ADDIS ABABA UNIVERSITY

SCHOOL OF GRADUATE STUDIES

SCHOOL OF EARTH SCIENCES

PETROGENETIC EVOLUTION OF THE BASALT AND ASSOCIATED RHYOLITE SUITI VOLCANICS (“ALAJE FORMATION VOLCANIC ROCKS’’) FROM AIBA AREA, TIGRAY, NORTHERN ETHIOPIA.

BY:

HAGOS HILUF ABRHA

ADVISOR: PROF. ASFAWOSSEN ASRAT

Thesis is submitted to School of Graduate Studies, Addis Ababa University, school of earth science for the Partial Fulfillment Requirement for Degree of Masters of Earth Sciences in Petrology.

30 May, 2018

Addis Ababa, Ethiopia

ADDIS ABABA UNIVERSITY
SCHOOL OF GRADUATE STUDIES
SCHOOL OF EARTH SCIENCES

PETROGENETIC EVOLUTION OF THE BASALT AND ASSOCIATED RHYOLITE SUIT VOLCANICS (“ALAJE FORMATION VOLCANIC ROCKS’’) FROM AIBA AREA, TIGRAY, NORTHERN ETHIOPIA.

BY
HAGOS HILUF ABRHA
ADVISOR: PROF. ASFAWOSSEN ASRAT

Thesis work is submitted to School of Graduate Studies Addis Ababa University, school of earth science for the Partial Fulfillment Requirement for Degree of Masters of Earth Sciences in Petrology.

30 May, 2018
Addis Ababa, Ethiopia

ADDIS ABABA UNIVERSITY

SCHOOL OF GRADUATE STUDIES

SCHOOL OF EARTH SCIENCES

PETROGENETIC EVOLUTION OF THE BASALT AND ASSOCIATED RHYOLITE SUIT VOLCANICS (“ALAJE FORMATION VOLCANIC ROCKS’’) FROM AIBA AREA, TIGRAY, NORTHERN ETHIOPIA.

BY

HAGOS HILUF ABRHA

Approved by Examining Committee

Dr. Balemwal Atnafu	_____	_____
Chairman school of Earth science	Signature	Date
Dr. Prof. Asfawossen Asrat	_____	_____
Advisor	Signature	Date
_____	_____	_____
Examiner	Signature	Date
_____	_____	_____
Examiner	Signature	Date

30 May, 2018

Addis Ababa, Ethiopia

ADDIS ABABA UNIVERSITY

SCHOOL OF EARTH SCIENCES

ANNEX 1: FORMAT FOR THESIS ORIGINALITY TEST REPORT.

Name of student	Hagos Hiluf
ID No.	GSR/2592/09
Stream	Petrology
Thesis title:	PETROGENETIC EVOLUTION OF THE BASALTS AND THE ASSOCIATED RHYOLITE SUIT VOLCANICS (“ALAJI FORMATION VOLCANIC ROCKS’’) FROM AIBA AREA, TIGRAY, NORTHERN ETHIOPIA.
Online site used for originally test	http://www.paperrater.com/plagiarisim_checker

No.	Particulars	Test I		Test II		Test II		Test IV		Test V		Average	
		Originality (%)o	Plagiarism (%)	Originality (%)	Plagiarism (%)	Originality (%)	Plagiarism (%)	Originality (%)	Plagiarism (%)	Originality (%)	Plagiarism (%)	Originality (%)	Plagiarism (%)
1	Abstract	100	0	100	0	100	0	100	0	100	0	100	0
2	Introduction	100	0	100	0	100	0	100	0	100	0	100	0
3	Literature review	100	0	100	0	100	0	100	0	100	0	100	0
4	Methodology	100	0	100	0	100	0	100	0	100	0	100	0
5	Result and Discussion	100	0	100	0	100	0	100	0	100	0	100	0
6	Conclusion	100	0	100	0	100	0	100	0	100	0	100	0
	Overall Thesis	100	0	100	0	100	0	100	0	100	0	100	0

NB: The results includes (geology and stratigraphy, petrography and geochemistry) chapter respectively and the literature review includes Regional geology chapter.

	Name	Signature
Student	Hagos Hiluf	
Advisor	Prof. Asfawossen Asrat	

Declaration of Originality

This is to announce that this thesis work is entitled "Petrogenetic Evolution of the Basalts and the Associated Rhyolite Suit Volcanics ("Alaji Formation volcanic rocks'') From Aiba Area, Tigray, Northern Ethiopia". This thesis is submitted for partial fulfillment of the requirements for the award of the degree of M.Sc. in petrology. It is supervised by Professor Asfawossen Asrat, Addis Ababa University, and School of Earth Science during the academic year 2017/2018 as part of Masters of Science program in Geological science (Petrology). In addition I announce that this thesis work is not presented, submitted, published to any institution/organization and it is well referenced and acknowledged.

HAGOS HILUF
Addis Ababa University
Date: June, 2017/2018
Sign: _____

I here by to declare this is original work as part of Masters of Science program in Geological science (Petrology)

Prof. Asfawossen Asrat: _____ _____

Signature Date

Acknowledgment

First, I would like to thank Adigrat University and Addis Ababa University for allowing me to pursue my postgraduate study.

I would like to thank my advisor Prof. Asfawossen Asrat for his genuinely constructive advice and moral support, and above all for his critical comments delivered always on time throughout the whole process, starting from my research proposal formulation until completion of my thesis writing.

In addition, I would also like to thank my colleagues for their unreserved support in the progress of my thesis work in some techniques and ideas: Hayelom Mengesha, Msgan Mola, Samuel Getachew, Angesom Resom, Belete Bychekign, Yemane Kelemework, Trhas Hadush and Azeb Gebremichael.

Last but not least, I would like to thank my family and the people of Aiba and Maichew area for their great support during the fieldwork, whose helped me to get access to the exposures on a generally difficult terrain.

Abstract

Continental flood basalts (Trap and shield basalts) of very large area and thickness, which occur in Ethiopia and Yemen are related to the Afro-Arabian continental break up. The current study deals with constraining the petrogenetic evolution of the mafic-felsic association of Alaje Formation in the Northwestern Ethiopian plateau, particularly at Aiba, Tigray, using detailed field mapping, petrographic analysis, as well as major and trace element geochemistry. The Alaje Formation is a succession of: rhyolitic tuff, olivine phyric basalt, rhyolitic ignimbrite, plagioclase phyric basalt, aphyric basalt. The basaltic rocks comprise phenocryst of plagioclase, clinopyroxene, Fe-Ti oxides and rare olivine phenocrysts. On average, the basaltic suite is plagioclase dominated, except the older basalt where olivine is dominant, and the younger basalt at Tsibet section where Fe-Ti oxide is dominant. The common phenocrysts of the silicic rocks are quartz and sanidine, though the banded rhyolitic lava is particularly quartz dominated. Although the basaltic rocks and the associated rhyolitic units have different phenocryst assemblages and textural relationship in between different unit of basalt and rhyolite, they do not show significant geochemical variation, while there is close genetic relationship between basalt and rhyolite. This is supported by the consistently constant similar trace element ratio Nb/Zr (0.09-0.14), Ce/Zr (0.20-0.29), La/Zr (0.10-0.012), Rb/Zr (0.05-0.14), Ta/Nb (0.05-0.07), La/Nb (0.85-1.05),Hf/La (0.21 0.26) and linear trend of two high incompatible trace element. Besides the geochemical data suggest that the basaltic units are more primitive than the associated rhyolites unites. However, the lower contents of MgO wt% (5.41 - 8.11) and compatible trace element content like Ni (19 – 151 ppm) and Cr (100-300 ppm) indicates that the basaltic units have undergone some fractionation except anomalous high Cr (670), Ni (421) of the lower basaltic unit. Furthermore, the rhyolites of the Alaji Formation have peralkaline affinity and show consistently similar geochemistry to the well-constrained rhyolitic rocks of Wegel Tena and Lima limo, which have been shown to be formed by low pressure crystal fractionation process. It is concluded that the rhyolites are derived by low pressure crystal fractionation of basaltic magma derived from enriched source component of the mantle.

Keywords: Continental flood basalts, Ethiopian plateau, enriched source, fractional crystallization, primitive source, co-genetic rocks

Table of Contents

List of figure **Page**

List of Table **Page**

List of Appendix

LIST OF ACRONYMS

- Ab Albite
- Ac Acmite
- ALS Ireland laboratory Science
- a.m.s.l Above mean sea level
- An Anorhtite
- Ap Apatite
- ASR Aygi section rhyolite
- CFB Continental flood basalt
- CIPW Cross Indings Pirsson Washngton
- CMER Central main Ethiopia rift
- Di Diopside
- EASR East Africa rift system
- E-W East West
- Fig Figure
- GPS Global positioning system
- Hm Hematite
- HREE Heavy rare earth element
- HT High titanium
- Hy Hypersthene
- ICP-AES Inductively coupled plasma atomic emission spectroscopy
- ICP-MS Inductively coupled plasma mass spectroscopy
- Km Kilometer
- LAB Lower Aygi basalt
- LOL Loss on ignition
- LAST Lower Aygi section tuff
- LREE Light rare earth element
- LT Low titanium
- LTSB Lower Tsibet section basalt
- m Meter
- ma Million year
- MER Main Ethiopia rift
- ME- ICP06 Multi element Inductively Coupled Plasma 06

- ME-MS81 Multi element Mass Spectrometry 81
- mm Millimeter
- MORB Mid oceanic ridge basalt
- NE North east
- NMER North main Ethiopian rift
- NE-SW Northeast south west
- NW North west
- REE Rare earth element
- Ru Rutile
- Ti Titanium
- Tn Titanite
- TSR Tsibet section rhyolite
- SMER Southern main Ethiopian rift
- SE South east
- OIB Oceanic island Basalt
- Opa Opaque
- Or Orthoclase
- PPL Plane polarized light
- Qtz Quartz
- UASB Upper Aygi section basalt
- UTSB Upper Tsibet section basalt
- Wt Weight
- XPL Cross polarizer light

CHAPTER ONE

INTRODUCTION

1.1. Background

The present study area is located in the Northwestern Ethiopian plateau volcanics, North of Maichew, particularly at Aiba Locality called Tsibet, Tigray, and Northern Ethiopia. This research work aims to study the petrological and geochemical evolution of the mafic–felsic association of the Alaje formation volcanic rocks, in addition to constructing the detailed stratigraphic successions and constructing the geological map of the study area. This study will contribute additional data and interpretations to understanding the evolution of the Ethiopian plateaus volcanic rocks. In order to achieve the objectives of the research, petrological, geochemical, and petrographic analysis have been performed on the upper sequence of the Aiba area (Tsibet and Aygi sections) (Fig.1.1) and Checkon section (Fig.1.4).

The Continental Flood Basalt (CFB) province of Ethiopia and Yemen are related to the Africa–Arabia continental break-up (Pik et al., 1998, 1999).According to Mohr and Zanettine (1988), the Ethiopian continental flood basalt is located at the junction of three rifts: two of them are developed into oceanic rifts (Red Sea and Gulf of Aden) whereas the third one is on the stage of continental rifting (East African continental rift) and the largest areal is covered in Ethiopia, which covers around seven times of Yemen flood basalt (Fig.2.2). The areal coverage of the Ethiopian flood basalts is 600,000 km^2 with an average total thickness of 2000m and total volume is about 350,000 km^3 (Mohr and Zanettine 1988).While the Yemen continental flood basalt covers an area of 80,000km^2(Ukstins et al., 2002). Lima limo, Maichew and Wegel Tena are example of thick continental flood basalt volcanics in Ethiopia. The earliest dated (35-45ma) south Ethiopia and Kenya flood basalt is covers small volume (George et al., 1998; Furman et al., 2006)

According to (Hofmann 1997, keiffer et al., 2004) the Northwestern Ethiopian flood basalt is composed of late Eocene and Oligocene fissure basalts, covered by Miocene shield volcanoes in some places. These Flood volcanic rocks in Ethiopia are uncomformably underlain by sandstones (Ukstins et al., 2002).

Traditionally, the Northwestern Ethiopian Plateau has been subdivided into three formations (Siefe Michael Berhe et al., 1987 and Mengesha Tefera et al., 1996): the Ashangi which is tilted in the lower stratigraphy and the horizontally layered Aiba basalt unit separated by an angular unconformity and the upper ignimbrite Alaji unit. The composition of the plateau volcanic rocks is both felsic and basaltic, though the felsic lavas and pyroclastic are found particularly at upper stratigraphic levels inter-layered with the flood basalts, mainly rhyolitic and less commonly trachytic compositions (Dereje Ayalew et al., 1999, 2011).

Southern Ethiopian pre-rift and syn-rift volcanics are study previously and accordingly the Plume contributions to the pre-rift basalts in the northern transect is less than the syn-rift basalt which is predominantly plume derived. Therefore the plume contribution is increase with rifting process increase (Stewart and Rogers 19996).

Pik et al. (1998; 1999) divided the northwestern Ethiopian plateau basalts geochemically into two high-Ti groups (HT1 and HT2) and one low-Ti group (LT) and these groups are found spatially zoned from the rift to the west of northern Ethiopian plateau.in addition Kurkura Kabeto (2010) identified the basaltic rocks of the Maichew area within the High-Ti group and divided them into six sequences (Fig. 1.1): alkaline lavas (basanites, basalts, and ankaramites, with basaltic agglomerate) at the base, felsic volcanics in the middle, and transitional to tholeiitic mafic lavas at the top of the transitional sequence.

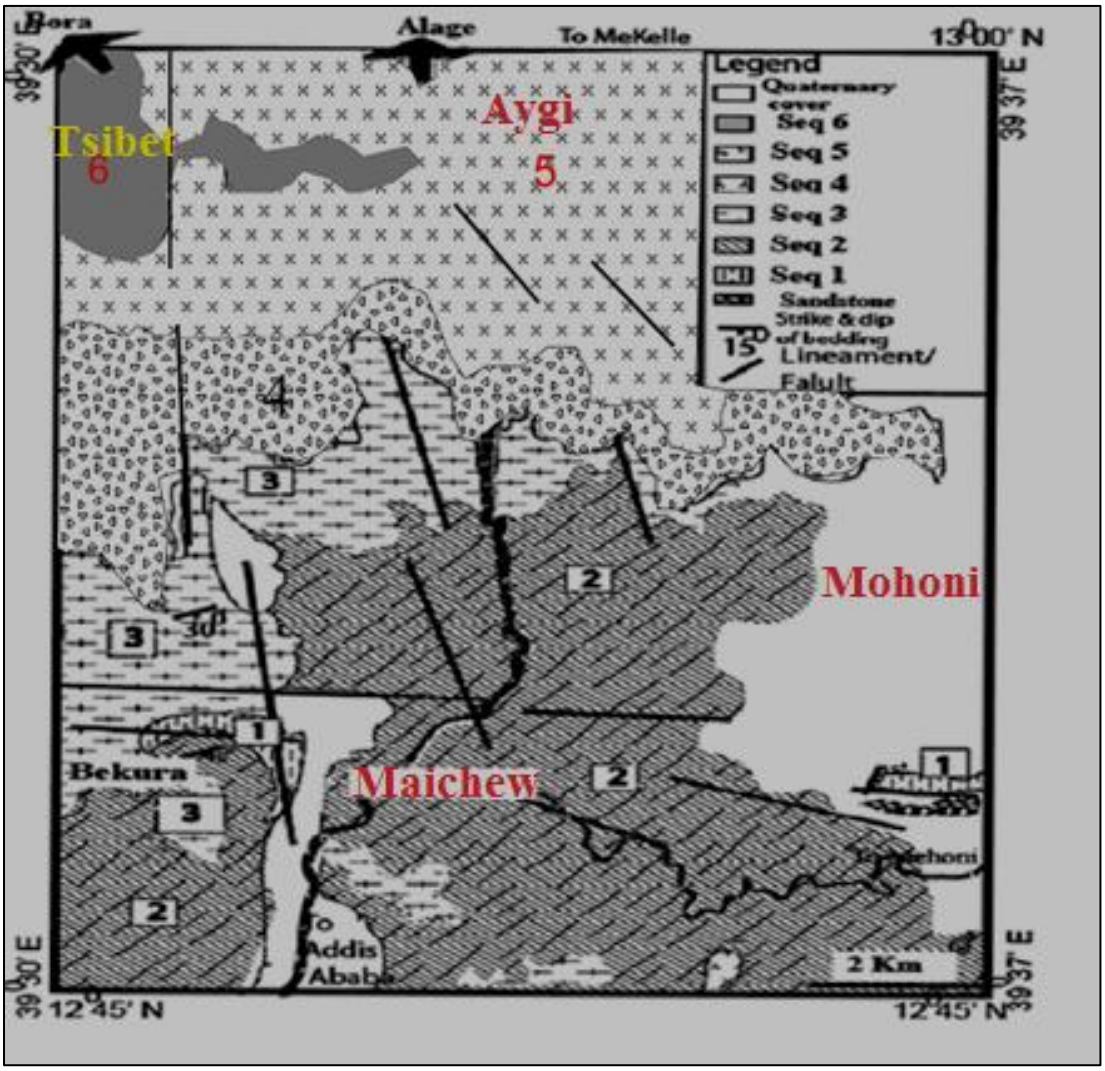

Fig. 1.1.Geological map of Maichew area, the number on the map indicates sequences of rock from the lower stratigraphy (Mohoni) up to the upper stratigraphy (Tsibet) as sequence 1, 2, 3, 4, 5, and 6, respectively. Number shows lithological variation or lava flow. (Modified after Kurkura Kebeto, 2010)

1.2. Methodology

The main methodologies have been utilized are basic geological mapping and data collection (primary and secondary data). Geological mapping has been done at the scale of 1:25,000 on a topographic base map of the Ethiopian Mapping Agency at scale of 1:50,000. Base maps have been produced and displayed using standard ARC GIS 10.3 software while images have been treated and analyzed using ERDAS, Global Mapper, Starter, Google Earth, and Surfer. In addition a hand-held GPS has been used to record sampling locations and other outcrop features of the primary data's. Major elements data's are analyzed using multi element inductively coupled plasma (ME-ICP06)

whereas, trace elements data's are analyzed using multi element mass spectrometry (ME-MS 81) techniques and Trace elements including the full rare earth element suites are reported from three digestions with either ICP-AES or ICP-MS finish. Geochemical data's have been compiled and analyzed using Excel and specialized geochemical software (Petrograph 2 beta and GCDKit 3.00) and Petrographic analysis was conducted using a Polarized Petrographic microscope.

During the course of the study a pre-fieldwork, secondary data and literature survey was conducted then based on research gaps were identified, objectives of the research were formulated. A base map at the scale of 1:25,000 was also prepared on which possible traverse lines for fieldwork were traced. During fieldwork, primary data including, lithological descriptions, contact relationships, structural data, were collected following the pre-defined traverses, geological map was prepared, sections were logged and representative samples were collected. Post fieldwork, samples were selected, prepared and analyzed for petrography and geochemistry; data were treated and interpreted, based on which the geochemical evolution of the rocks is characterized.

1.3. Basic research questions

The basic research questions of this study are the following:

- ✓ How did the felsic pyroclastic rocks in the Alaji series evolve within the flood basalt sequence? Felsic pyroclastic rocks are found interbeded with in the flood basalt sequence interchangeable from the lower stratigraphic unit and goes continuously to the upper unit, then how did this felsic evolves and related?
- ✓ What is the Petrogenetic relationship between the basaltic unit and the felsic units? Three sequence of basalt and three sequences of felsic rocks are found interbeded interchangeably within the outcrop unit, and then is there any Petrogenetic relationship in between the basalt of the different suit and felsic pyroclastic rocks unit or no?
- ✓ What Petrogenetic process was responsible for the formation of the felsic pyroclastic rocks? Different Petrogenetic process are responsible for the felsic pyroclastic rock such as partial melting underplate basic igneous rock , fractional crystallization mantle derived basalt with or without crustal contamination and partial melting of the continental crust.

1.4. Statement of the problem

Most studies on the plateau magmatism are conducted at a regional scale (e.g.Zanettine, et al.,1978; Mohr, 1983; Mohr and Zanettine, 1988; Hart et al., 1989; Berhe et al., 1987; Mengesha Tefera et el., 1996; Stewart and Rogers, 1996; Pik et al., (1998; 1999); Kieffer et al., 2004, Bacculava et al., 2009). The Petrogenetic process responsible for the formation of the pyroclastic rocks within the flood basalts has also been a major question. Various models have been proposed in the previous study of flood basalts and the associated rhyolite such as: partial melting of continental crustal rocks; fractional crystallization of mantle-derived basaltic magmas with or out crustal contamination; or partial melting of underplated basic igneous rocks. Some authors put that the rhyolitic rocks are derived from fractional crystallization of the associated basaltic magma with little crustal contamination (Peccerillo et al. (2003, 2007); Dereje Ayalew and Gezahign Yirgu (2003); Ayalew et al. (2006; 2011); Kabeto et al., 2009; Rooney et al., 2012; Angesom et al., 2018. In contrast Boclleti et al., (1995) explain different origin of the basaltic rock and the associated felsic pyroclastic rocks. According to Dereje et al.,(2002) the plateau ignimbrites are derived by fractional crystallization of basaltic magmas consistent in composition to the exposed flood basalts. In addition in Axum-Adwa basalt and associated trachyte and syenites are related through fractional crystallization (Miruts Hagos et al., 2010). While, Black et al.(1997)and Mahoney et al.(2008) rhyolite is related to the crustal derived or re-melting of under plate basic igneous rock in the lower crust in Kenya and Madagascar complex respectively. The current study focuses on a single section of the Alaji formation in the Aiba area and around; where the petrogenetic evolution of the felsic and basaltic units is investigated using detailed stratigraphic logging, mapping and sampling. The results of the investigation will help to characterize the relationship between the felsic and basaltic units at the local scale and to correlate various sections at regional scale. In addition, the Petrogenetic evolution of the felsic pyroclastic rocks will be investigated.

1.5. Objective and scope of the work

1.5.1. Major objective

The major objective of the study is to determine the Petrogenetic evolution of the basalt and associated rhyolite rocks of the "Alaji Formation" in the Aiba area and its surrounding based on field, petrographic, and trace and major element geochemistry.

1.6.2. Specific objectives

The specific objectives are to:

- Produce detailed geological map at scale of 1:25,000 of the area.
- Construct the detailed stratigraphic log of the study area.
- Constrain the geochemical suits of the units.
- Constrain the petrographic associations of the various rocks units.
- Characterize the petrological and geochemical variation of all the basic and felsic units.

1.6. The study area

1.6.1. Location and Accessibility

The study area is located around Aiba area, 15km north of Maichew town, 672 km north of Addis Ababa, and 120km south of the Mekelle, in Tigray regional state, Northern Ethiopia. It is specifically located at the Tsibet mountain range at an elevation of 2900 - 3935m a.m.s.l. Geographically it is bounded by UTM 37 E554000 to 562000m longitude /N1418000 to 1425000 m latitude (Fig. 1.2). The eastern part of the study area is crossed by the Addis Ababa-Mekelle highway (Fig. 1.2). However, most parts of study area are accessed only along footpaths, due to the high cliffs and rugged terrain nature of the topography. In general, the accessibility in the area is very limited.

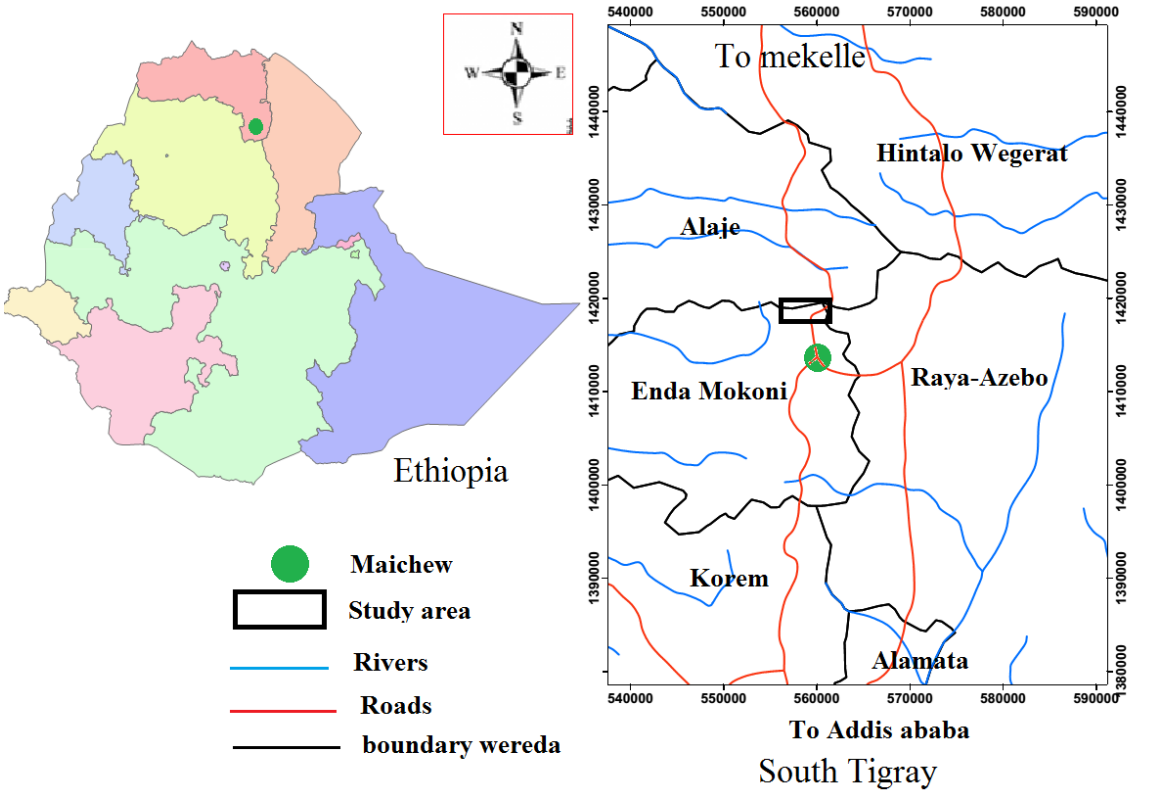

Fig. 1.2. Location map of the study area, at the junction of wereda Emba Alaje, Enda mokoni, Raya –Azebo.

1.6.2. Climate and vegetation cover

The average annual temperature of the study area is 16.7^{0}c and the average annual rain fall is 753mm.However, there is high seasonal variability in temperature and rain fall, where highest temperatures are measured during May and June with average temperature of 20.2^{o}c, while the lowest temperatures are measured in August and October, December with average temperature of 14^{0}c. In addition the peak rain fall is measured in August month (http://En.climate-data.org). In general the area has good climatic condition. Except the eastern part of the study area with cliffs and ridges topography, the study area

is nearly bare land with little permanent vegetation cover. Therefore due to the agricultural activities the area led to erosional landscapes and becomes scarce vegetated.

1.6.3. Population and settlement

Population density in the study area is high owing to the presence of fertile soil on the basaltic bedrocks which support significant agricultural activities. Settlements are in scattered villages on the plateau where rain fed agriculture and animal rearing are practiced. According to the 2007E.c central statistical agency of Ethiopia the maichew town has 23,419 people are present, which is nearer town of Aiba village area (http://en.m.wikipidia.org.>wiki>mayc...).

1.6.4. Drainage pattern

The drainage of the study area is characterized by dendritic pattern form. All streams in the study area are intermittent, and they generally flow from the high plateau passing through the Maichew and Aiba escarpments to the Mohoni marginal graben in the rift, in the eastern direction (Fig. 1. 2) and to Gereb Tsana River in the western direction. Due to the high elevation from sea level all the river including Gereb Tsana starts from this point.

1.6.5. Physiography and soil cover

The study area is very rugged plateau, forming topography the Tsibet ridge, one of the highest ranges in southern Tigray, bounded to the east by the major Maichew-Mohoni fault escarpment, which exposes the volcanic sequences (Fig. 1.4a). A continuous, E-W extending ignimbrites cliff exposes the on the high plateau and the Aiba valley at the northern foot of this ridge extends in the same direction. This valley and the foothills south of the main ridge are filled by thick soil accumulated from erosion of the adjoining tuffaceous hills. The generally flat Aiba valley forms a permanent wetland while the southern foot hills are generally drained due to the appreciable slope and form excellent agricultural fields.

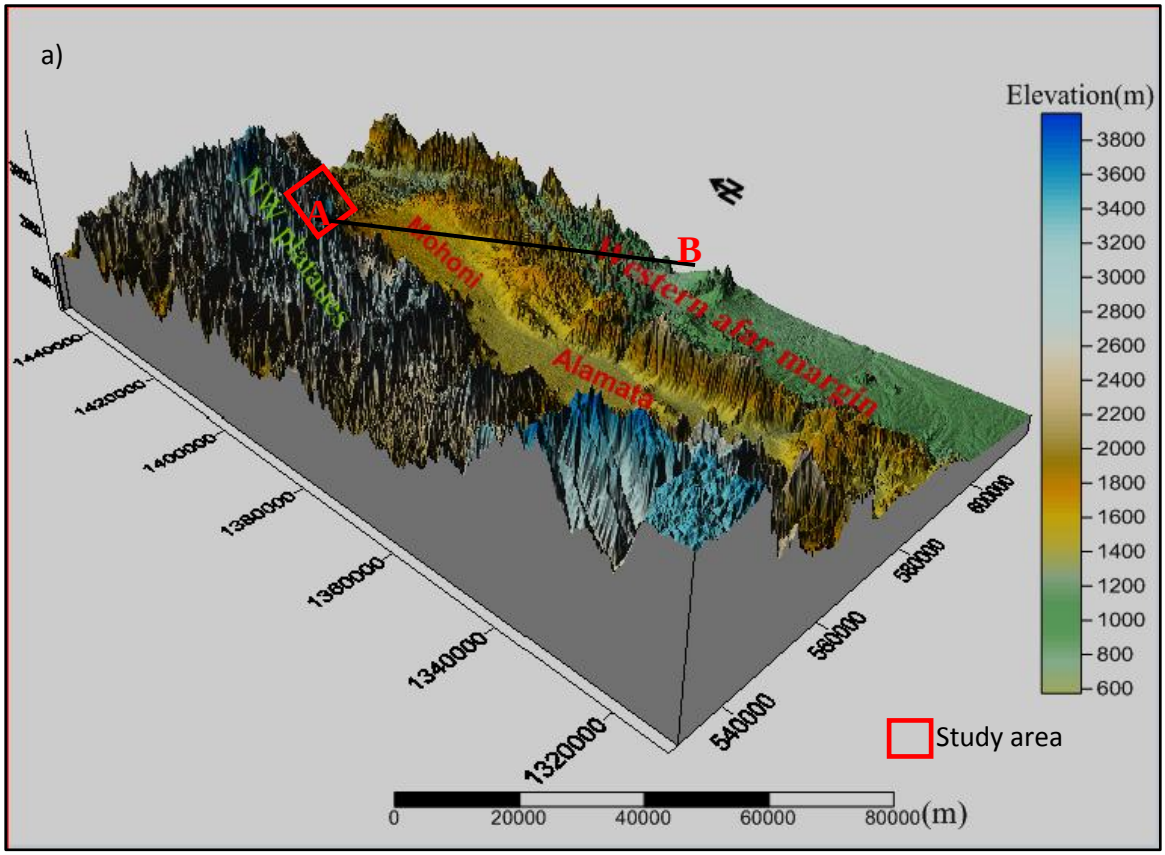
a)
Elevation(m)
3800
3600
3400
3200
3000
2800
2600
2400
2200
2000
1800
1600
1400
1200
1000
800
600
A
B
NW Plateaus
Mohoni
Extern afar margin
Alamata
Study area
0
20000
40000
60000
80000(m)

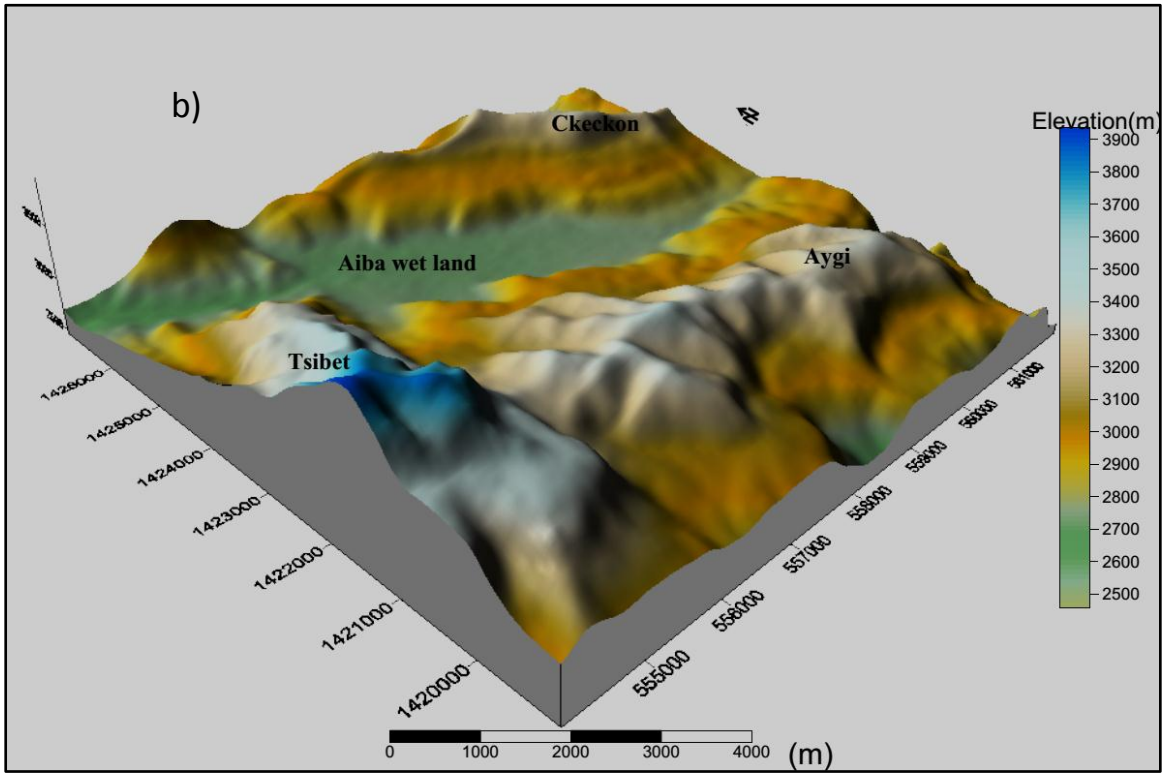
b)
Ckeckon
Aiba wet land
Aygi
Tsibet
Elevation(m)
3900
3800
3700
3600
3500
3400
3300
3200
3100
3000
2900
2800
2700
2600
2500
0
1000
2000
3000
4000
(m)

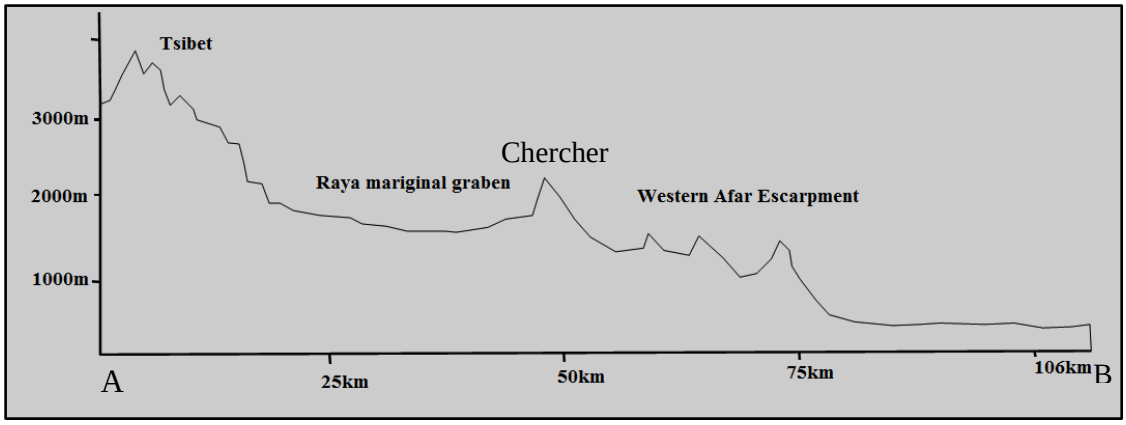

Fig. 1.3. Digital Elevation map (physiography) of the study area. (a), raya marginal graben. (b), study area found at the NW margin of raya marginal graben. (c)Trace of profile section from study area to west afar escarpment

1.7. Literature review

According to Siefe Michael Berhe et al. (1987); Mohr and Zanettine (1988); Ebinger et al. (1993); Pik et al (1998, 1999); Peccerillo et al. (2003; 2007) Kieffer et al., 2004; Beccaluva et al. 2009; Natali et al. (2011; 2013), Furman et al., 2016), Volcanism in Ethiopia has occurred since the Oligocene related to the Afro-Arabian continental separation, while the currently active volcanism is centered in the Afar and Main Ethiopian Rifts. According to Furman 2007, Furman et al., 2016 and Sembroni et al., 2016, Ethiopian is a naturally occurred laboratory to study process operating on crust and mantle due to the existence of recent active rift volcanism and existing plateau volcanics.

Hence most current studies of volcanism in Ethiopia focus on these volcanically and tectonically active regions (Peccerillo et al. (2003; 2007). The Oligocene volcanism of the Northwestern Ethiopian plateau has been subdivided into three formations from the lower to the top of the basaltic sequence as Ashangi Formation, Aiba Basalt, and Alaji Series which is bimodal in composition (Siefe Michael Berhe et al., 1987).The volcanic rocks of the Maichew sheet are mapped at a very small scale (1:2,000,000 scale) which indicated a succession of Ashangi Formation consisting of often tilted flood basalts with rare intercalation of tuff; the massive Aiba basalt, the Alaji series and the Tarmaber Gussa Formation. The Ashange and Aiba basalts are marked by an angular unconformity where the titled Ashangi basalts are overlain by the generally horizontally layered Aiba basalts while the Aiba and Alaje is basalts are marked by tuffaceous material (Mohr and

Zanettine 1988; Mengesha Tefera et al., 1996). However, this stratigraphic classification is generally arbitrary and based only on field associations without any detailed petrological and geochemical characterizations. The classification could work for the type locality but could not be easily replicated elsewhere in the flood basalt province.

Pik et al. (1998; 1999) divided the Northwestern Ethiopian plateau basalts into two high-Ti groups (HT1 and HT2) and one low-Ti group (LT). However, limited number of samples from the Maichew area was included in these studies. Therefore it is difficult to draw conclusion with little sample for the whole Maichew area and its surrounding.

Kurkura (2010) investigated the volcanic rocks of the Maichew area using petrological and geochemical methods, and identified six sequences of lavas from bottom to top as: basanite, alkaline basalts, transitional ankaramite, silica rich tholeiitic to transitional sequence, mafic-felsic volcanism, and tholeiitic to transitional basalt (upper part of flood basalt). The alkaline basalt and the transitional ankaramite can be grouped in the HT2, and the other younger sequences can be grouped in the HT1 of Pik et al. (1998; 1999).however the present study area(Aiba) classify into two stratigraphic unit and more concentrated in Maichew and around ridges. Then the basalts and felsic are grouped together as one unit and its main concentration to the basalt but not to the rhyolite. As the present study is one of the objective is to characterize the rhyolite, and the petrological and geochemical variation with the basalts.

According to Dereje et al. (1999), felsic lavas and pyroclastic rocks of rhyolitic and trachytic composition are interlayered with the flood basalts particularly at upper stratigraphic levels. Dereje et al. (2002) further indicated that bimodal mafic-silicic volcanism initiated in northern Ethiopia at 30.2 Ma, consistent with the flood volcanism in Yemen at 30 M. Petrological and geochemical characteristics of the plateau ignimbrites show their derivation by fractional crystallization of basaltic magmas, Dereje Ayalew and Gezahign Yirgu (2003) showed that little crustal contamination contributed to the genesis of basalt and rhyolite geochemical provinciality on the Ethiopian plateau.

1.8. Expected outcome /significance of the study

The possible outcomes / significance are:

- ✓ A detailed section of the Alaji Series with detailed description of the rock units, which could serve as a reference section.
- ✓ A detailed geological map of the Aiba area.
- ✓ A clear understanding of the petrogenetic relationship between the basaltic and felsic pyroclastic units in addition, the petrogenetic relationship in between the same unit of different stratigraphy.
- ✓ A Petrogenetic model/characterization of the felsic pyroclastic rocks of the Alaji formation.

CHAPTER TWO

REGIONAL GELOGICAL SETTING

2.1. Cenozoic continental flood basalt volcanism of East Africa

The Cenozoic continental flood basalt volcanism in Ethiopia and Yemen is the youngest flood basalt activity which is associated with continental break-up and ocean basin formation and it is located at the junction of three rift: two of them are developed into oceanic rifts (Red Sea and Gulf of Aden) whereas the third one is at the stage of continental rifting (East African continental rift). The flood basalt volcanism covers an enormous area from southwestern and eastern Ethiopia, Eritrea, Djibouti and including Yemen and southern Saudi Arabia, with areal coverage of ~600,000 km^2, an estimated volume of >350,000 km^3 and an average thickness of 2000m in Ethiopia (Mohr, 1983; Mohr and Zanettine, 1988; Baker et al., 1996; Tedious Chernet et al., 1998; Pik et al., (1998; 2006, 2009); Kieffer et al., 2004; Corti et al., 2009). The Ethiopian and Somalian plateau is dissected by the EARS which extends over 2000 km from the Red Sea southward to Mozambique and provides an opportunity to study the mantle plume- driven continental rift volcanics rocks (Furman et al., (2004; 2006,2007).

The Continental Flood Basalt (CFB) province of caped in Ethiopia and Yemen are consistently related to the of Afar plume head (Hofmann et al. 1997;Pik et al. 1998; 1999); Furman et al.(2004;2016), Kieffer et al., 2004;Beccaluva et al. 2009; Natali et al. (2011;2013).Various views have been proposed concerning to the source region of the East African Rift System magmatism which is exposed in Ethiopia ,Yemen, Kenya and other area . Ebinger & Sleep (1998) considered that the Cenozoic magmatism throughout the EARS, West Africa and central Africa was the result of single large mantle plume beneath the Ethiopian lithosphere at ~45 Ma. However, other researchers uses geochemical and geochronological data, and they suggest that more than one mantle plume might have been involved in the magmatism of the Ethiopian (Afar) and Kenyan sectors of the East Africa Rift System (George et al., 1998; Rogers et al., 2000; Pik et al., (1998; 1999). Dereje Ayalew et al. (1999) have also explained that the difference in age of basaltic volcanism in the southwestern and northern Ethiopian volcanic provinces may imply that the two provinces are originated from different mantle plumes.

The Cenozoic Ethiopian continental flood basalt province embraces the Afar triple-rift junction which connects the East African Rift System with the Red Sea and Gulf of Aden sea-floor spreading zones, where three main stages of volcanic episodes are distinguished (Mohr and Zanettine, 1988; Ukistins et al., 2004). The age of the Ethiopian volcanics according $^{40}Ar/^{39}Ar$ data ranges between late Oligocene and early Miocene (32-21 Ma), and is characterized by eruption of huge flood basalt sequences (known as Ashangi and Aiba Basaltic Formations) followed by alternating basalt and rhyolitic sequences forming the so-called Alaji Rhyolitic Formation (Zanettine, 1980 cited in Mohr and Zanettine 1988). However, the most voluminous volcanic activity occurred between 30 and 29.5 Ma within a short 1 Myr period (Hofmann et al., 1997). The subsequent volcanic episodes are central eruption of the Termaber basalt formation at 13 to 9 Ma (Peccerillo et al., 2007) and Pliocene to Quaternary volcanism directly related to the main episodes of the opening of the Main Ethiopian rift and Afar depression at 4.5 Ma to present (Peccerillo et al., 2007). However, older volcanic episodes are dated at 45 Ma from the southwestern Ethiopian plateau. These volcanic rocks have small volume and are unrelated in composition to the volcanic rocks of the Northern plateau (George et al., 1998, Ebinger et al., 1993; Ukstins et al., 2002). In addition, Merla et al. (1979) the southern Ethiopian plateau is significantly different from the northern Ethiopian volcanic plateau, in that flat lying thick piles of basalts (traps) are rare and large volcanic shield volcanoes are not common in the south, while phonolitic lavas are abundant.

Most of the Ethiopian continental flood basalt erupts at around 30 Ma during the pre-rift tectonic stage are characterized by the eruption of huge volume of basaltic (tholeiitic to alkaline) lava flows, with varying magmatic characteristics in different regions of the volcanic plateau (e.g., Kieffer et al., 2004). While the felsic lava flows and pyroclastic rocks of rhyolitic, and less commonly of trachytic composition, are interbeded within the flood basalts, particularly at upper stratigraphic levels (e.g., Mohr and Zanettine, 1988; Dereje Ayalew et al., 1999; 2002; Kieffer et al., 2004).

2.2. Cenozoic flood basalt and shield volcanism

The Ethiopian plateau flood basalt volcanics provenances are mainly distributed in the northwestern, southeastern and southwestern plateaus. The Southeastern plateau covers less area while the northwestern and southwestern plateau are covers wide area, the plateau composed of late Eocene and Oligocene fissure basalts covered in places by upper Miocene shield volcanoes (Hofmann, 1997; keiffer et al., 2004), in addition the plateau basalts are comprise felsic pyroclastic rock particularly in the upper stratigraphy (Dereje Ayalew et al., 2002).

The volcanic pile exposed in the Alaji-Aiba-Maichew area has been divided into two groups based on the tilting nature of the lava flows (Mohr and Zanettine, 1988): the lower group, which is a S- to SE-dipping basalt lava sequence; and the upper group, which is horizontally bedded and uncomformably overlaying the lower group with cliff forming. Later these rocks were subdivided into three formations based on their field relationships (Berhe et al., 1987): the Ashangi and Aiba basaltic units, separated by an angular unconformity (Mohr Zanettine, 1988; Mengesha et al., 1996) and the upper Alaji ignimbrite unit.

According to Mohr and Zanettine (1988), the Aiba Formation and the Alaji series are lithologically similar except welded and unwelded pyroclastic rocks become more abundant in the Alaji series. The Aiba Formation is typically composed entirely of massive flood basalt flows of dense, dark, fine-grained olivine basalt, with or without intervening agglomerate beds. The individual flows are 15 to 50 m thick and commonly form columnar joints. The Alaji Series is composed of basalts of similar composition and abundant silicic (trachyte/rhyolite) ignimbrites flows. In some localities, such as at the Amba Alaje, the Aiba basalts are directly conformably overlain by laterally extensive and constantly thick, horizontal layers of welded rhyolitic ignimbrite successions (Mohr and Zanettine, 1988). In the current study area, the unwelded rhyolite tuff is overlaying the Aiba basalts.

The lithological characteristics of the Aiba Formation is easily distinguishable over the northern Ethiopian Plateau owing to the presence of thick, massive and frequent columnar flows of fine-grained basalt and upper contact of the silicic horizon. However, the initiation of Miocene silicic volcanism was not uniform throughout the Ethiopian volcanic province. Therefore, the absence of this interbeded silicic volcanic horizon in

some place makes distinction between the Aiba and Alaji formations difficult, as the two formations comprise basalts of virtually identical mineralogy and chemistry (Mohr, 1983).

The Termaber formation overlies the Alaje formation, although it is removed in some places by erosion (Mohr and Zanettine, 1988). It can be distinguished from the other formation because it forms large, low angle shields up to tens of kilometers in diameter, although smaller and steeper edifices also occur. In addition, the shield basalts are composed of pyroclastic beds, lava flows of commonly scoriaceous and/or amygdaloidal, porphyritic varieties including olivine-pyroxene basalts, basanites and, less abundant coarse feldspar-phyric basalts.

According to Dereje Ayalew et al. (1999; 2003), the Ethiopian continental flood basalt province contains a significant volume of large felsic eruptive rocks (>$63x10^4$ km^3) overlaying the flood basalt, mostly interbeded with the upper levels of the flood basalt sequence. The age of these felsic volcanics is relatively uniform in the Northwestern Ethiopian plateau (e.g., the Lima Limo rhyolite sequence is 30.6±0.79 Ma and the Wegel Tena rhyolite sequence is 30.17±0.54 Ma old) The rhyolites follow similar pattern to the basalts in terms of the Ti distribution, where the low-TiO2 rhyolites are associated with low-TiO2 basalts and the high-TiO2 rhyolites are associated with the high-TiO2 basalts (Dereje Ayalew et al., 2002.

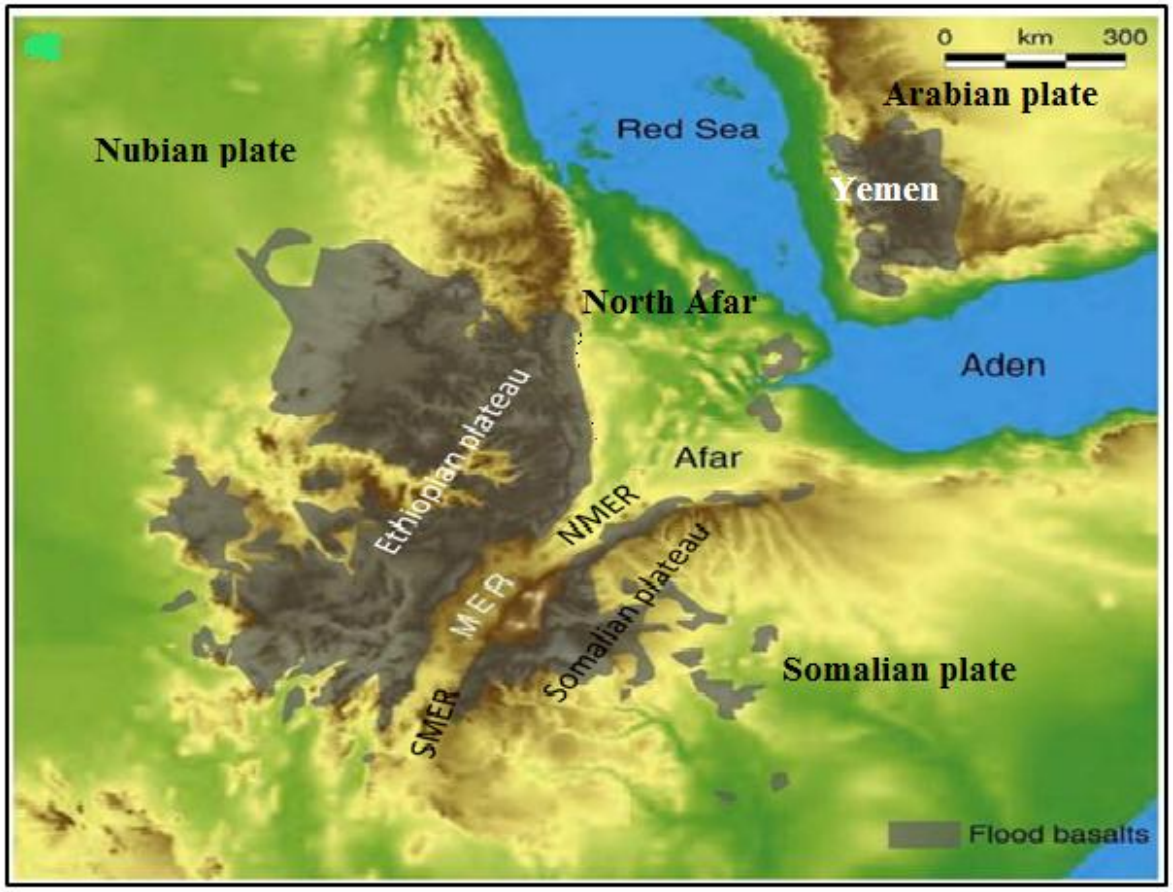

Fig. 2.2. Schematic distribution of flood-basalt volcanism in Ethiopia and Yemen (modified after Chorowitz, 2005; Corti et al., 2009).

Pik et al. (1998; 1999), based on geochemical and isotopic studies concluded that the effect of lithospheric signature in the Ethiopian flood basalts is less in the high Ti basalts than in the low Ti basalts, and suggested that the northern Ethiopian flood basalts have two mantle source component, i.e., depleted mantle source and OIB like mantle component. They further elaborated that as continental break-up increased, the geochemical signature of the lavas generally evolved toward that of oceanic magmas (OIB, ocean island basalts; and MORB, mid ocean ridge basalts), suggesting the increasing involvement of the asthenosphere mantle. The Oligocene volcanic products of the northern Ethiopian plateau also show a strongly bimodal distribution of basalts and rhyolites although the province is predominantly basaltic. Dereje Ayalew et al. (1999; 2002) later concluded that the consistency in composition of the basalts and rhyolites provinciality indicates the rhyolites associated with the flood basalts were derived either by fractional crystallization of the associated basalt.

2.3. Quaternary volcanism

The Alaje-Aiba-Maichew area is bounded to the east by the volcanically and tectonically active rift. The Main Ethiopian Rift is the northern segment of the East African Rift System that connects with Afar depression, at the Red Sea–Gulf of Aden triple junction in the northeastern direction, and connects with the Turkana depression and Kenya Rift to the south. It is key sector of the EARS to analyze the evolution of continental extension and the dynamics of continental deformation (Mohr, 1983; Wolfden et al., 2004; Roony et al., (2005; 2012); Peccerillo, 2007; Corti et al., 2009). The Afar region is a triangular depression and bounded by the Ethiopian plateau volcanics and it is the intersection of the Red Sea and the Gulf of Aden oceanic rifts with the continental rift of MER (Chernet et al., 1998).

The Main Ethiopian Rift (MER) is an ideal place to study the transition from continental rifting to ocean basin formation because it captures rifting processes during continental breakup (Roony et al., 2012, Furman et al., 2016, and Sembroni et al., 2016). MER lies in a unique transitional zone between the continental rifting of East Africa and the seafloor spreading of Northern Afar and the Red Sea (Rooney et al., 2005). Initial rifting in the southern and central Main Ethiopian rift (MER) commenced between 18 and 15 Ma, but little is known of rift initiation in the northern MER (Giday Weldegebriel et al., 1990; Ebinger, 2000; Wolfden et al., 2004). Chernet et al. (1998) sample sequences throughout the northern MER and suggested that rifting commenced at 7 Ma. The MER, which marks the incipient plate boundary between Nubia and Somalia, formed long after the flood basaltic magmatism, and not as a consequence of the separation (Wolfden et al., 2004).

The MER is characterized by bimodal volcanism where intermediate composition rocks are rare. The rift floor is dominated by silicic volcanic rocks in the form of pyroclastic flow and fall deposits, rhyolitic ignimbrite and pumice (e.g.Berhe et al., 1987; Mohr and Zanettine, 1988, Peccerillo et al., 2003; 2007). The rhyolitic rocks are derived by fractional crystallization of basaltic rocks; though heterogeneous sources various levels of crustal interaction is possible (Peccerillo et al., 2007). Bimodal volcanism seems to be a common feature of both the plateau and rift volcanic provinces, though the relative volume of felsic rocks on the plateau volcanic rocks is less significant than that in the rift.

Recent work in the Petrogenesis of the basalt in the MER indicates the presence of three distinct mantle reservoir (Afar plume, depleted mantle, and enriched mantle) and there is with small amount of crustal contamination with the basalt (Marty et al., 1996; Rooney et al., 2012, Mulugeta Alene et al., 2017; Muruts Hagos et al., 2016; Dereje Ayalew et al., 2016).

CHAPTER THREE

GEOLOGY AND STRATIGRAPHY

3.1. Introduction

The geology of Southern Tigray is underlain by continental flood basalts, except some exposures of the Upper Sandstone (‘‘Ambaradam Sandstone’’) at uplifted fault escarpments, such at the Mohoni marginal Graben to the east, or at deeply incised gorges in the Bora area (Gereb Tsana River) North West of the study area. The thickness of the continental flood basalts in the Maichew area reaches up to 2200m (particularly in the study area), from the lowest contact at the foot of the Mohoni escarpment to the upper levels at the Tsibet ridge (Fig. 3.1). Basaltic and rhyolitic units of various textures and thickness are exposed in the study area. The basalts are mostly porphyritic to aphyric, but could be aphanitic, and/or vesicular in places. In some localities, they show strong alteration. The rhyolitic rocks show variable degrees of welding and show spary porphyritic to porphyritic texture. Both basalt and rhyolite of the formations are exposed in the Aygi, Checkon, and Tsibet ridges while the lower basalt is covered its most portions by the Aiba Wet land area. The volcanic units are affected by NE-SW oriented faults and joints.

3.2. Lithology and stratigraphy of Aiba

The major stratigraphic units in the study area are the lower basalt (Aiba basalt); the Alaje formation (the rhyolitic tuff, olivine-phyric basalt, rhyolitic ignimbrite, plagioclase-phyric basalt, aphyric basalt) and alluvial and reworked materials (Fig. 3.1).

3.2.1. Lower basalt (Aiba basalt)

The lower basalt is mostly exposed at a cliff face in the eastern and southeastern part of the study area, though small patches are also exposed in the southern and northern parts of the area. In the northern portion of the study area Aiba basalt is covered by thick the Aiba wet land soil though the wet land area is companied as Aiba basalt in the map provided (Fig.3.1). The lower basalt is underlain by the tilted basaltic layers of the Ashange Formation and overlain by the rhyolitic tuff of the Alaje Formation. The layers are massive, aphanitic and vesicular (Fig. 3.2.), and in many places affected by quartz

veining. In addition it is uniquely cliff-forming, where a maximum thickness of ~200 m is exposed at the North eastern and eastern part of the study area around the Ksad Gudo and Bolenta Georges locality respectively. This unit exposed in the Tsibet section is more massive and aphanitic. It is underlain by the tilted basalt of pyroxene-phyric, vesicular, and plagioclase-phyric basalts with high degree of alteration and weathering and overlain by yellowish rhyolitic tuff in this locality.

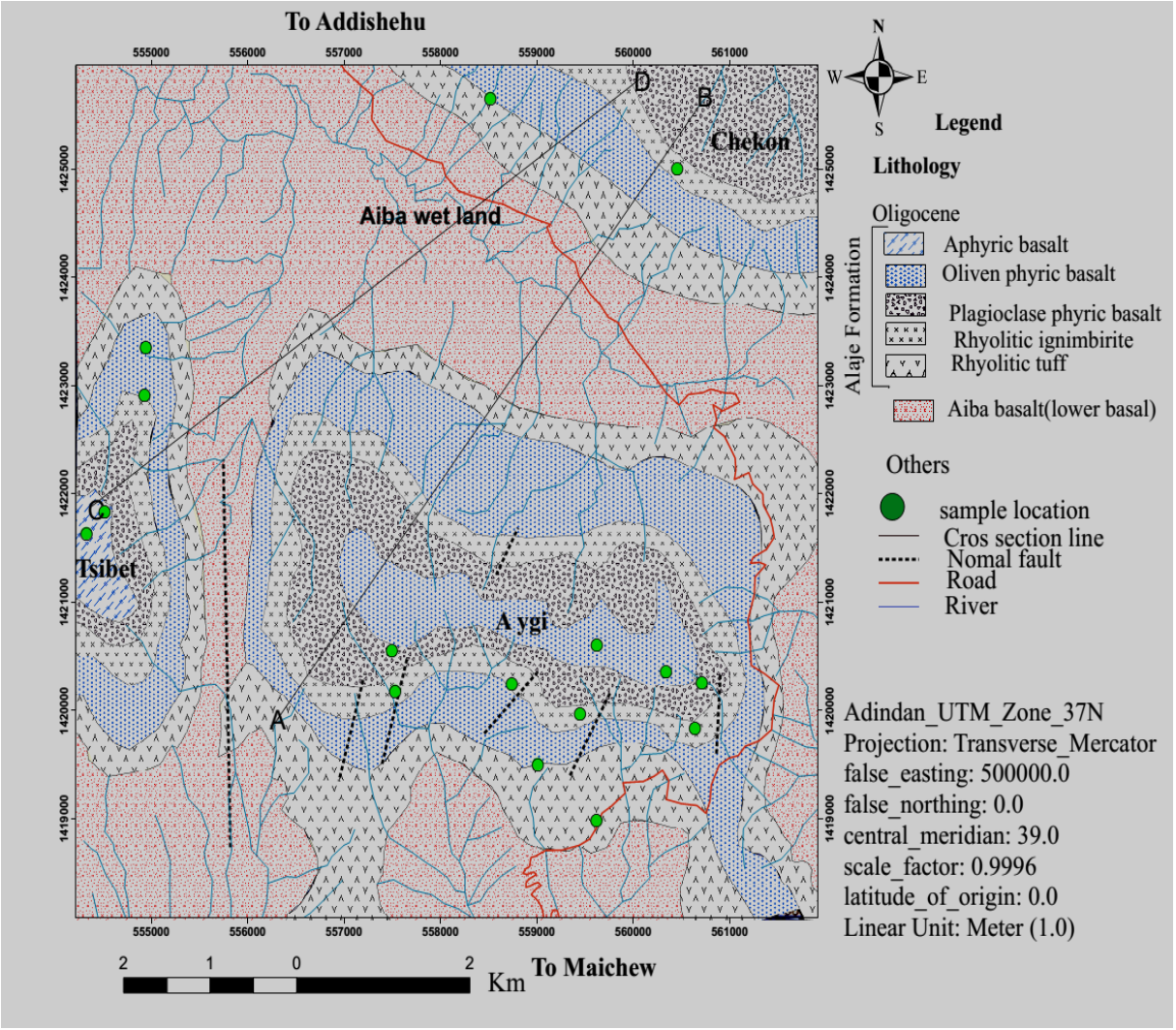
To Addishehu
555000
556000
557000
558000
559000
560000
561000
1425000
1424000
1423000
1422000
1421000
1420000
1419000
D
B
Chekon
Aiba wet land
C
Tsibet
A ygi
A
To Maichew
2 1 0 2 Km
N
W
E
S
Legend
Lithology
Oligocene
Alaje Formation
Aphyric basalt
Oliven phyric basalt
Plagioclase phyric basalt
Rhyolitic ignimbirite
Rhyolitic tuff
Aiba basalt(lower basal)
Others
sample location
Cros section line
Nomal fault
Road
River
Adindan_UTM_Zone_37N
Projection: Transverse_Mercator
false_easting: 500000.0
false_northing: 0.0
central_meridian: 39.0
scale_factor: 0.9996
latitude_of_origin: 0.0
Linear Unit: Meter (1.0)

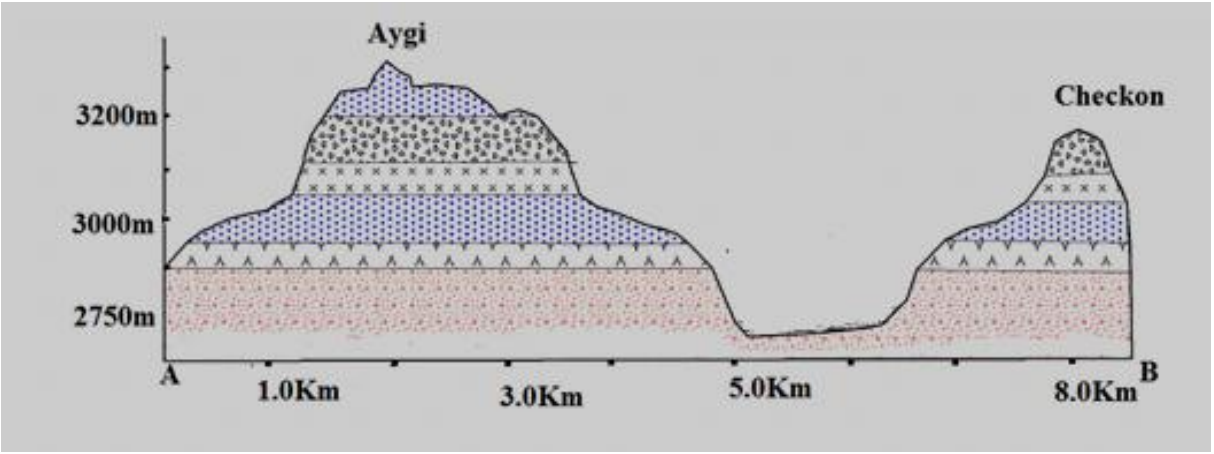
Aygi
Checkon
3200m
3000m
2750m
A
B
1.0Km
3.0Km
5.0Km
8.0Km

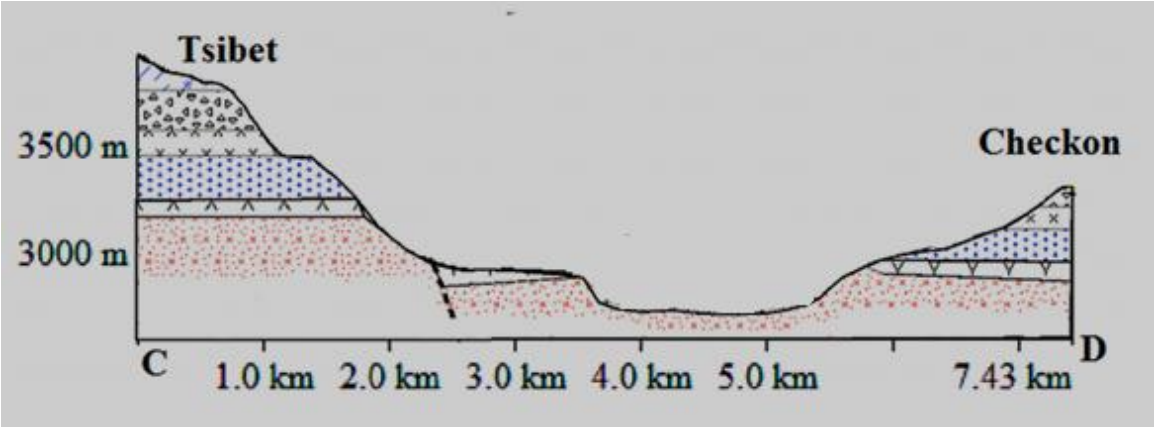

Fig.3.1. Geological map of Aiba area, and geological cross sections along line AB and CD On the geological map.

Fig.3.2.The Lower basalt (Aiba basalt), exposure in the eastern part of the Aiba area around Ksad Gudo.

3.2.2. Rhyolitic tuff

The rhyolitic tuff is the older unit of the Alaje formation overlaying over the Aiba basalt (lower basalt). It is composed mainly of quartz, alkali feldspar, and rock fragments. It is characterized by variegated color (yellow, greenish, to gray), fine- to coarse-grained, with alternating friable and compact beds of various thicknesses and colors, and highly altered, especially when friable (Fig. 3.3). The rhyolitic tuff at the Tsibet section is dominated by

rock fragments than the one at Aygi, and Checkon and it contains a 10m thick layer of welded pyroclastic rock inter-bedded within the friable rhyolitic tuff. This unit is affected by NE-SW trending parallel series of joints and normal faults mainly at the locality of the Belego Michael church. In the northern part of the study area, the rhyolitic tuff forms both layered and massive beds and dominated with coarse quartz grains. A layer of palaeosol separates the rhyolitic tuff from the overlaying olivine-phyric basalt in some places (e.g. North Belego Michael church).

Fig. 3.3. Rhyolitic tuff exposure at a road cut showing a coarsening upward layers, where moderately compacted and coarse layer is exposed at the top.

A moderately welded rhyolitic tuff layer, with 3-6 m variable thickness, is sparsely exposed in the middle levels of the rhyolitic tuff and at the lower levels of the rhyolitic ignimbrite (Fig. 3.4). These moderately welded rhyolitic tuffs are mainly exposed at the Belego Michael and Tsibet sections. These pyroclastic fall units have similar composition to the rhyolitic tuff however only vary by their degree compactness. It is mainly composed of quartz, alkali feldspar and generally large rock fragments, where the quartz is the most dominant component, and its colour ranges from dominantly yellowish to occasionally greenish.

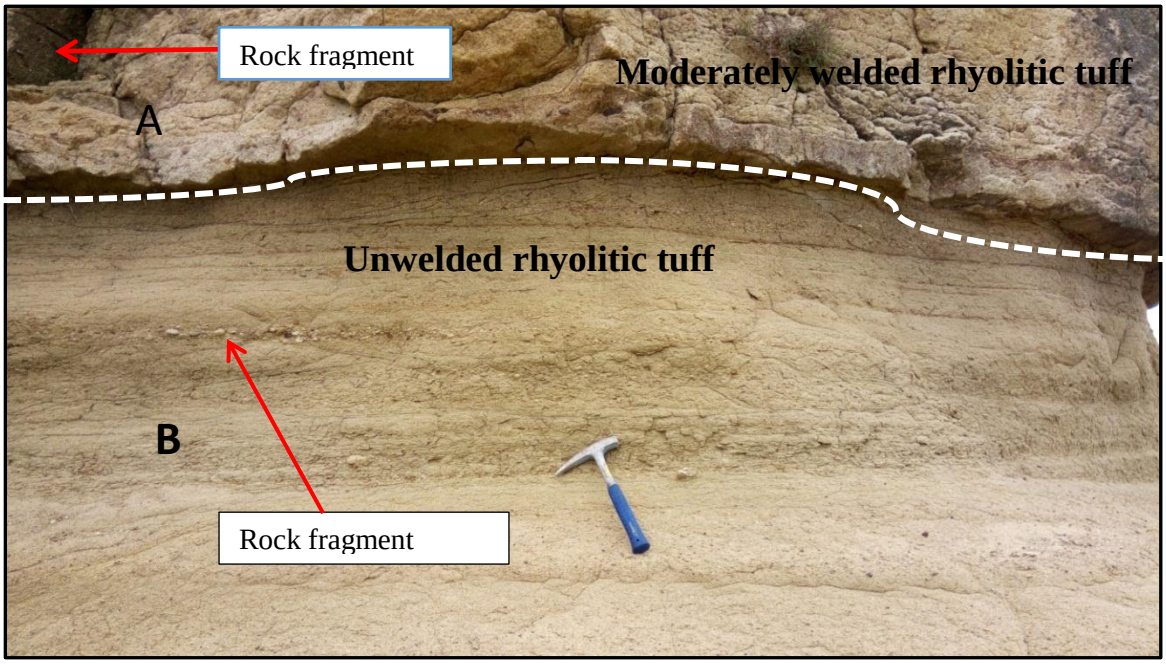

Fig. 3.4. A road cut exposure of succession of the rhyolitic tuff and the moderately welded rhyolitic tuff at the Belego Michael church section. The upper part of the photo (A) represents moderately welded rhyolitic tuff with rock fragment and the lower (B) shows the generally fine-grained rhyolitic tuff with scattered linear arranged small rock fragment.

3.2.3. Olivine-phyric basalt

The olivine-phyric basalt overlies the rhyolitic tuff and underlies the rhyolitic ignimbrite. This unit is composed of dark, olivine-phyric porphyritic basalts (brown to yellowish when weathered), exposed as rounded spheroidally-weathered and strongly altered boulders and cobbles, generally exposed on the gentle slope (Fig. 3.5). The average thickness of oliven-phyric basalts is ~150 m and have a clear sharp contact with the overlaying rhyolitic ignimbrites, while the lower contact is marked by a palaeosol layer, though it could not be traced elsewhere in most parts of the area, because of the soil cover above the contact zone due to the deep weathering and erosion of the olivine-basalt, which form a gentle agricultural slope at its foot. This basalt is also strongly altered and contains several secondary inclusions such as quartz. The oliven -phyric basalt has two distinct units separated by a layer of palaeosol and dark, friable lignite seams which can be traced throughout the area in the Aygi, and Tsibet sections in similar stratigraphic positions: a thinner around 40M thick pyroxene-phyric layer at the top and a thicker 110M thick, olivine thick layer at the bottom.

In addition a layer of dark strongly weathered an altered, cobble-forming, oliven-phyric basalt is also exposed at the upper levels of the Aygi area overlaying the plagioclase-phyric basalt marked with a palaeosol layer, and it is a flat forming topography.

Fig. 3.5. An exposure of olivine-phyric basaltic at the lower levels of the Aygi section. The spherical shape of the photo indicates the high degree of weathering with onion skin (exfoliation) type of weathering.

3.2.4. Rhyolitic ignimbrite

The rhyolitic ignimbrite is a strongly welded, cliff forming unit, laterally extended from eastern part of the study area to the west direction the study area and goes in to Bora area with a uniform thickness throughout. The rhyolitic ignimbrite unit is underlain by the olivine-phyric basalt and overlain by the plagioclase-phyric basalt unit at sharp contacts. The colour of the layer changes from greenish to yellow at the lower levels to gray towards the top. The degree of compactness increase from the lower levels less welded to the upper levels more welded relatively. The ignimbrites are composed of quartz, feldspar, obsidian and pumice fiammes, and large mafic rock fragments (Fig. 3.6). The upper most part of this unit contains a thin (5-7 m thick) layer of rhyolitic lava with clear flow banding.

Fig. 3.6. Highly discontinuous rhyolitic ignimbrite exposed at the Tsibet section, with prominent mafic rock fragments (greenish spots).

Throughout the whole area the rhyolitic ignimbrite grades to a fine-grained, strongly and visibly banded, strongly discontinuous, gray rhyolite lava flow (Fig. 3.7), with no visible rock fragments, and which laterally extends with uniform thickness of about 7m in all the logged section at(Tsibet, Checkon and Aygi). The Fig.3.7shows the discontinuity nature of the rhyolitic lava flow(A)and banding nature of the rhyolitic lava flow(B).the rhyolitic lava flow in the out croup differ from rhyolitic ignimbrite by texture ,discontinuity nature, and presence of banding nature while both are very compacted and resisting to weathering and alteration than the pyroclastic fall deposit lower part.

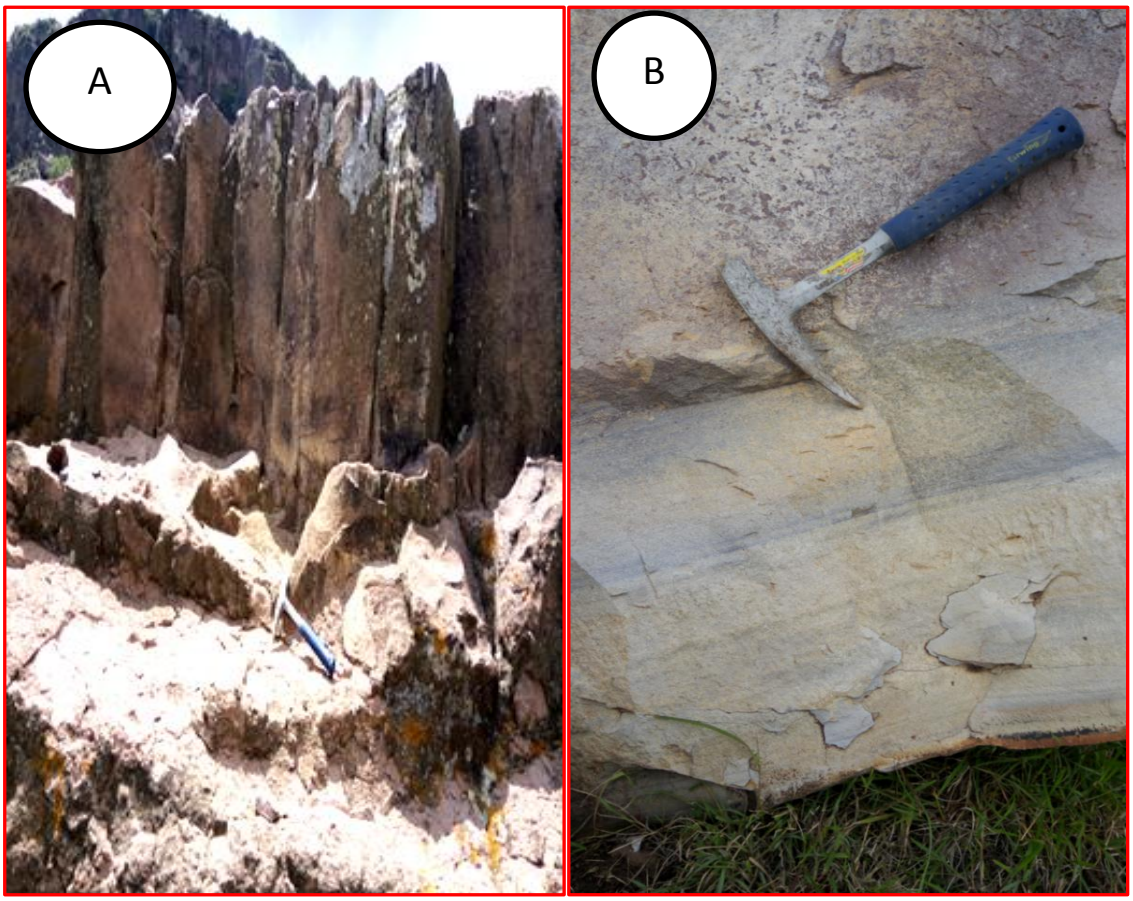

Fig.3.7. Rhyolitic lava at the Aygi section :(A) highly discontinuous rhyolite flows; and (B) banded rhyolite lava flow.

3.2.5. Plagioclase-phyric basalt

The dark colored plagioclase-phyric basalt is exposed overlies the rhyolitic ignimbrite and traced in the whole sections with an average uniform thickness of ~170 m. The upper contact is overlain by a layer of olivine phyric basalt separated with a palaeosol at the Aygi section while overlaying by the aphyric basalt at the Tsibet section without a marker bed of palaeosol unit. The surface geomorphology shows ropy flow nature in the Tsibet ridge however its broken surface is massive (Fig. 3.8). This outcrop unit is strongly weathered and altered by exfoliation weathering in the Aygi ridge while in the Tsibet section it is moderately weathered and altered. Secondary quartz and zeolite fillers are the common feature of plagioclase phyric- basalt due to its high degree of weathering and alteration. Therefore due to the accumulation of thick weather products on gentle slopes, this unit is used for agriculture for the local people.

Fig. 3.8. Plagioclase-phyric basalt exposed at the Tsibet section with ropy surface texture appearance.

3.2.6. Aphyric basalt

A very dark, aphyric, massive, and series of horizontally bedded basalt is exposed at the upper most levels of the Tsibet section (Fig. 3.9).The aphyric basalt is only found Tsibet ridge and missing other Aygi and Checkon rigde.The average thickness of this unit about ~260m and the thickness of the is individual flows is about ~15 m. The lower part of the unit is underlaying by more plagioclase phyric basalt and the contact is easily distinguishable with the surface geomorphology in the outcrop.

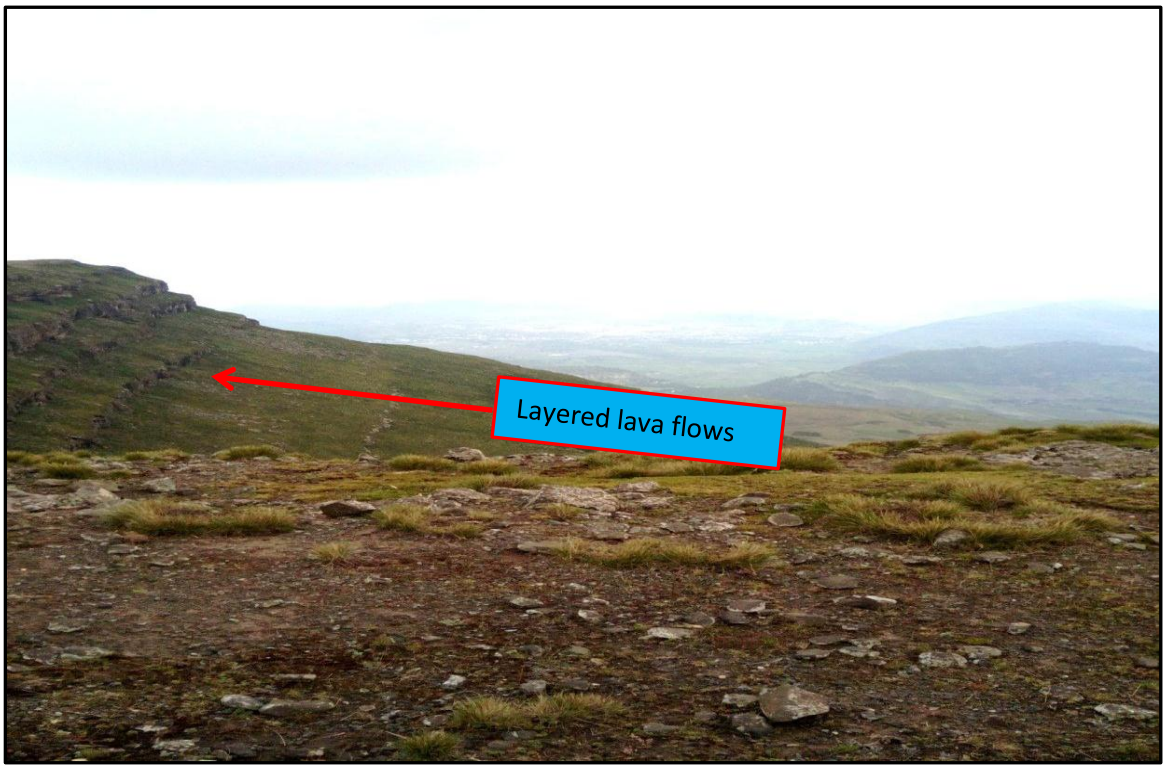

Fig.3.9. A distance views of an aphyric basalt ridge at the Tsibet section. The arrow indicates line of different thickness lava flow.

3.2.7. Palaeosol layers

Several 1 to 1.5 m thick palaeosol layers among the various units and marks as eruption gab in the different rock type and is not considered as major lithologic unit. in some cases it occurs between different layers of the same unit in the study area and in between layer of different unit (e.g. Fig. 3.10). The palaeosol are generally reddish to brownish owing to the leached and mature soil protoliths, and generally more compacted, welded, and baked at their upper parts than their lower part.

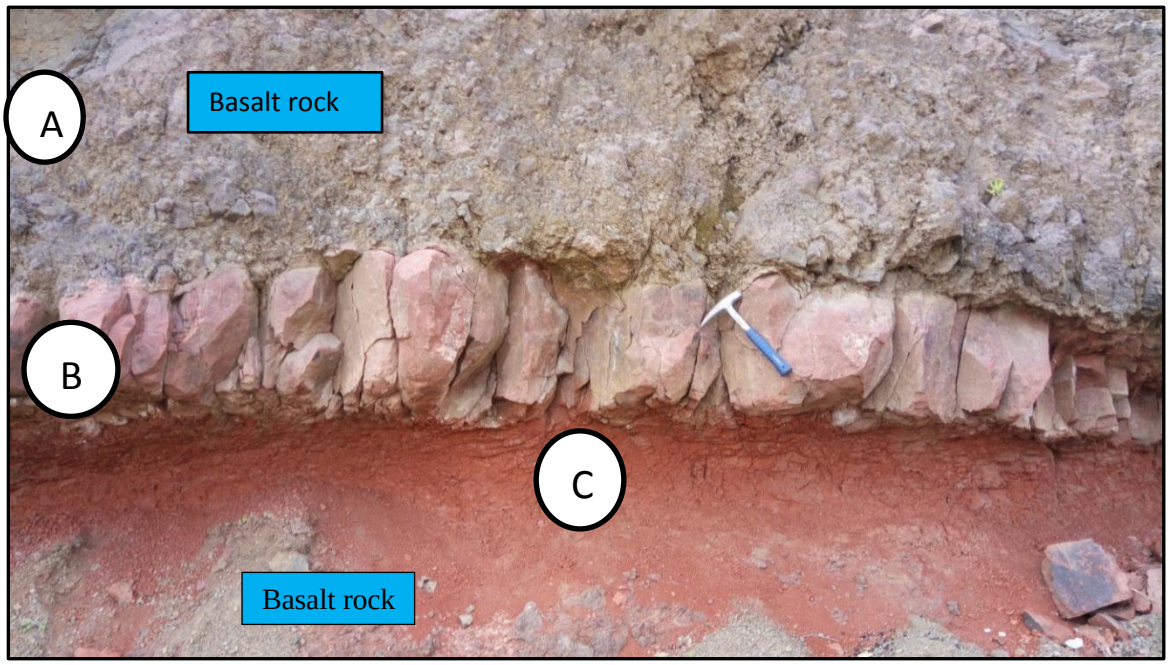

Fig. 3.10. A palaeosol exposure within the lower basalt, in the southern part of the study area. (A) Fine grained aphyric basalt; (B) highly compacted palaeosol; (C) friable, loose palaeosol.

3.2.8. Quaternary Alluvial and Colluvial deposits

The Aiba wetland valley and the adjoining gentle slopes at the northern part of the study area are filled by a thick deposit of colluvial and alluvial sediments produced by the weathering and erosion of the volcanic units on the adjoining ridges, and develop in-situ black soil. The foot hills at the southern side of the ridges are mostly covered by weathering products of the felsic rocks.

3.3. Geological structures

3.3.1. Contact relationships

Most of the contacts among the various volcanic units are sharp, though there are some gradational contacts within the same basaltic units. The contacts between the basaltic and rhyolitic units can be easily discerned at sharp boundaries, such as between the olivine-phyric basalt and the rhyolitic ignimbrite unit (Fig. 3.11) in many cases, the contacts among the different basalt units are marked by palaeosol layers.

Gradational contacts are less common in the area. The olivine-phyric basalt grades to a pyroxene-phyric basalt towards its top, and the rhyolitic ignimbrite grades to rhyolitic lava flow.

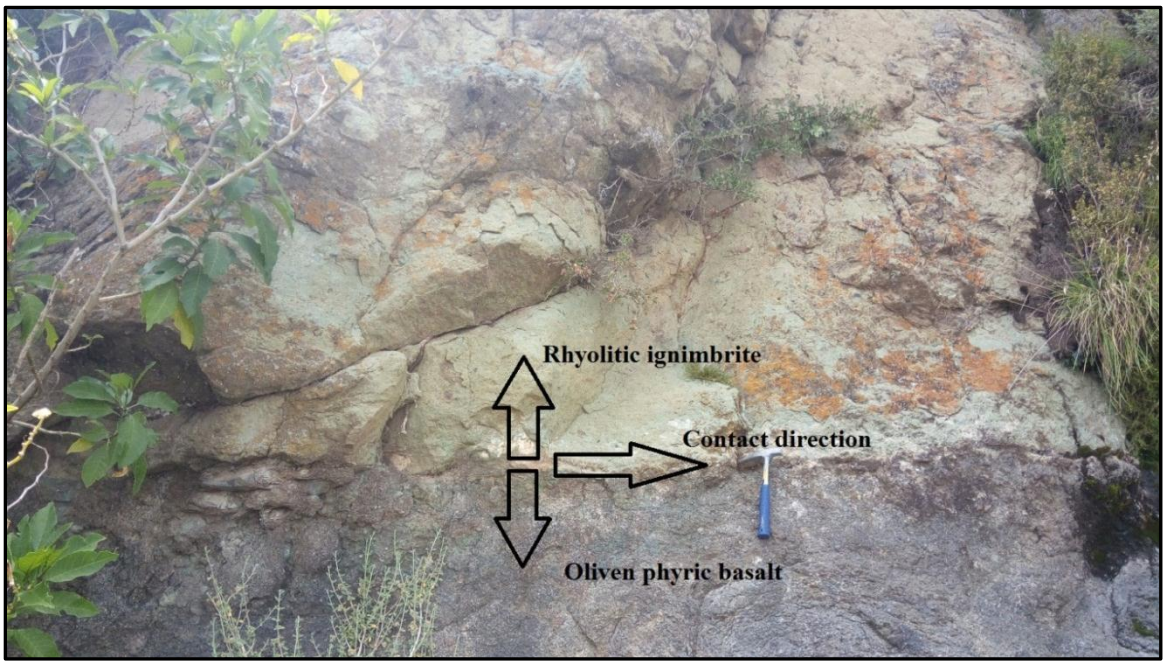

Fig. 3.11. A sharp contact between the friable olivine-phyric basalt and the rhyolitic ignimbrite.

3.3.2. Layering

The rhyolitic tuff is characterized by prominent horizontal bedding (Fig. 3.12). The basaltic units at the Tsibet section are also horizontally bedded lava flow. In most cases, particularly at the rhyolitic rocks, the beds are affected by discontinuities and subsequent weathering.

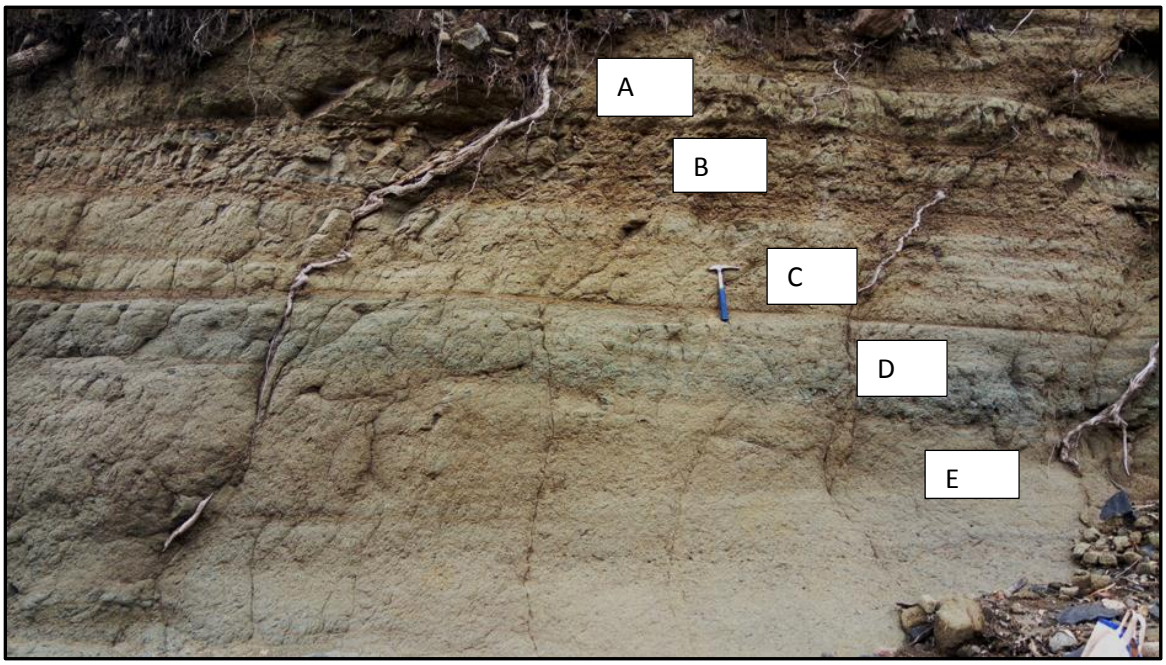

Fig. 3.12. Layers of different thickness ranges from centimeter thickness up to one meter thickness of rhyolitic tuff unit. Each layer is varying in thickness, grain size and color.

3.3.3. Normal Faults and joints

A series of NE-SW oriented faults affect the volcanic units, particularly the rhyolitic ignimbrite (Fig. 3.13). The normal faults have a general orientation which is consistent with the regional trend of the faulting in the Ethiopia rift system and with nearby marginal graben of trending from Mohoni to Alamata and kobo. Similarly oriented (NE-SW) joints and fractures affect the rhyolitic tuff unit and the basaltic rocks (Fig. 3.14). Most of the joints in the rhyolitic rocks are unfilled, while those in the basalts are filled by secondary materials such as quartz veins. The jointing and fracturing is more prominent in the southwestern part of the study area particularly in the rhyolitic tuff Belego Michael, while the joints in the northern part are mostly common on the basaltic units.

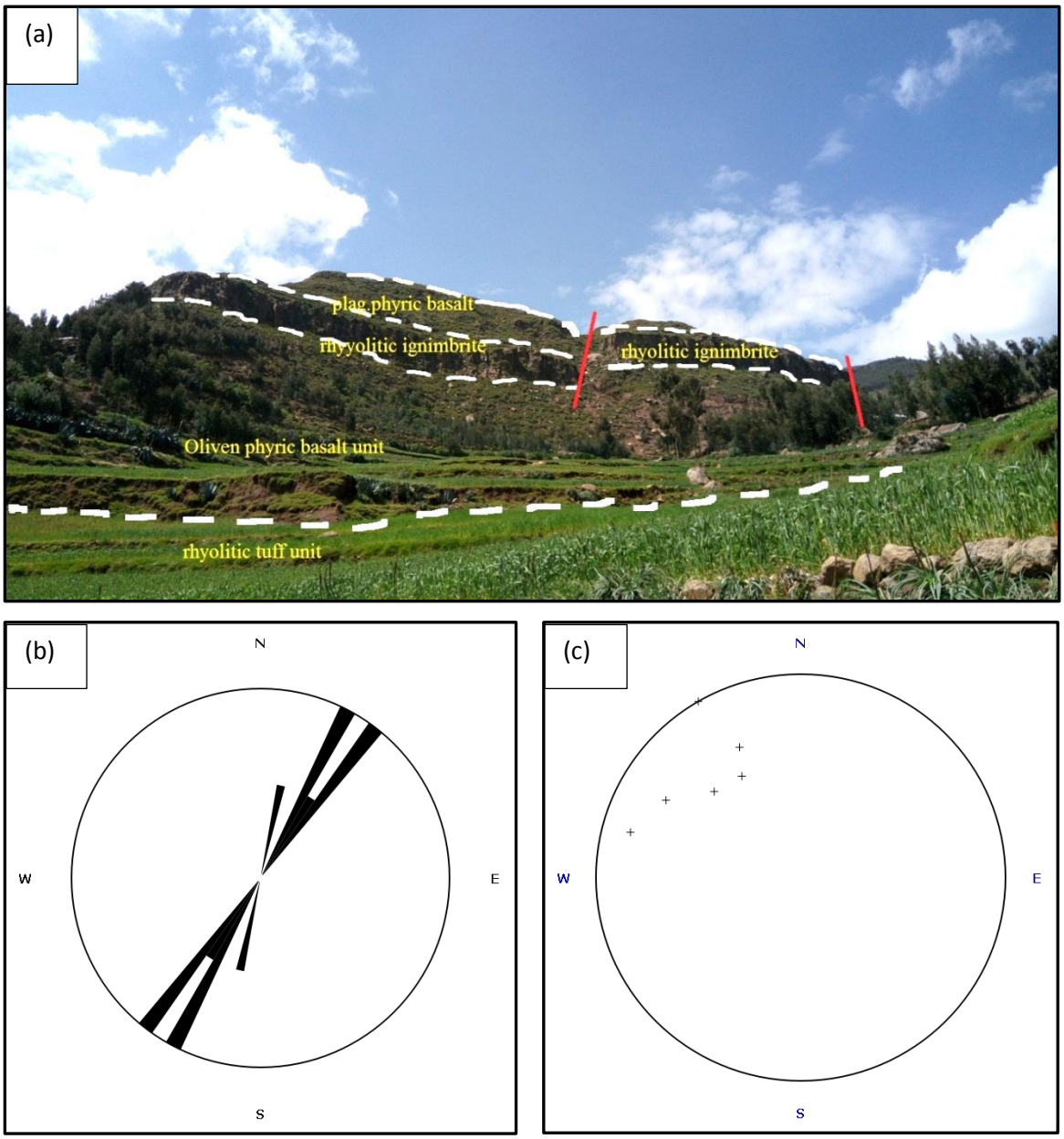

Fig. 3.13. (a) Series of normal faults affecting the volcanic units, particularly the rhyolitic ignimbrite at the Aygi section; red lines are the fault traces and dashed white lines are the lithological contacts; (b) Rose diagram of fault orientations, with the longest wedge of the rose diagram (the major trend) oriented at N30°E to N35°E ;(c) stereonet plot show pole concentrated on the NW and represents SE dipping of the faults.

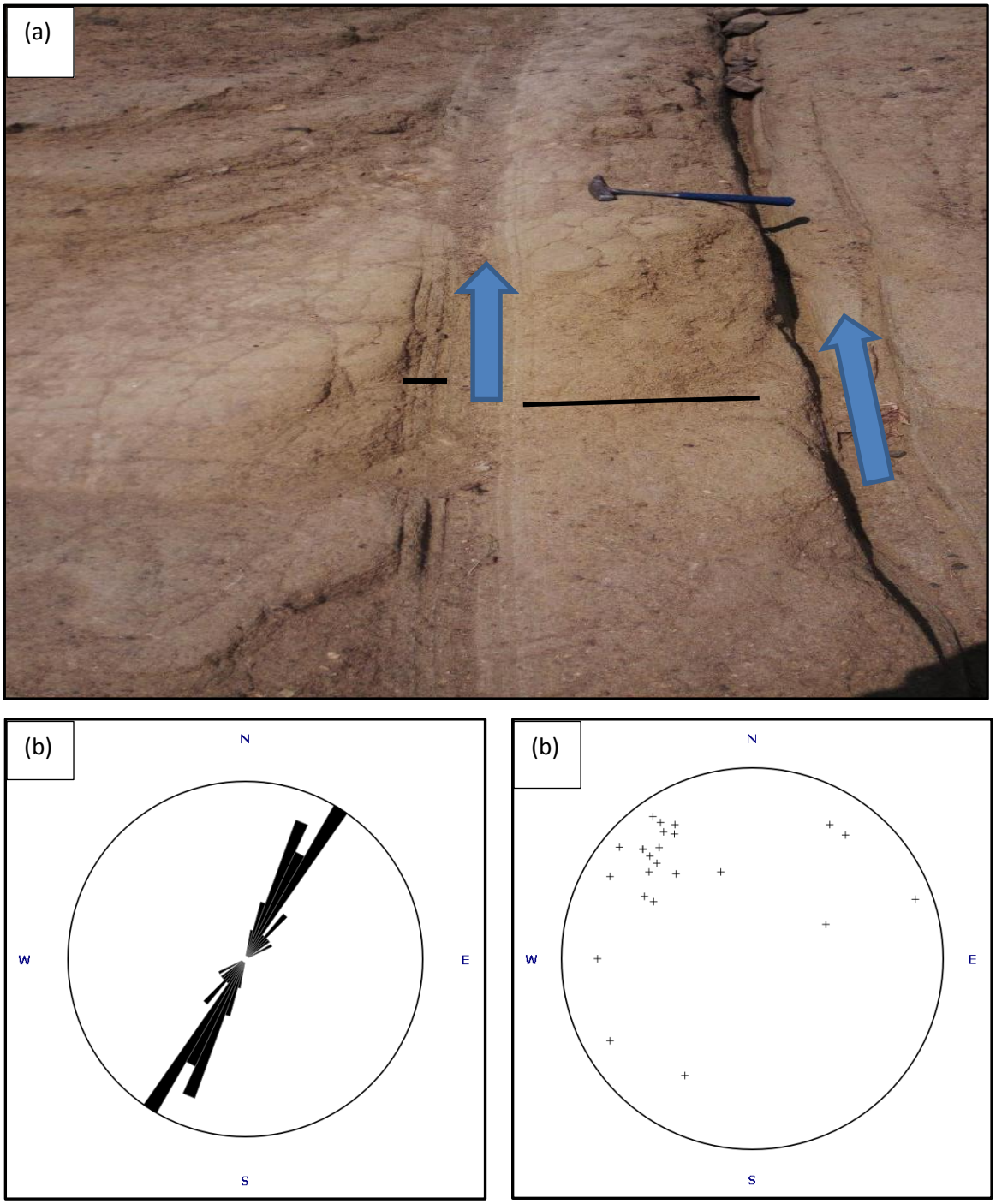

Fig. 3.14. (A) A jointed rhyolitic tuff at the Belego Michael area. Joint spacing ranges from few cm to 1m(black line) and the arrow indicates joint orientation; (B) Rose diagram of joint orientations, with the longest wedge of the rose diagram (the major trend) oriented at N20°E to N25°E;(c) c)stereonet plot show pole concentrated on the NW quadrant and represents SE dipping of the joints

3.5. Correlation of the three sections

The logged sections, though found at different elevations, show similar stratigraphic successions and similar thickness of the individual units. However few lithologic layers are missing in one or another section due to erosion and faulting (Fig. 3.15). There are also some lateral variations in texture in some of the units. A 10m thick welded rhyolitic ignimbrite layer within the rhyolitic tuff unit and the aphyric basalt at the top of the Tsibet section are not represented in the Aygi and Checkon sections. In addition presence of oliven phyric basalt in the Aygi section though missing in the other section.

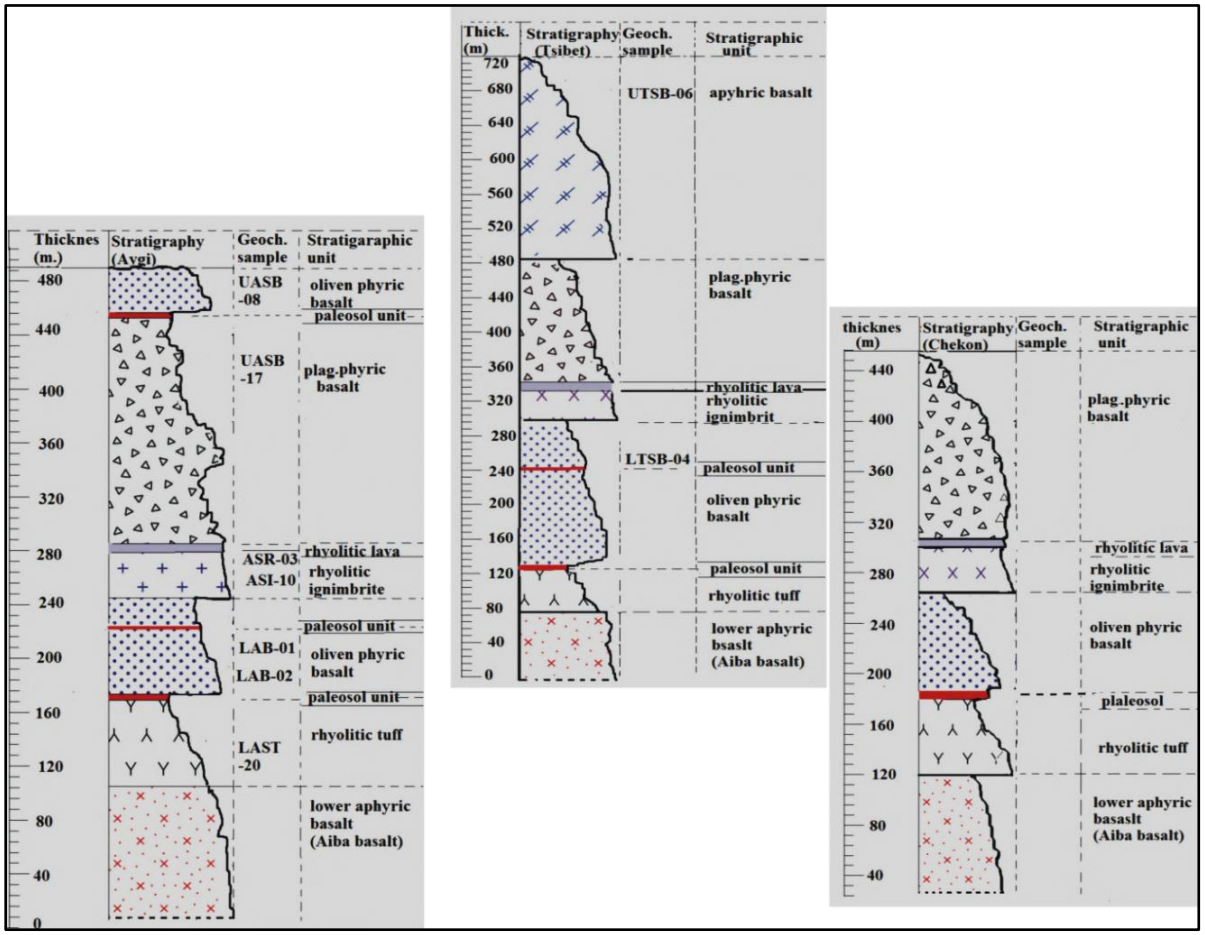

Fig. 3.15. Stratigraphic correlation of basalts and rhyolite of the three sections in the Aiba area. The palaeosol are simply to show contact but their thickness is not drawn based on the scale of major unit.

CHAPTER FOUR
PETROGRAPHY

4.1. Introduction

Most of the analyzed basalts are variably porphyritic with total phenocryst content up to 20% although some are aphyric to sub-aphyric with microphenocrysts, while the rhyolitic tuff and ignimbrite contains large rock fragments. A total of 16 samples were selected from all the basaltic and rhyolitic rocks based on the petrological variation observed in the outcrop level, stratigraphic and the percent of rock fragment in the felsic rocks. The thin sections were prepared from these samples at the Geological Survey of Ethiopia, and studied at the School of Earth Sciences, AAU petrology laboratory. Among the thin section analyzed 7 of them are rhyolitic (3 rhyolitic ignimbrites, 3 rhyolitic lavas, 1 rhyolitic tuff) and 9 basalts from the different stratigraphic levels. The rhyolitic rocks are composed of quartz, alkali feldspar, volcanic glass, rock fragment, plagioclase feldspar, Fe-Ti oxides minerals, and small amounts of clinopyroxene. The common phenocrysts in the basaltic units are plagioclase, clinopyroxene, Fe-Ti oxide and very few Olivine. All the rhyolitic lava and rhyolitic ignimbrites show clear flow banding with large phenocrysts of alkaline feldspar minerals embedded within the glass flow. The basaltic rocks at the lower levels are porphyritic while those towards the intermediate and top levels (for instance, of the Tsibet section) are more aphyric.

4.2. Basaltic units

4.2.1. Olivine - phyric basalt

The olivine phyric basalts exposed at the lower levels of the Alaje formation, contain more prominent olivine phenocrysts than the oliven phyric basalt at the upper levels of the Aygi section. Olivine phenocrysts are the dominant phenocrysts with small amount of clinopyroxene in the former while phenocrysts of olivine, clinopyroxene, and plagioclase, in almost equal proportion are dominant in the latter, with some Fe-Ti oxides, all set in fine-grained matrix. While the proportion of Fe-Ti oxide is more prominent in the upper Aygi section basalt than the lower one. The olivine are highly altered and affected by randomly oriented fractures filled by greenish to yellow intra-fracture mineralization (Fig. 4.1).

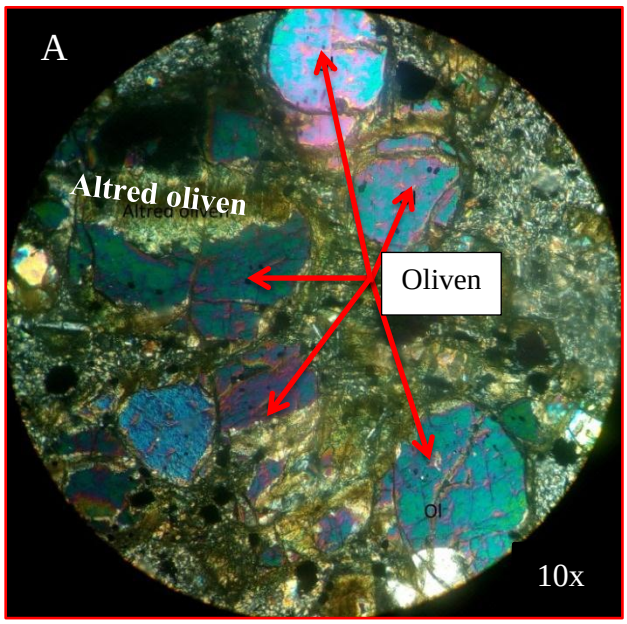

(A) Is a field of view almost is covered by olivine phenocrysts; while (B) field of view shows olivine, clinopyroxene, and plagioclase phenocrysts in a fine-grained matrix of plagioclase, clinopyroxene, and Fe-Ti oxide. Olivine is euhedral and reaches up to 3mm x 1mm size. The modal proportion of phenocrysts in (A) is 100% olivine, with few micro phenocryst Fe-Ti oxides and matrix of clinopyroxene and plagioclase

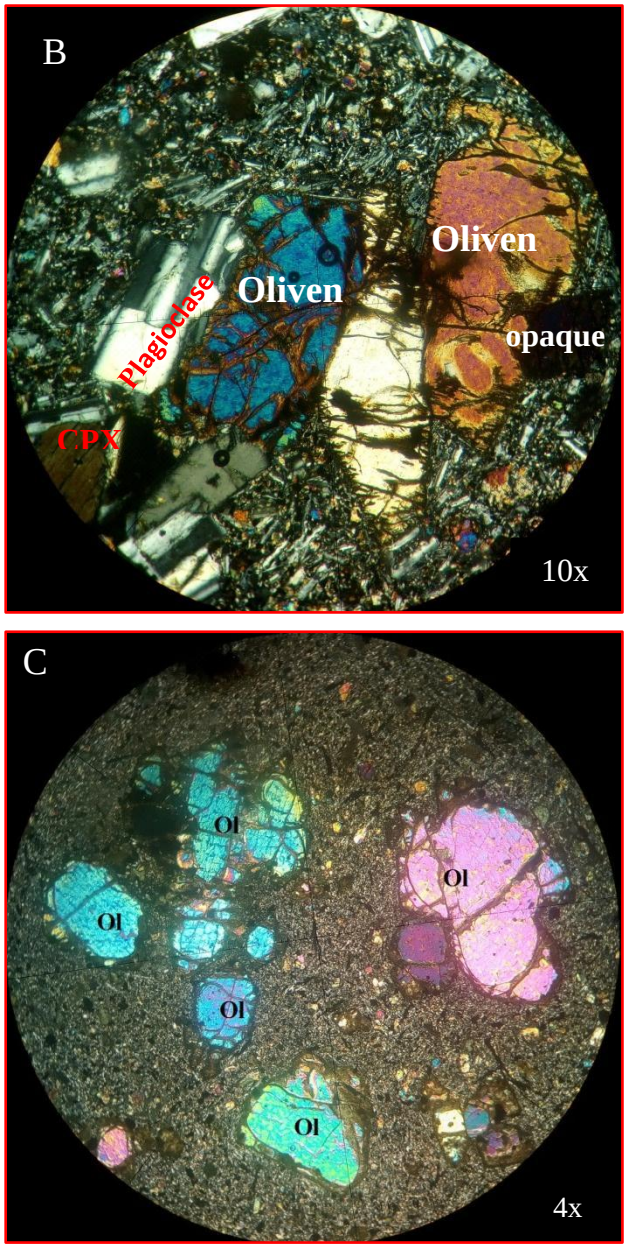

are dominantly covered. Field of view (B), covers phenocryst of 60% Olivine, 20% plagioclase and 20% clinopyroxene, while the proportion of the matrix is nearly 40% plagioclase, 30% clinopyroxene, 20% is olivine and Fe-Ti oxides; (C) 100% olivine phenocryst. With very fine matrix of plagioclase, Clinopyroxene, Fe-Ti oxide and oliven. In general field of view (A) and (C) are covered with very large phenocryst and two of the are from the lower Aygi section oliven phyric basalt with different magnification. While (B) is from the Upper Aygi section and it less covered by oliven phenocryst, have more plagioclase and Fe-Ti oxide mineral.

Fig. 4.1. Photomicrographs of thin sections of the olivine-phyric basalt; XPL view and 10x magnification in A and B and 4x in C. A&C are from the lower Aygi section and whereas B is from the upper Aygi section. Ol: olivine, Cpx: clinopyroxene.

4.1.3. Plagioclase-phyric basalt

Plagioclase-phyric basalt is less porphyritic (<15% phenocrysts) compared with the lower basalt while it is more porphyritic compared to the upper Tsibet section basalt. The common phenocrysts in this unit are plagioclase, clinopyroxene, and Fe-Ti oxides, and few oliven, while the most dominant is plagioclase (about ~90% of all phenocrysts), which shows some chloritization along fractures. In the studied thin section from this unit

plagioclase accounts 60%, olivine and pyroxene 20%, while Fe-Ti oxides 20%. The olivine is nearly completely altered leaving ghosts.

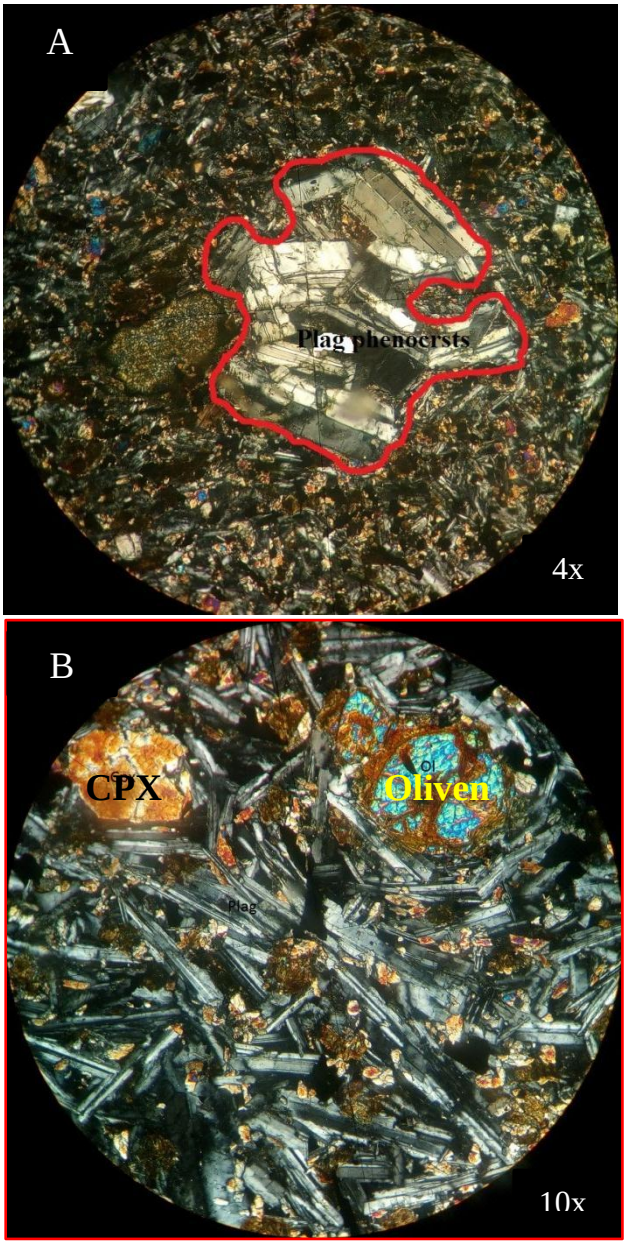

These thin sections are prepared from the same unit and but different rock samples. In both samples, the dominant phenocrysts are: plagioclase (50%), clinopyroxene (30%), and Fe-Ti oxides (20%) in this selected field of view. Plagioclase is elongated with 4mm x 1mm size. Olivine and clinopyroxene are more rounded and have up to 2mm diameter. While the matrix is generally constituted by: plagioclase (40%), clinopyroxene (25%), Fe-Ti oxides (25%) and olivine (10%).

As indicated in (A) field of view plagioclase shows glomerphorphritic texure. The Lower photo in figure (B) in the right upper corner it shows fracture olivine and left upper corner fractured and altered clinopyroxene and it is nearly plagioclase dominated.

Fig. 4.2. Photomicrographs of thin sections of the plagioclase-phyric basalt; XPL view and 4x magnifications in A and 10x in B and both are from Aygi section. Cpx: clinopyroxene.

4.1.4. Aphyric basalt

The aphyric basalts contain randomly oriented plagioclase microphenocrysts with glomerporphyritic texture, and high accumulation of Fe-Ti oxides, which are only visible in high magnifications (Fig. 4.3).Generally it is matrix dominated (~95%) and only about 5% plagioclase phenocrysts. The rocks are hardly altered. The aphyric basalt is more fractionated than the other basaltic units, containing 30% plagioclase, 20% clinopyroxene, 15% olivine and 35% Fe-Ti oxides minerals. Plagioclase and clinopyroxene phenocrysts are usually clustered and generally elongated.

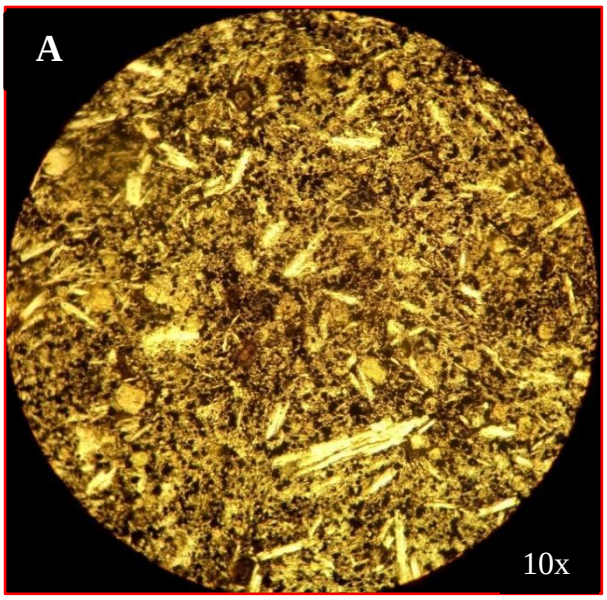

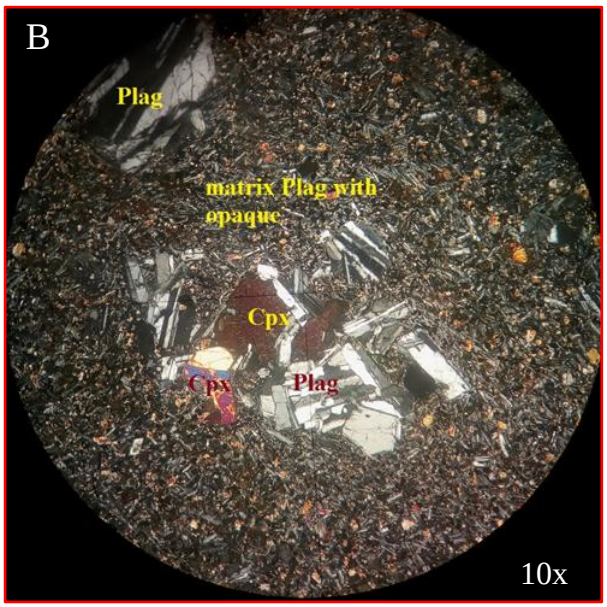

In field of view (A,B, and C) shows aphyric texture, with nearly equal proportion of plagioclase, pyroxene, olivine and opaque minerals. Lath-shaped, with 2mm x 0.5mm, randomly oriented plagioclases, and more rounded olivine are common. The modal proportions are 35% plagioclase, 25% clinopyroxene, 25% Fe-Ti oxides and 20% olivine. (B) Shows accumulation of plagioclase phenocrysts within fine matrix of clinopyroxene, Fe-Ti oxide, and plagioclases forming cummulo-porphyritic texture.

All the thin section (A, B and C) are only studied at high magnifications 10x while under this magnification still it is fine and microphenocrysts dominated.

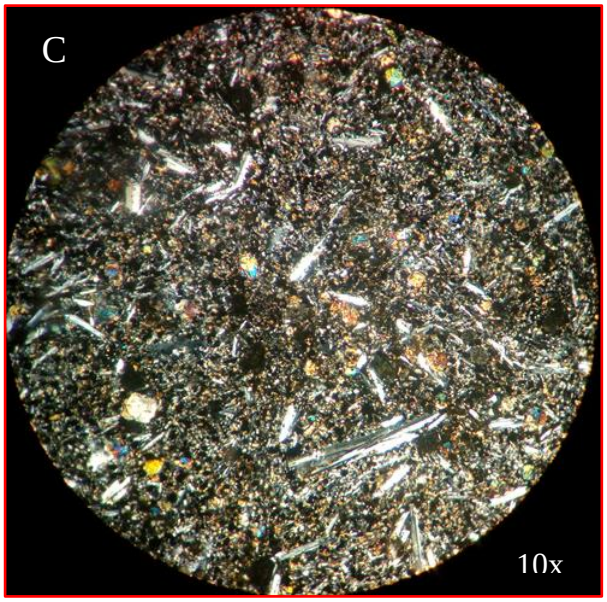

Fig. 4.3. Photomicrographs of thin sections of the aphyric basalt from the upper levels of the Tsibet section; PPL view and 10x magnification in A and XPL view and 10x magnification in B and C. Plag: plagioclase; Cpx: clinopyroxene.

4.2. Rhyolitic rocks

4.2.1. Rhyolite tuff

Rhyolitic tuff (Fig. 4.4) is generally more crystal rich and composed of randomly oriented, sanidine, quartz, plagioclase, orthoclase, clinopyroxene, Fe-Ti oxides, and appreciable amount of large rock fragments with volcanic glass. While the volcanic glass are does not show any flow nature and recrystallization features like in the rhyolitic ignimbrite and rhyolitic tuff. The mineral abundance decreases from volcanic glass, sanidine, quartz, Fe-Ti oxide, to clinopyroxene respectively. Some of the Fe-Ti oxides are embedded in the pyroxenes. The possible order of crystallization of the minerals is Fe-Ti oxides, clinopyroxene, plagioclase, alkali feldspar and quartz. Both alkali feldspar and clinopyroxene has simple twinned. The feldspars are highly altered and show sieved texture.

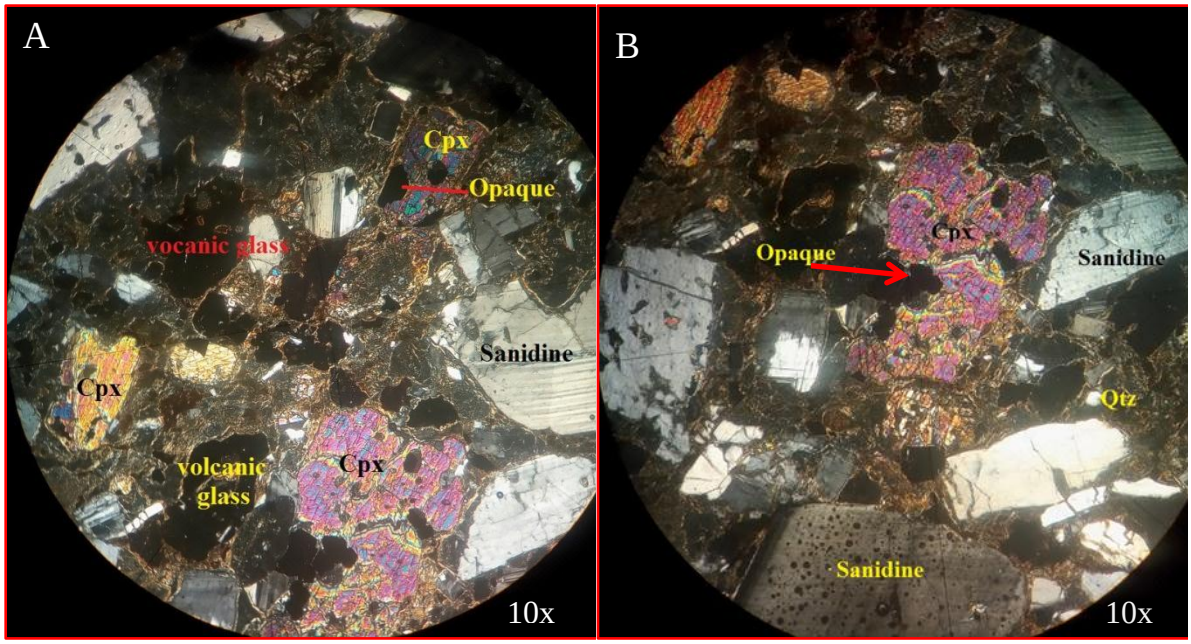

Fig. 4.4. Photomicrographs of thin sections of unwelded rhyolitic tuff from Aygi section. XPL view and 10x magnification. Altered alkali feldspar and Cpx are partially removed due to weathering (B). Cpx: clinopyroxene; Qtz: quartz.

4.2.2. Rhyolitic ignimbrite

The rhyolitic ignimbrite is slightly porphyritic to porphyritic, and composed of volcanic glass which shows flow banding, sanidine, quartz, plagioclase, lithic rock fragments, Fe-Ti oxide, and small amount of clinopyroxene (Fig. 4.5).Typically the feldspars (alkali and plagioclase feldspar) shows simple twining while the clinopyroxene both show simple twining and clear zonation, though both plagioclase and clinopyroxene are strongly altered. The rock fragments are composed of up dominantly of plagioclase and altered clinopyroxene. The order of mineral crystallization is the same to that of the rhyolitic tuff and the rhyolitic lava flow. The quartz show some deformation resulting in sharp edges and the alkali feldspars are cloudy and sieve-textured, and in some cases spherulitic texture with aggregate of minerals radiating from a common center are shown on the recrystallized glass.

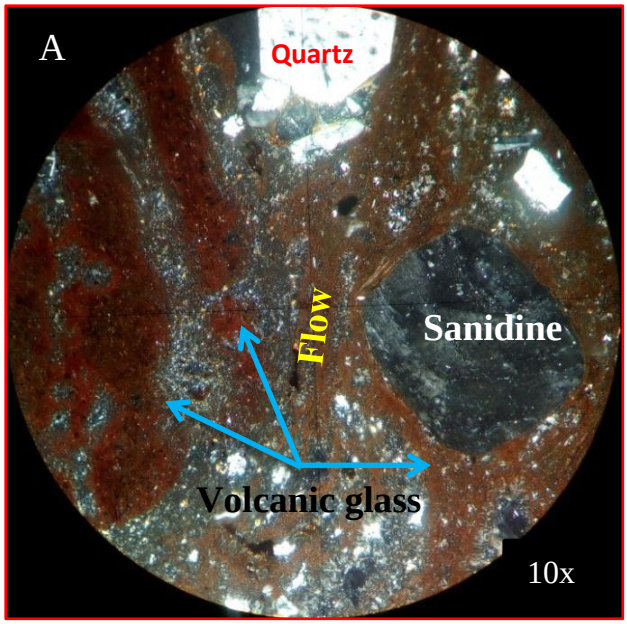

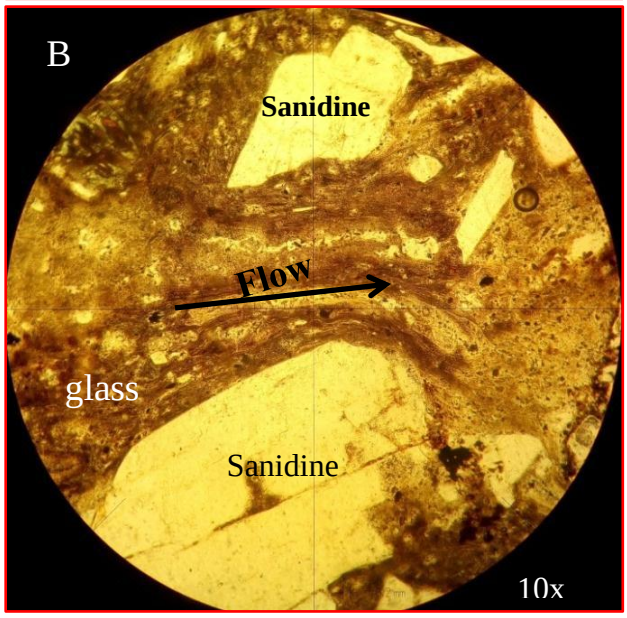

Representative field of view (A, B, and C) are show form the rhyolitic ignimbrite. While sanidine mineral is the common mineral in all the field of view. Quartz is euhedral, 2mm x 0.5mm in size. The glassy matrix shows flow banding. The common phenocrysts are sanidine, quartz, Fe-Ti oxide, clinopyroxene within volcanic glass matrix. The sanidine is twinned (C), and the dark brown volcanic glass shows flow banding around the sanidine in all (A,B, and C).

Generally thin section 'A' and 'C 'are more glass dominated and they shows strong welded. Photo 'A and B' is shows more flow nature and more brownish color than 'C'.

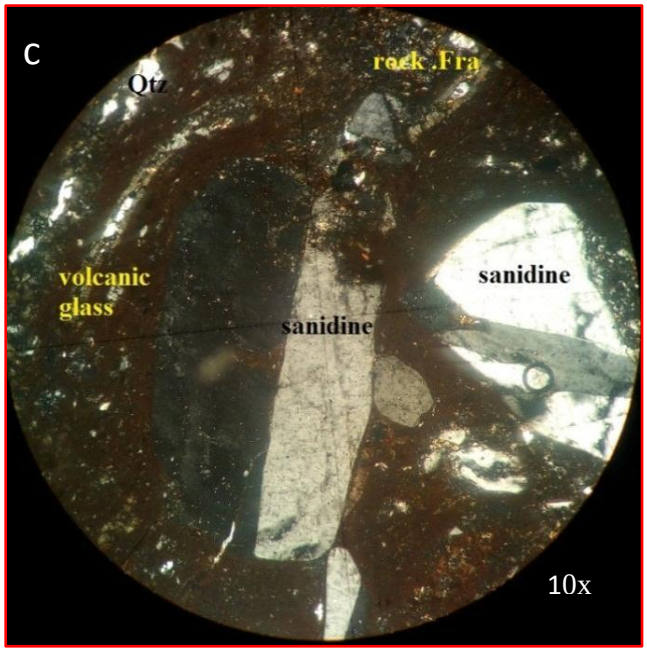

Fig. 4.5. Photomicrographs of thin sections of the rhyolitic ignimbrite from the Aygi section (A and C) and the Tsibet section (B); XPL view and 10x magnification (A and C); PPL view and 10x magnification (B).Qtz: quartz, Fra: fragment

4.2.3. Rhyolitic lava

The rhyolitic lava is aphyric to spary porphyritic and comprises volcanic glass, sanidine and quartz, small proportion clinopyroxene, rare plagioclase and few rock fragments. Nearly all the minerals are embedded within the volcanic glass. The order of crystallization is Fe-Ti oxide, clinopyroxene, plagioclase, Sanidine, quartz, and glass. The glass shows increasing recrystallization from the rim to the center (Fig. 4.6). The recrystallized glass shows a star shaped extinction. The distinct feature of this rock is the presence of very clear flow banding, dominant volcanic glass with high amount of Quartz. The quartz and feldspars are also strongly altered resulting in resolved, and fractured grains, and in spot-textured surfaces on the feldspars. Most of the plagioclase are nearly completely altered leaving ghosts.

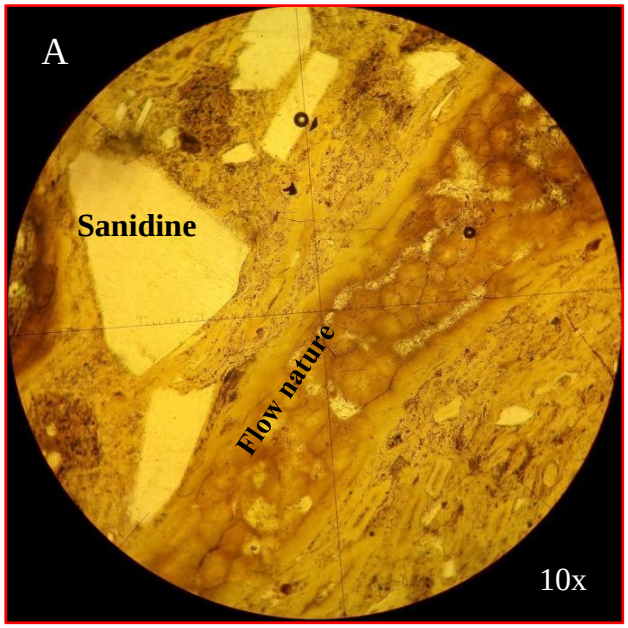

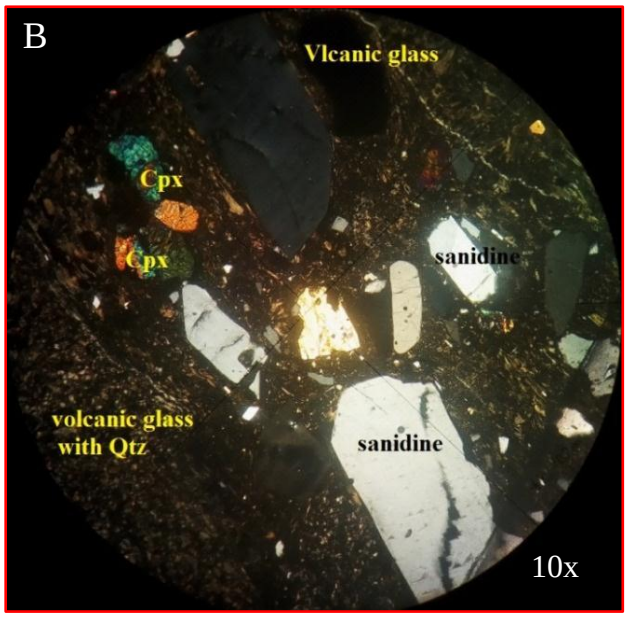

Representative selected field of view from the rhyolitic lava from Aygi and Tsibet section. Field of view (A) and (C) show clear flow around large alkali feldspars. Sanidine phenocrysts are as big as 3mm x 1.5 mm. (B) shows clinopyroxene in the left upper part and Fe-Ti oxide embedded within it and it is more glass dominated, have high proportion of sanidine mineral than (A and C).

The common phenocryst observed in (B) is volcanic glass, Sanidine, clinopyroxene and Fe-Ti oxide minerals.

(C) The recrystallized and fractured flow show radiating texture from a common center.

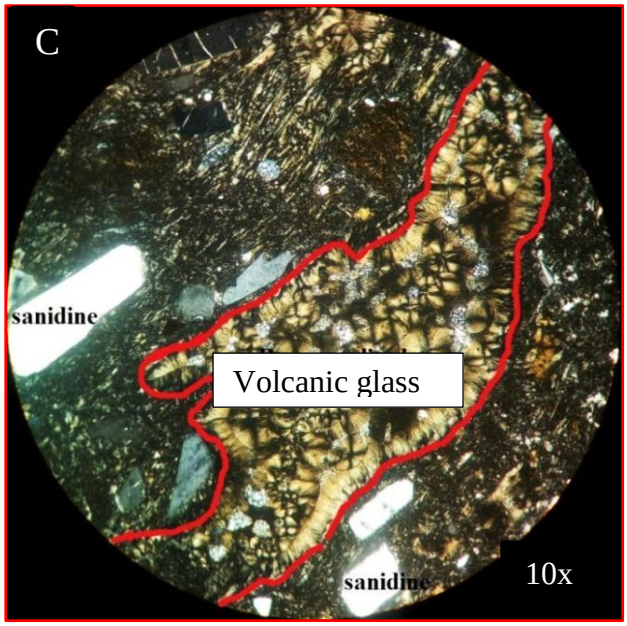

Fig. 4.6. Photomicrographs of thin sections of the rhyolitic lava from the Aygi and Tsibet sections; and shows the vein development in A and C. (A) PPL view and 10x magnification; XPL view and 10x magnification (B and C).

4.3. Petrographic relationships

4.3.1. Basalt units

The basaltic rocks of the Alaje formation show some textural and compositional variation, followed by plagioclase, clinopyroxene, Fe-Ti oxide, and olivine mineral phenocryst assemblage. The lower basaltic unit is more olivine phenocrysts dominated, the basalt above the rhyolitic ignimbrite unit is more plagioclase and pyroxene dominated, while the upper basaltic unit exposed at the Tsibet section is aphyric and comprises of more Fe-oxides, possibly indicating more fractionated basalts, compared to the older basalts. The Clinopyroxene, plagioclase and Fe-Ti oxides minerals show wide range of fractionation from the basaltic to the rhyolitic units with decreasing their modal proportion from basalt to rhyolite. The olivine phenocrysts are limited to the basaltic units only. The high amount of zoned clinopyroxene (Ca-rich and Ca-poor) and Fe-Ti oxides and small amount of olivine in the basaltic rocks, particularly in the upper part of Tsibet section, and the presence of plagioclase phenocrysts in all the suites, and its association with sanidine in the rhyolitic suites, indicates the tholeiitic characteristics of the basalts.

In generally, Most of the thinscetion analyzed in basaltic rocks of the study area is plagioclase dominated phenocryst and followed by, clinopyroxene, Fe-Ti oxide and few oliven and this assemblage suggested that the low pressure crystal fractionation process and most are porphyritic texture. With the exception of upper stratigraphic section of Tsibet which is aphyric with micro phenocrysts of oliven, plagioclase, and Clinopyroxene and Fe-Ti oxide.

4.2.2. Rhyolitic units

The petrography of both the lower and upper rhyolitic units and different stratigraphic section is nearly the same. However, the upper rhyolitic lava is significantly different from the rhyolitic tuff and rhyolitic ignimbrite, where the lava flow is less porphyritic, contains more quartz and rare rock fragments, and shows clear flow banding even though the rhyolitic ignimbrite also shows flow banding. These are possibly suites of rhyolitic lava flow, ignimbritic flow and rhyolitic fall.

CHAPTER FIVE
GEOCHEMISTRY

5.1. Sample preparation and analysis

Samples for geochemical analysis were selected based on stratigraphic position, field petrological variations, and petrographic characteristics, and based on the proportion of rock fragments and degree of alteration for the rhyolitic rocks. Among the 16 samples analyzed petrographically, 10 samples (6 basaltic and 4 rhyolitic rocks) were analyzed for major and trace element geochemistry. These samples were crushed and milled into powders at the Ethiopian Geological Survey. Whole rock major and trace element geochemistry of the samples has been determined at the Analytical Testing Services (ALS, Ireland). Major elements were analyzed using Multi-Element Inductively Coupled Plasma-06 (ME-ICP06) whereas trace elements were analyzed using Multi-Element Mass Spectrometry-81 (ME-MS 81) techniques. Trace elements including the full rare earth element suites are reported from three digestions with either ICP-AES or ICP-MS finish: a lithium borate fusion for the resistive elements, a four-acid digestion for the base metals, and an aqua regia digestion for the volatile gold related trace elements. The detection capacity of the method ranges between 0.01 and 100% for major elements and generally 0.01 to 10,000 ppm for trace elements except for Cr (10 - 10,000ppm) and V (5 - 10,000ppm).

Among the 10 samples analyzed for major and trace element geochemistry 9 of them have loss on ignition (LOI) between 0.04-2.61 % while. The 2.61% LOI is with the more porphyritic sample (LAB-01). The range of LOL for the rhyolite rocks is low it ranges from 1.39-1.75% .However, one rhyolitic sample has anomalous high LOI of 15% and it is discarded during classification and interpretation. The major element percentages are recalculated to LOI-free base and the classification diagram is based on the recalculated value. Finally Petrograph 2 beta and GCDKit 3.00 are used for these geochemical diagrams and Microsoft Excel 2010 for trace element ratio calculations.

5.2. Results

The geochemical data (major and trace element data) are given in (Table 5.1 and Table 5.3). As shown in these Tables, the basalt of different stratigraphic unit shows similar geochemical result and same also for the rhyolitic rock suites. Furthermore, most of the basaltic rock are fractionated with low Mg# <55.56, low concentration of compatible elements (e.g., Ni: 19-423 ppm, Cr: 100-670ppm, Co: 31-59 ppm and Sc: 26-31 ppm), high incompatible element concentrations and low ratio, such as HFSE, low LREE/HREE.

The CIPW norms (Table 5.2) show Acmite as a normative mineral in the rhyolitic rocks (ASR-03 and LAST-20) indicating per alkalinity of the rhyolitic rocks. All the sample show quartz and hypersthene normative minerals indicating that they are silica saturated to over saturated rocks. The major normative minerals in both the suit of rocks are; anorhtite, albite, hematite, quartz, orthoclase, Diopside, hypersthene, and titanite and Acmite.

Table 5.1. Whole rock major element geochemistry of the basalt and associated rhyolitic rocks of Aiba area, recalculated on LOI-free base.

	Basaltic rocks						Rhyolitic rocks		
Sample code	LAB-01	LAB-02	LTSB-04	UASB-08	UTSB-06	UASB-17	ASR-03	TSR-15	LAST-20
SiO_2	46.1	47.8	48	48.7	48.7	48.4	66.3	80.5	65.8
TiO_2	2.48	2.53	2.76	2.6	2.98	2.59	0.96	0.47	0.94
Al_2O_3	10.95	15.4	15.2	15.15	13.3	11.85	14.7	8.54	14.65
Fe_2O_3	12.7	11.75	12	11.35	13.85	13	4.87	2.4	4.7
MnO	0.17	0.15	0.15	0.17	0.18	0.18	0.22	0.07	0.23
MgO	12	6.34	5.82	5.41	6.53	8.11	0.73	0.42	0.68
CaO	9.82	10.2	10.25	10.2	10.8	11.2	0.76	0.58	0.75
Na_2O	1.86	2.86	2.91	2.81	2.46	2.09	5.88	1.91	5.94
K_2O	0.61	0.88	0.89	0.93	0.38	0.58	4.98	3.93	5.3
P_2O_5	0.24	0.33	0.32	0.32	0.27	0.24	0.13	0.06	0.13
LOI	2.61	1.63	1.6	0.93	0.04	1.2	1.75	1.7	1.39
Total	99.7	99.99	100.03	98.67	99.56	99.53	101.4	100.6	100.3
Mg#	50	51.6	50	50	48.48	55.56	25	7.69	14.29
CaO/ Al_2O_3	0.89	0.66	0.67	0.673	0.81	0.945	0.05	0.06	0.05

N.B. Major element data are reported in wt%. Total Fe reported as Fe_2O_3.

Table 5. 2. CIPW norms: Calculated Normative Minerals

Mineral	LAB -01	LAB -02	LTSB -04	UASB -06	UTSB -08	UASB -17	ASR -03	TSR -15	LAST -20
Q	0.709	2.209	2.766	6.696	4.696	5.585	11.85	53.269	10.38
Or	3.664	5.260	5.319	2.246	5.614	3.487	29.55	23.461	31.617
Ab	16.16	24.624	25.047	20.900	24.454	20.90	48.13	16..33	46.287
An	20.43	29.09	26.239	24.472	26.569	24.47	0.000	2.535	0.000
Ac	0.000	0.000	0.000	0.000	0.000	0.000	1.578	0.000	3.875
Di	15.58	0.727	11.040	14.049	11.302	14.05	0.342	0.000	0.439
Hy	23.61	11.092	9.627	9.852	8.560	9.852	1.660	1.046	1.540
Ti	0.385	0.321	0.321	0.385	0.364	0.385	0.471	0.150	0.492
Hm	13.10	11.90	12.210	13.930	11.620	13.93	4.354	0.420	3.401
Tn	5.762	5.919	6.459	6.867	6.060	6.806	1.749	0.000	1.696
Ap	0.592	0.805	0.782	0.640	0.87	0.640	0.308	0.42	0.308
Sum	99.99	100.01	99.810	99.998	100.02	99.99	99.99	99.984	100.04

NB: CIPW is calculated using GCDKit 3.00.

Table 5.3. Whole rock trace element data of the basalt and associated rhyolitic volcanic rocks of Aiba area. Composition is reported in ppm.

	Basaltic rocks						Rhyolitic rocks		
Sample	LAB-01	LAB-02	LTSB-04	UASB-08	UTSB-06	UASB-17	ASR-03	TSR-15	LAST-20
Sc	27	25	27	26	30	31	8	4	8
V	328	284	292	286	356	322	23	16	23
Cr	670	250	180	150	100	300	20	10	10
Co	59	39	38	31	49	50	<1	<1	2
Ni	423	61	37	19	99	151	9	3	5
Rb	10.7	17.6	14.3	16.6	9.5	11.1	110	85.1	120.5
Sr	362	621	610	496	385	337	117.5	91.5	113.5
Y	23.1	28.4	29.7	32.3	28.8	26.6	65.2	67.8	69.4
Zr	165	214	218	226	198	194	1080	587	1090
Nb	24.3	22.9	23.1	21.3	20.5	20.1	128.5	67.2	129.5
Cs	0.14	0.18	0.07	0.13	0.15	0.1	0.69	0.39	0.68
Ba	139.5	282	271	272	130	133.5	978	363	949
Hf	4.7	5	5.3	5.6	5.1	5	26.6	14.8	25.5
Ta	1.2	1.5	1.4	1.3	1.5	1.3	8.6	4	8.3
Pb	8	3	3	9	4	<2	20	9	21

Th	2.17	1.41	1.53	1.88	1.85	1.78	14.05	9.22	13.85
U	0.55	0.45	0.39	0.54	0.55	0.46	3.81	2.68	3.75
La	20.8	22.1	21.5	22.5	19	19	112.5	68.4	116.5
Ce	47.9	49.8	48.1	50.3	42.8	42.9	224	146	248
Pr	5.99	6.7	6.65	6.71	5.79	5.66	29	19.4	31.9
Nd	26.8	29.2	28.5	30.2	26.7	25.7	113	81.5	126.5
Sm	5.81	6.59	6.55	7.02	6.08	6.51	21.4	16.7	24.6
Eu	2.02	2.32	2.25	2.27	2.22	1.99	5.65	4.21	6.51
Gd	5.97	6.49	6.52	7.31	6.83	6.58	17.35	15.95	19.65
Tb	0.88	0.96	0.97	1.01	1.08	0.94	2.55	2.46	2.82
Dy	4.77	5.91	5.68	6.15	5.96	5.53	14.2	14.5	14.85
Ho	0.91	1.08	1.08	1.21	1.04	1.02	2.59	2.62	2.68
Er	2.07	2.7	2.68	3.3	2.92	2.65	7.02	7.09	7.01
Tm	0.31	0.41	0.34	0.46	0.38	0.33	0.95	0.94	0.87
Yb	1.91	2.23	2.43	2.77	2.24	2	5.57	5.92	5.57
Lu	0.25	0.36	0.33	0.36	0.32	0.32	0.76	0.76	0.8
∑REE	127.9	136.8	133.5	141.57	123.36	121.2	556.5	386.5	608
La/Sm_N	1.69	1.84	1.8	1.75	1.71	1.6	2.88	2.25	2.59
La/Yb_N	6.6	6.0	5.36	4.92	5.14	5.76	12.24	7.0	12.67

5.4. Major element geochemistry

The SiO_2 in the basalts range between 46.1 to 48.7 wt%, while the rhyolites it ranges between 65.8 to 80.5 wt%. With no intermediate values. In the other major oxides do not show significant variation within the suites of rocks. K_2O/Na_2O (0.28-0.89) is low in all the basalt and rhyolite except in the high SiO_2 (80.5%) rhyolitic lava sample TSR-15 is 2.06. The basalts have generally low Mg# (48.48-51.6%) except one 55.56%, and low ratio of CaO/Al_2O_3 (0.66-0.95), with no major variation among the basalt samples. In general, major element geochemistry is fairly uniform among the samples from the different stratigraphic levels of both the basalts and rhyolites

5.4.1. Major element variation diagrams

Major element variation diagrams are given in Fig. 5.1, which clearly show the bimodality of the rocks, with a gap of ~17 wt% in SiO_2 in between them. Most of the major oxides show clustering of the basaltic suites and the rhyolitic suites within each group and show some differentiation trend between the two groups. A differentiation trend between the basalt rocks is not shown and the major oxide doesn't show considerable scatter. Na_2O and k_2O shows positive trend with the exception of sample

(TSR-15), inflected trend of P_2O_5 and Al_2O_3 are observed. Major Oxide such as Fe_2O_3, MgO, TiO_2 and CaO shows negative trend.

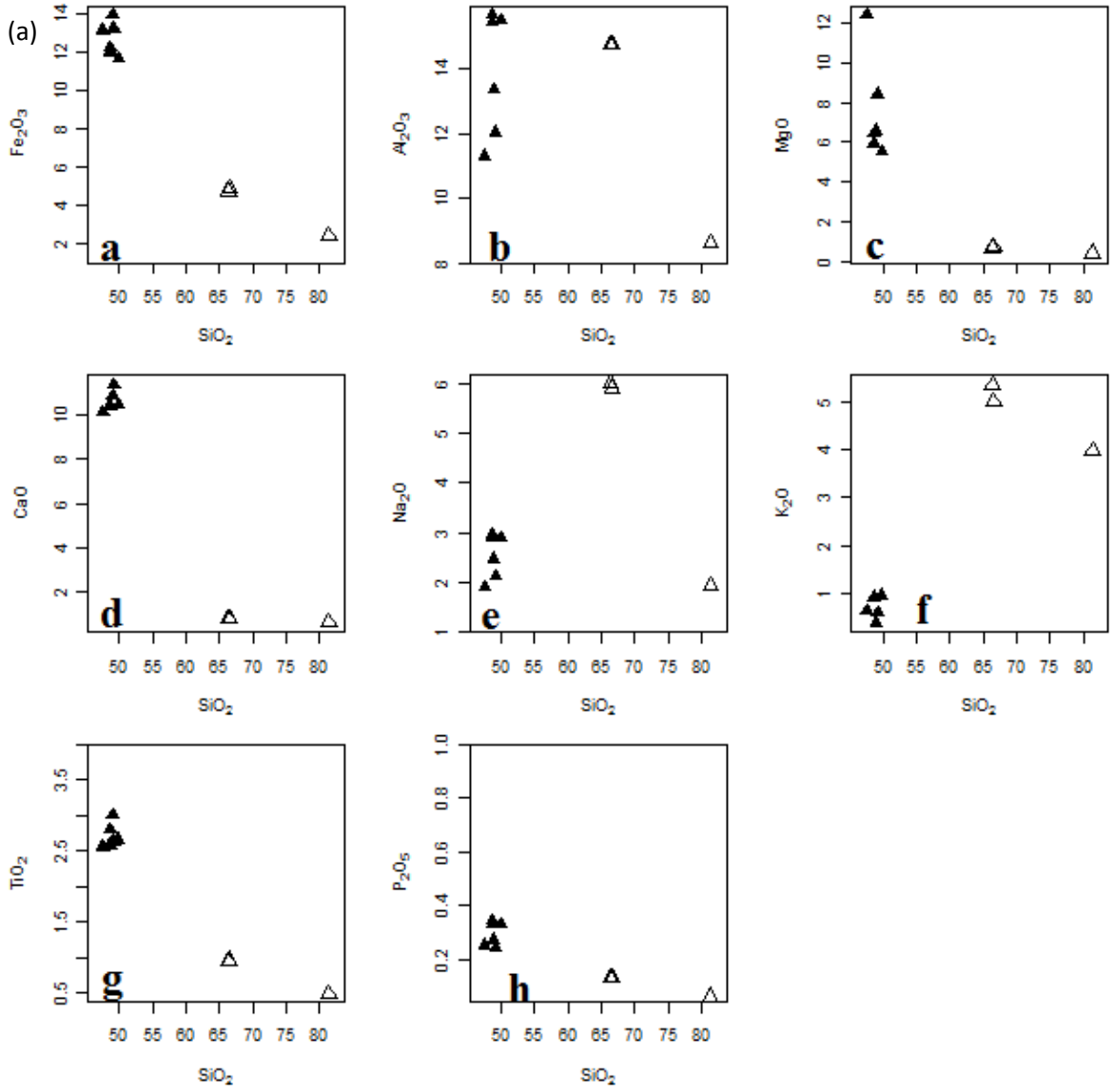

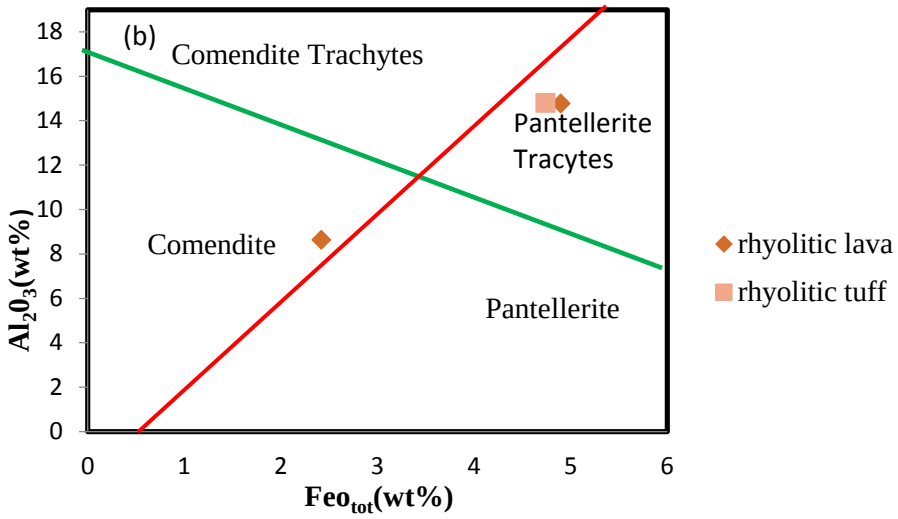

Fig. 5.1. Major element variation diagrams of the basaltic and rhyolitic rocks. SiO_2 versus (a);a Fe_2O_3; (b) MgO; (c) Al_2O_3; (d) CaO; (e) Na_2O; (f) K_2O; (g) TiO_2; and (h) P_2O_5. And (b) further rhyolite classification based on the proportion of Al_2O_3 and FeO_{tot} (Fe_2O_3) the lines are (after Macdonald, 1974 as cited in Angesom resom et al., 2018. Symbol as in fig.5.2

The concentration of TiO_2 is decrease with increase SiO2 consistently with the whole sample of rhyolite. In addition, The rhyolitic samples have lower concentration of CaO, Fe_2O_3, MgO, TiO_2, and P_2O_5 and high concentration of Al_2O_3,K_2O and Na_2O; however, comendite rhyolitic rock (TSR-15) is anomalous low amount of Al_2O_3 with relative to Na_2O, K_2O, CaO,MnO_2,P_2O_5 at high SiO_2 (80.5wt%) and, it has high K_2O/Na_2O (2.06).The rhyolite rocks are per alkaline affinity with one sample comendite (TSR-15) As show in the (Fig. 5.1).While the other two (ASR-03 and LAST-20) are pantellerite trachyte in composition with high Al_2O3 and Fe_2O_3 content.

5.4.2. Total alkali verse silica classification

The TAS diagram classification (after Middlemost, 1994) in (Fig. 5.2a) show the Aiba volcanic rocks fall in three major categories of the classification. All the basaltic samples fall in the "basalt" field, while two of the rhyolitic samples (ASR-03 and LAST-20) fall in the "trachyte to trachy dacite" fields, while one rhyolitic (TSR-15) from the Tsibet section falls in the "rhyolite" field. In addition, the basalts fall in the sub-alkaline field (K_2O+Na_2O=2.53-3.8%), while the rhyolites fall in the alkaline field with (K_2O+Na_2O = 5.9-11.34%) with the exception of TSR-15. Sample (LAB-01) has low total alkali content from the basalt suit, while the highest total alkaline content is occurring with sample

(LAST-20) from the rhyolite. In the alkali diagrams (Peccerillo et al., 1979), the basalts fall from tholeiitic to transitional field, which is close to the boundary line of tholeiitic and transitional (Fig. 5.2b)?

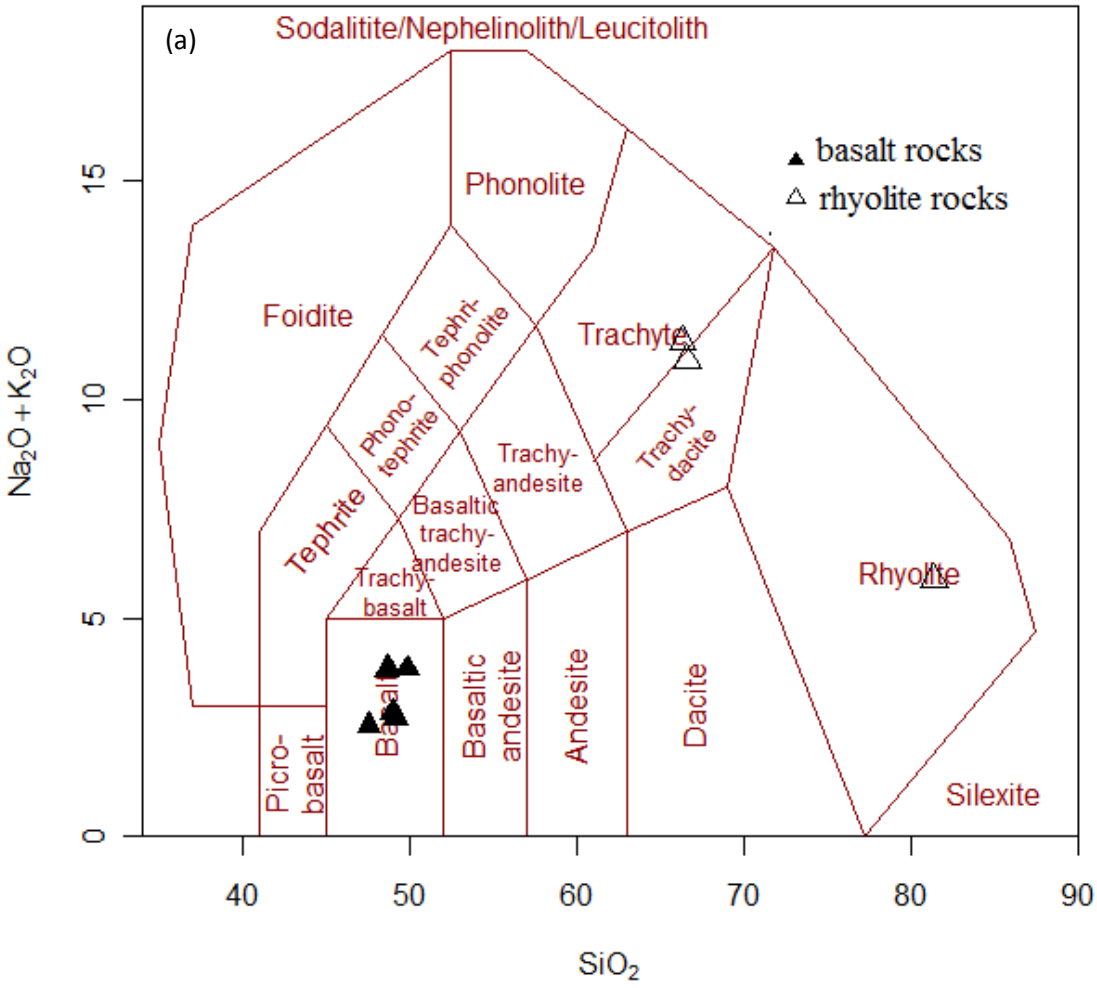

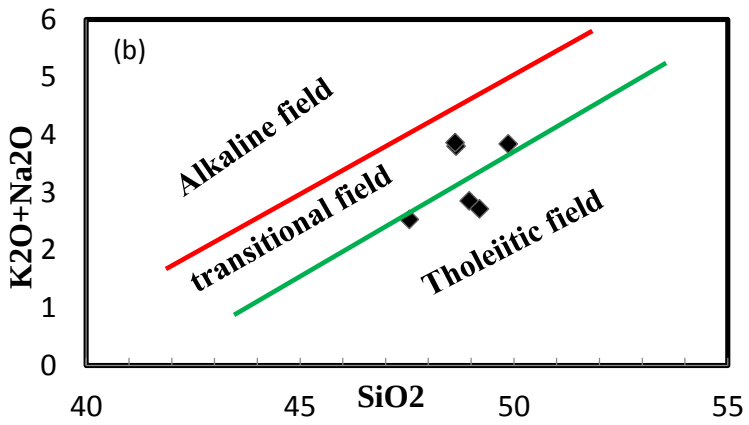

Fig. 5.2. Classification of the Aiba volcanic rocks (basalt and rhyolite) (a) Total Alkaline-Silica classification diagram (Middlemost, 1994).Further classification or identification of transitional basalts. Boundary lines are (after Peccerillo et al., 1979 as cited in Mohr and Zanettine, 1988)

5.5. Trace element geochemistry

The volcanic rocks have low compatible element (Ni, Cr, Co) concentration, and are enriched both in the LREE (La, Ce, Pr, Nd, Sm,) and highly incompatible element (Cs, Rb, Ba, Th, U, Zr, Ta and Y), low LREE/HREE ratio (La/Sm, La/Yb). In addition, the ratio of two highly incompatible elements such as Nb/Zr (0.09-0.14), Ce/Zr (0.20-0.29), La/Zr (0.10-0.012), Rb/Zr (0.05-0.14), Ta/Nb (0.05-0.07), La/Nb (0.85-1.05), Th/La (0.06-0.13), and Hf/La (0.21-0.26) is nearly constant within the basalt and rhyolite suites. The lower stratigraphic basalt, olivine-phyric basalt (LAB-01) has more primitive compositions with MgO: 12wt% and Mg#50%, and high amount of compatible elements (Ni: 423 ppm, Cr: 670 ppm, and Co: 59 ppm) than the other basalts unit.

Table 5.4. Highly incompatible Trace element Ratio

Sample Code	LAB - 01	LAB-02	ASR -03	LTSB-04	UASB-08	UTSB-06	TSR -15	UASB-17	LAST -20
La/Nb	0.85	0.96	0.87	0.93	1.05	0.92	1.01	0.94	0.89
Hf/La	0.22	0.22	0.23	0.24	0.24	0.26	0.21	0.26	0.21
Th/La	0.10	0.06	0.12	0.07	0.08	0.09	0.13	0.09	0.11
Ta/Nb	0.05	0.06	0.06	0.06	0.06	0.07	0.06	0.06	0.06
Rb/Nb	0.44	0.76	0.85	0.61	0.77	0.46	1.26	0.55	0.93
Th/Nb	0.08	0.06	0.10	0.07	0.09	0.09	0.14	0.09	0.11
Ta/Nb	0.05	0.07	0.07	0.06	0.06	0.07	0.06	0.06	0.06
La/Zr	0.13	0.10	0.10	0.10	0.10	0.10	0.12	0.10	0.11
Nb/Zr	0.14	0.10	0.12	0.11	0.09	0.10	0.11	0.10	0.12
Rb/Zr	0.06	0.08	0.10	0.07	0.07	0.05	0.14	0.06	0.11
Ce/Zr	0.29	0.23	0.20	0.22	0.22	0.22	0.25	0.22	0.23
La/Lu	0.25	0.23	0.46	0.23	0.2	0.13	0.67	0.22	0.47
Tb/Yb	1.96	1.83	1.94	1.69	1.5	2.05	1.77	2	2.15
Th/Ta	1.81	0.94	1.63	1.09	1.45	1.23	2.30	1.37	1.67
Zr/Nb	6.79	9.34	8.40	9.43	10.61	9.65	8.73	9.65	8.41
Ba/Nb	5.74	12.31	7.61	11.73	12.76	6.34	5.40	6.64	7.32
Ba/La	6.70	12.76	8.69	12.60	12.08	6.84	5.30	7.02	8.14

5.5.1. Trace element variation diagrams

Trace element variation diagrams against Zr (Fig. 5.3) and SiO_2 (Fig. 5.4) as differentiation index are given below. These diagrams show that the compatible elements are rapidly fractionated with slight change in Zr within the basalt suite, while they are nearly constant in the rhyolites, whereas the incompatible elements (e.g., Th, Nb, Ta, Ce and Hf) shows generally good linear trend in both rock suites with less considerable scattern, suggesting that these rocks could be linked by fractionation process of the same magma source. The similarity the incompatible trace element ratio of the above table 5.4, in both rock suites also supports this. The trace element variation diagrams with SiO_2 Fig.5.4 show little variation of both highly incompatible element and SiO_2 within the basalts, in addition no trend or fractionation variation between the basalts, while there is a slight fractionation trend in the rhyolites. This is also supported by the consistent

similarity in CaO/Al_2O_3 ratio (0.63-.0.94) which might indicate genetic relationship between the basalts and rhyolites.

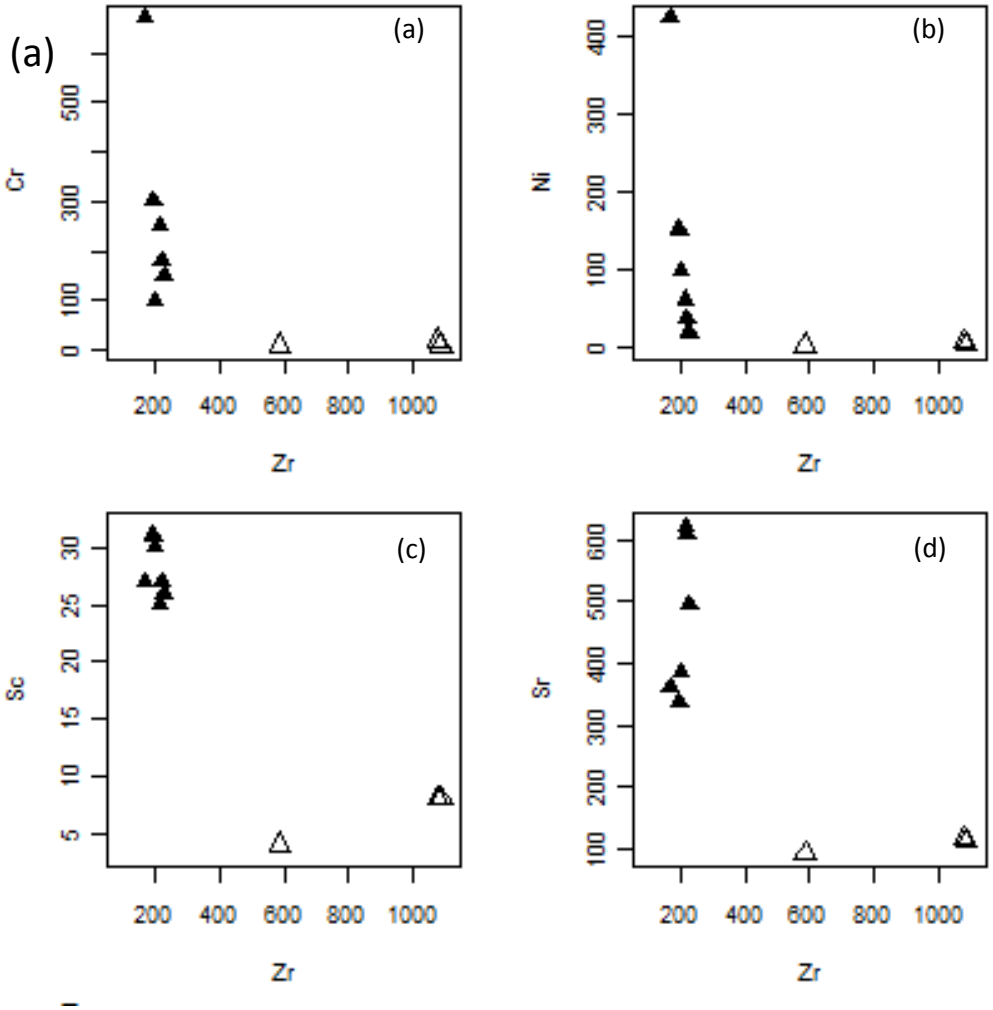

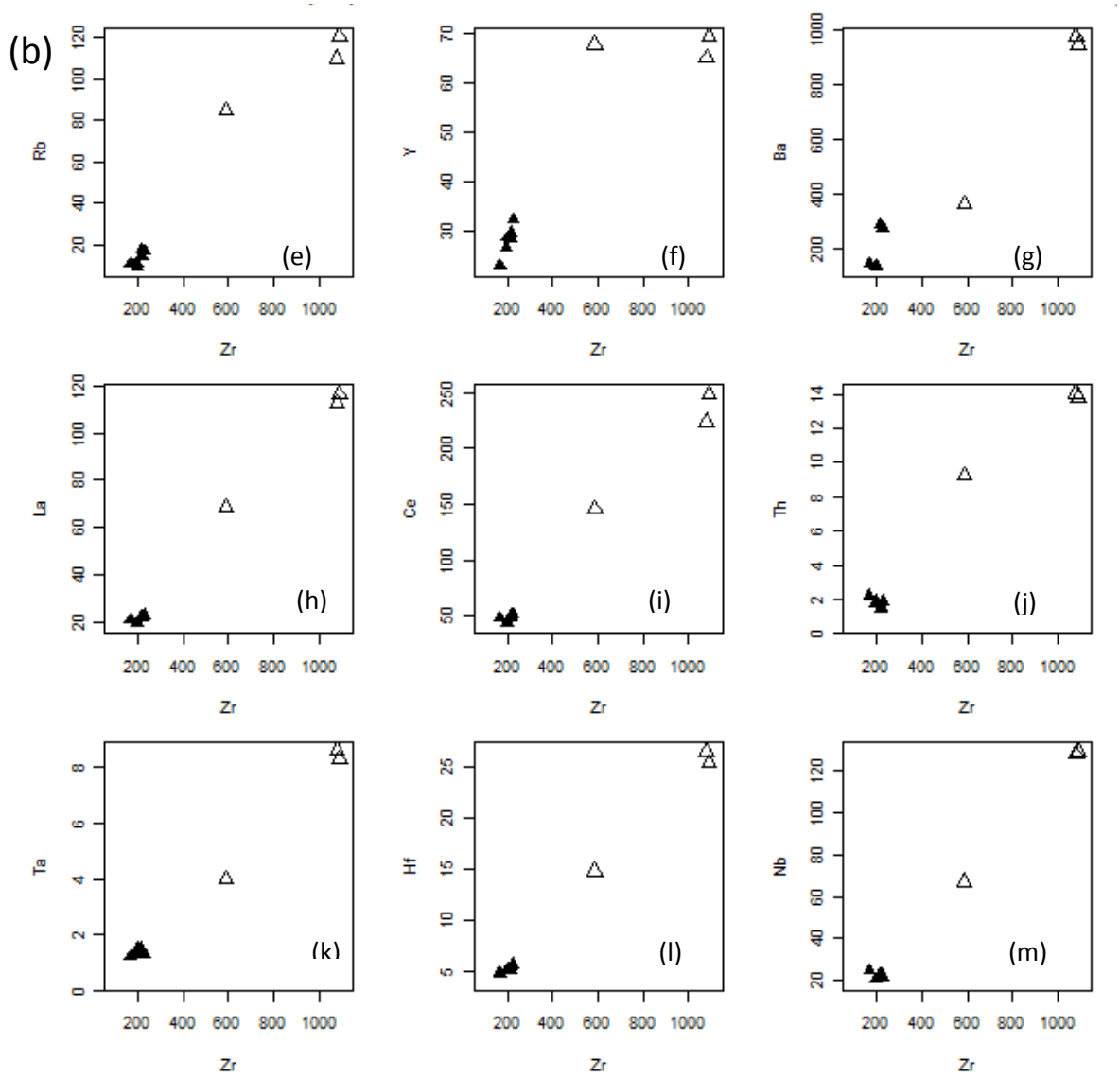

Fig. 5.3 (a) Compatible (Cr, Ni, Sc, Sr) versus incompatible (Zr) trace element variation diagram. (b) Incompatible (Rb, Y, Ba, La, Ce, Th, Ta, Hf, Nb) versus incompatible trace element (Zr) variation diagram. Symbol as in fig 5.2

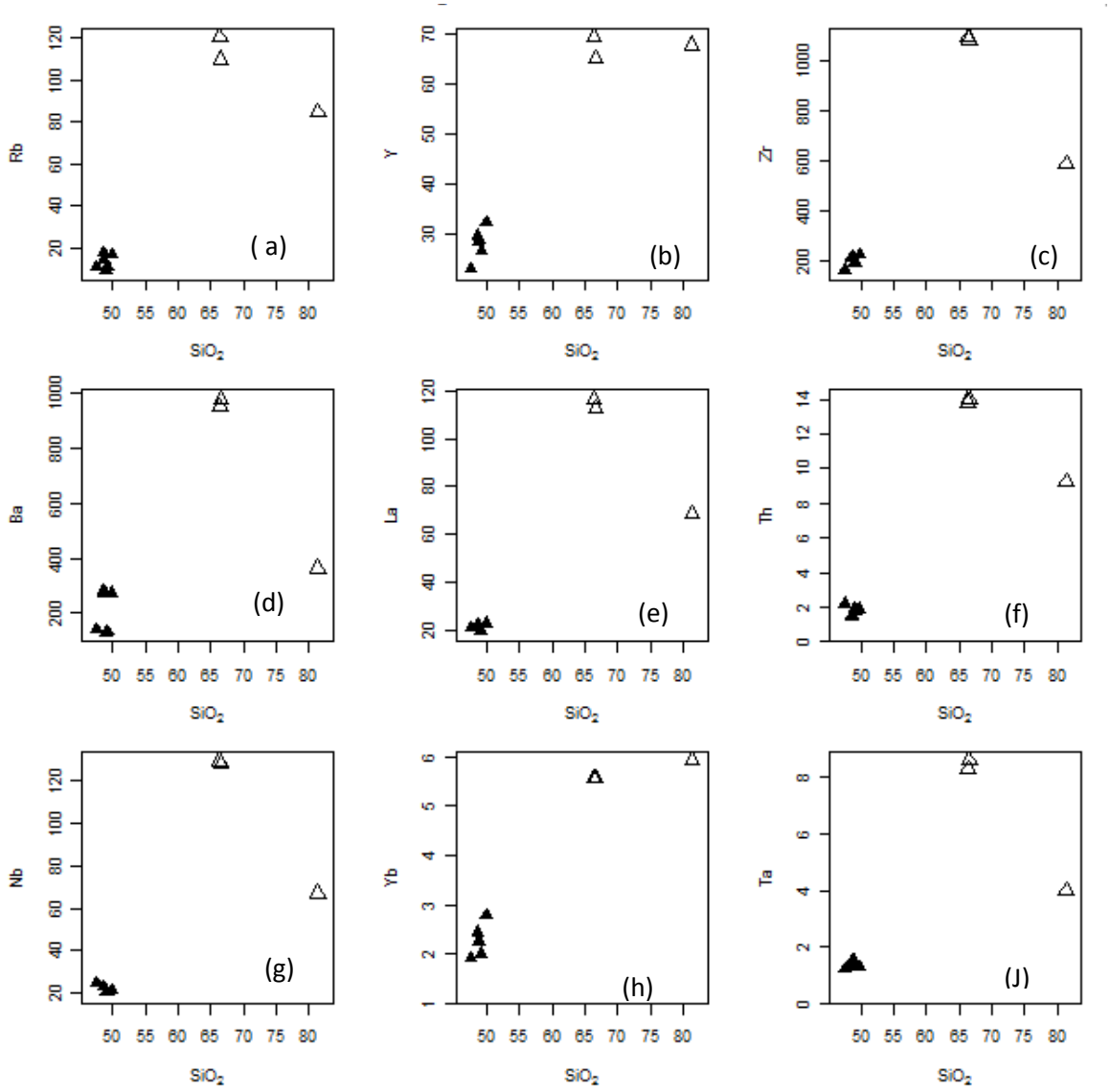

Fig. 5.4. Incompatible trace element (Rb, Y, Zr, Ba, La, Th, Nb, Yb, Ta) versus SiO_2 variation diagrams. Symbol as in fig 5.2

5.5.2. Multi-element variation diagram (spider diagram)

Primitive mantle normalized multi-element (Sun and McDonough, 1989) diagram (Fig. 5.5) shows enrichment of the high field strength elements (HFSE) such as Cs, Th, U, Zr, Ta, Y, Hf, Nb, and Pb, and shows a large considerable depletion in Ti, P, Sr and slight Ba in the rhyolitic samples. The basalts show nearly uniform fractionating trend both in the most incompatible and less incompatible trace elements except slight depletion in K and strong enrichment in Pb in many of the samples.

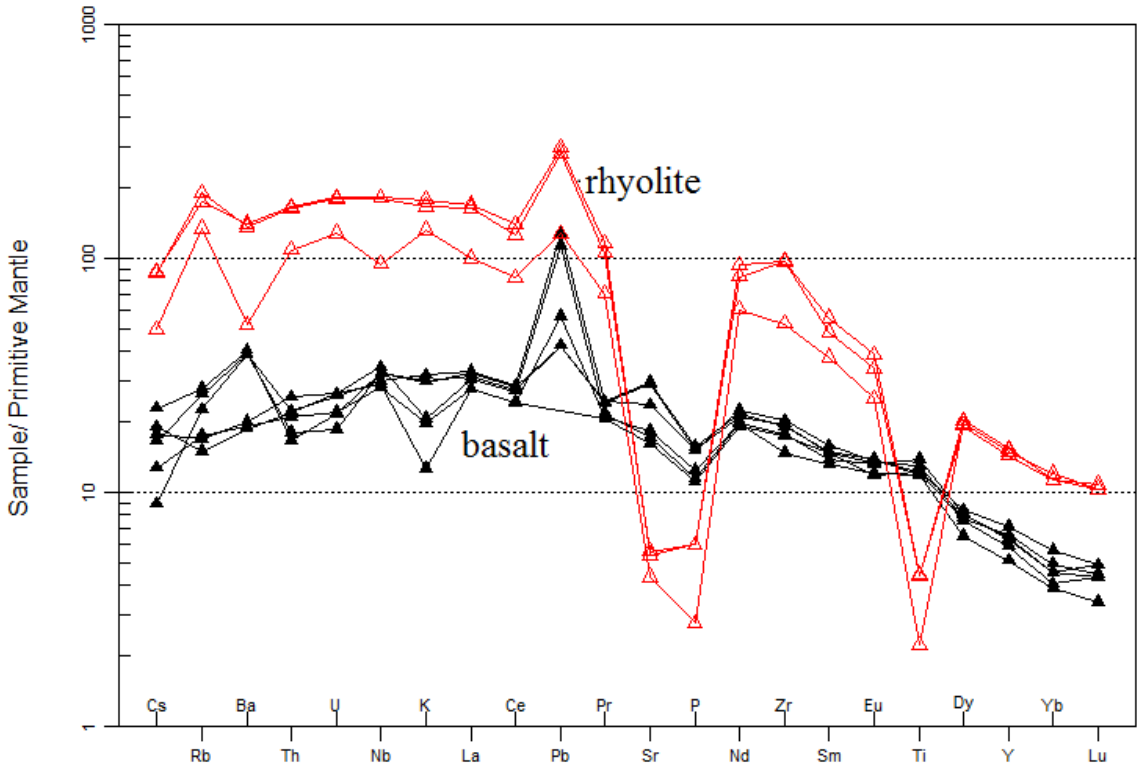

Fig. 5.5. Primitive mantle normalized incompatible trace element variation diagram (Sun and McDonough, 1989).

5.5.3. Rare earth element variation diagram

The chondrite normalized REE variation diagram (Fig. 5.6) shows that basaltic and rhyolitic rocks are LREE enriched and HREE depleted, and evolve with uniform slope, smooth parallel trend from the LREE to the HREE, though the rhyolites are generally more enriched than the basalts and no considerable depletion and peak is observed in both the volcanics. Both the basalts and the rhyolites are enriched in the REE compared to chondrite. The basaltic rocks are shows nearly constant value of LREE compared to the HREE in contrast the rhyolitic rocks show nearly constant HREE and slightly vary LREE relatively. Generally all the basalt and rhyolite lay above the 10 times chondrite value except one basaltic sample with Lu and Yb below the chondrite value.

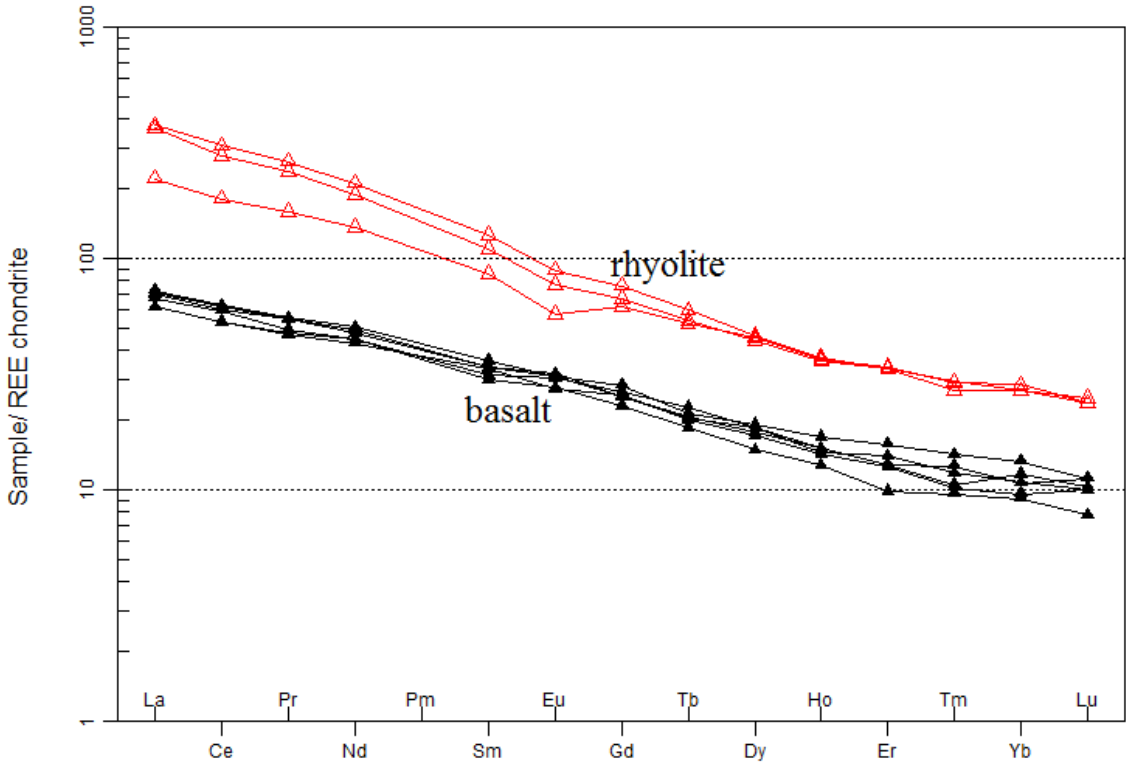

Fig. 5.6. Chondrite normalized REE variation diagram for basaltic and rhyolitic rocks from the Aiba area (normalizing values are from Boynton, 1984).

CHAPTER SIX

DISCUSSION

6.1. Petrogenesis of the Northwestern plateau basalts and rhyolites

Previous study on the North Ethiopia plateau volcanic rocks have identified the presence of variation of geochemical and isotope data, and they conclude the presence of different mantle source reservoir. The volcanic rocks of northern Ethiopia plateau are spatially zoned from the west of the plateau (LT) to the center of the rift (HT2) and HT1 is zoned intermediated in between them (Bacculava et al., 2009). Further studies indicated that the High-Ti and Low-Ti flood basalts of the Northwestern Ethiopian plateau are sourced from enriched mantle with OIB like geochemical signature, and from depleted mantle with MORB like geochemical signature, respectively (Pik et al., 1998; 1999) and this classification includes the present study area and they classify with HT flood basalt in composition which is consistent with the present result. As show in the Fig.6.1 (a.b, c), the basaltic rocks of the present study is lay transitional with the HT2 and LT of the northern Ethiopia Oligocene flood basalt from (Pik et al., 1998, 1999).Recently, Miruts hagos et al.(2016), further describe the zonal separation of the of HT and LT basalt in the Danakil depression of northern Afar depression rift and rift shoulders with HT in the rift while LT on the rift shoulder. In contrast, Kieffer et al. (2004) described that the large difference in the content of incompatible trace elements is not only indicative of the source composition but also shows the variation of the degree of partial melting of the source rock. Other works (e.g. Mohr and Zanettine, 1988; Hart et al., 1989; Peccerillo et al., 1997; Dereje Ayalew et al.,(1999; 2002); Miruts Hagos et al., 2010, Kurkura Kebeto et al., 2010) show that the Ethiopian flood basalts evolved through fractional crystallization of mantle derived sources. Many studies of the rift and rift margin plateau rocks also indicate that the silicic rocks evolved by fractional crystallization of basaltic magmas with variable degree of crustal contamination (e.g. Dereje Ayalew et al.,(2006; 2011),Peccerillo et al., (2003, 2007), Kurkura Kebeto et al., 2009; Gasparon et al., 1993; Giordano et al., 2014;TadiosChernet and Hart, 1999; Rooney et al., 2012 Angesom Resom et al., 2018).In contrast others such as Trua et al.(1999)the origin of rhyolite is partial melting of lower crust basalt followed by low pressure fractionation in the eastern rift shoulder of main Ethiopian rift. While, Bocalleti et al.(1995) explain different origin of the basaltic rock and the associated felsic pyroclastic rocks. Beside, Peccerillo et al.

(2007) the strong bimodal volcanic rock in the Northern sector of Main Ethiopian Rift is due to the shallow level fractional crystallization of the magma generates, zoned magma chambers of basaltic at lower and rhyolitic melts at the top in addition the presence of large amount of felsic rock relative to the basalt is due to the trap of felsic to the basalt in the magma chamber, the rhyolite have a chance to erupted to surface than the basalt. Basalt only erupt following fracture if it get open space.

6.2. Petrogenesis of the Alaje Formation basaltic rocks

The petrography, major and trace element geochemistry of the basaltic rocks, irrespective of their stratigraphic position, show little variation except the slight textural difference and the relative proportion of the various phenocrysts. Though the numbers of samples are limited to draw definitive conclusions, the basalts show limited variation of fractionation within the suite. This is supported by the uniform trace element ratio and REE patterns. The present study area is part of the northwestern Ethiopian plateau flood basalts and according to the trace and Major element data, the area is grouped with in the HT1 of Pik et al. (1998; 1999) with TiO_2 content of 2.48-2.98 wt% fig.6.1c. In addition, REE chondrite of fig.6.1 (a, b) shows the Aiba basalt which is dark field place below HT2 and above the LT on the LREE of the north western plateau basalt, and are tholeiitic to transitional in character, which is consistent with (Mohr and Zanettine, 1988 and Kurkura, 2010). In contrast, Miruts Hagos et al. (2010) identified the Axum-Adwa area basalt rock on northern periphery of northern plateau basalt into alkaline to transitional basalts. The Aiba volcanic rocks display a smaller range of incompatible trace element variations while the Axum-Adwa basaltic rocks show a wide range of incompatible trace element variations possibly indicating uniformity of source in the former and wider range of partial melting or source heterogeneity in the latter.

The lower stratigraphy of Alaje formation basaltic unit (lower olivine-phyric basalt) has relatively high MgO and is enriched in the compatible trace elements, and depleted in the incompatible trace elements. The positive correlation of MgO with the high compatible elements (Ni, Sc and Cr) is also consistent with the relatively higher proportion of olivine phenocrysts in this unit. These possibly indicate a little fractionated magma erupting to the surface. On the other hand, the depletion of the highly compatible element (Ni, Cr and Sc) and the enrichment of most incompatible elements in the plagioclase-phyric basalt,

suggests fractionation of olivine and clinopyroxene, consistent with petrography of this unit.

All the basaltic rocks in suit show nearly flat LREE to HREE variation with slightly enriched values than chondrite, while most incompatible elements are enriched in these basalts. This enrichment in LREE and in highly incompatible trace elements suggests either crustal contamination or derivation from enriched mantle source (Thompson, 1984, as cited in Dereje Ayalew et al., 1999).Trace element ratio of Y/Nb to Zr/Nb Fig.6.1 (d)all the basalt rocks of Aiba area lie on the enriched source of (Wilson,1989) classification and this supported also by the positive anomaly of Nb,U,Th on the multi–element variation diagram.

Further, the HREE are shows above the chondrite value therefore it represents the garnet free source (Wilson, 1989). The major oxide variation diagram Na_2O and k_2O shows positive trend with in the suite of rhyolite and basalt may indicating no fractionation of Albite and k-feldspar whereas the inflected trend of P_2O_5 and Al_2O_3 are may also show to indicate the fractionation of apatite and plagioclase feldspar in the late stage of fractionation. On the other hand, the negative trend Major Oxide such as Fe_2O_3, MgO, TiO_2 and CaO indicates that the fractionation of oliven, clinopyroxene, Fe-Ti oxide, and plagioclase bearing minerals from the system respectively (Rollinson, 1993)

The smaller difference in the content of Major and trace element, REE, most incompatible element concentration and ratio, clustering of the basalt in the small range of SiO2 in the variation diagram, and the linear trend of two high incompatible element plot diagram suggested that the basaltic rocks of the different stratigraphic suits is may indicate a homogenous source parental magma.

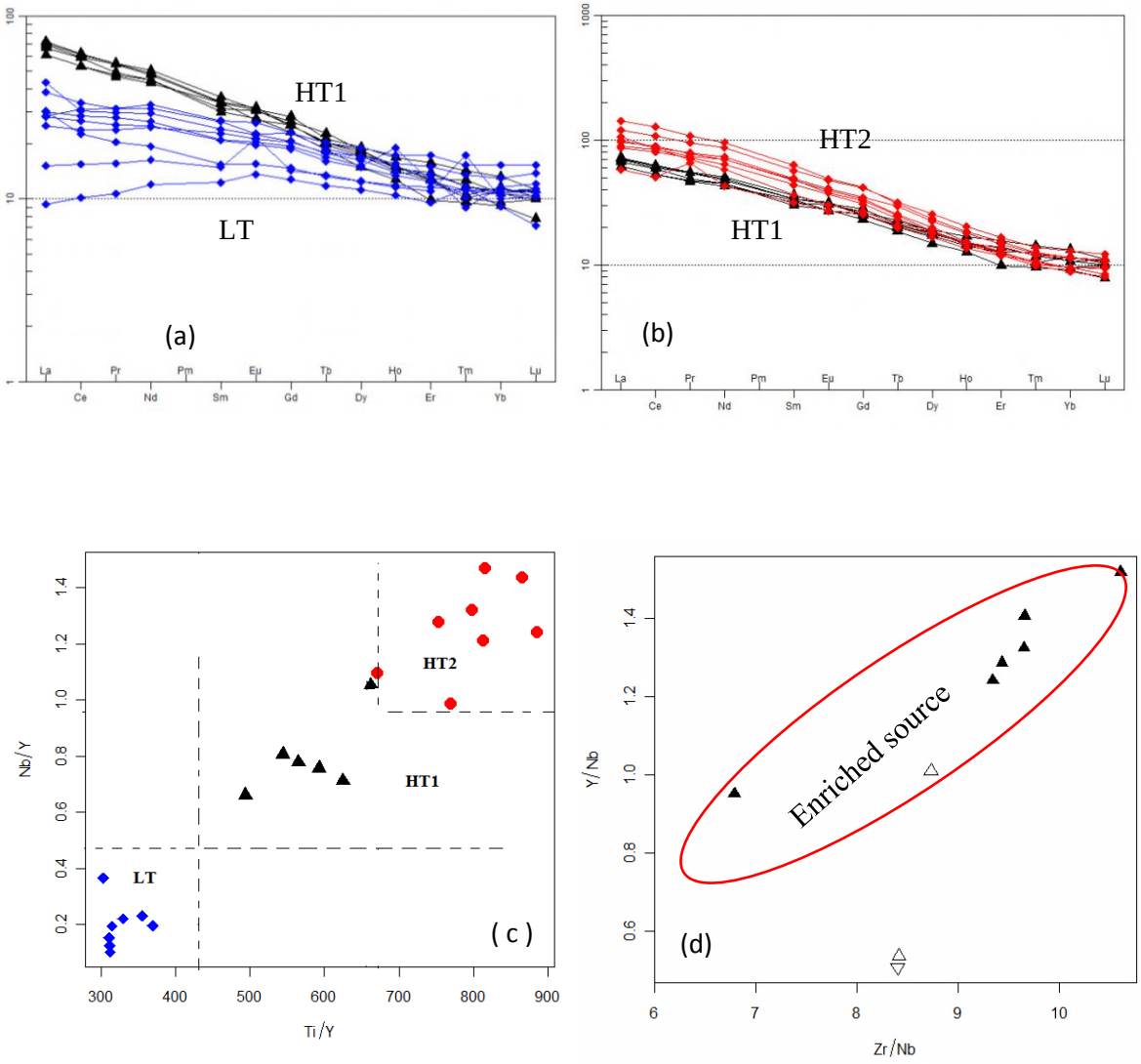

Fig. 6.1.Comparistion of REE chondrite value for northwestern plateau LT and HT2 basalt With HT1 basaltic rock from Aiba area (dark field) in (a, b). (c): Ti/Y versus Nb/Y values of basaltic rocks of the Aiba area with northwestern plateau LT and HT2 basalt. (d) Zr/Nb versus Y/Nb value of Aiba basaltic rock (after Wilson, 1989). Source of the REE data for LT and HT2 is Pike et al., 1999.The trace element ratio of HT and LT (c) is from Pik et al., 1998.

6.3. Petrogenesis of the Alaje Formation rhyolitic rocks

The analyzed rhyolitic samples are few to make any definitive conclusions. However, the rhyolitic rocks of the Aiba area show consistently similar geochemistry to the well-constrained rhyolitic rocks of Wegel Tena and Lima limo, which have been indicated to be formed by low pressure crystal fractionation process (Dereje Ayalew et al., 2002; Dereje Ayalew and Gezahign Yirgu, 2003), and show closely related geochemical evolution to those of the basaltic rocks of the study area, suggesting that they are

genetically related. The dominance of plagioclase as the mafic phenocryst in the rhyolitic rocks supports this conclusion. The analyzed thin section in volcanic rocks of the study area is plagioclase dominated with clinopyroxene and Fe-Ti oxide and few oliven, this assemblage suggested that the shallow level low pressure crystal fractionation process (Wilson 1989).

The rhyolites on the plateau are geochemically related to the associated basaltic rocks though, the high-Ti rhyolites are associated to the high-Ti basalts and the low-Ti rhyolites are associated to the low-Ti basalts (Dereje Ayalew et al., 2002; Dereje Ayalew and Gezahign Yirgu, 2003), who have also showed that the rhyolitic rocks are derived from the associated basalts through fractional crystallization. The Aiba rhyolitic rocks have similar Ti content ($0.48 < TiO_2 < 0.96$ wt%) with those of Wegel Tena rhyolites ($0.45 < TiO_2 < 1$ wt%), and similar concentration of incompatible trace elements and REE, falling in the High-Ti suites (Dereje Ayalew et al., 2002; Dereje Ayalew and Gezahign Yirgu, 2003). Dereje Ayalew and Gezahign Yirgu (2003) have compared the trace element ratios (La/Nb and Rb/Nb) and isotopic ratios of rhyolitic rocks from the Ethiopian highlands to those form various parts of the word derived from crustal melt, and showed that the rhyolitic rocks of the Ethiopian highlands (such as from Wegel Tena and Lima Limo) show much lower values of La/Nb (Lima limo: 1.7 – 3.0 and Wegel Tena : 0.8 – 1.2) and Rb/Nb (Lima limo: 1.4 – 2.9 and Wegel Tena: 0.8 – 1.3) values compared to those derived from crustal melts. The Aiba rhyolites have similarly low ratios of La/Nb (0.85 - 1.02) and Rb/Nb (0.85- 1.23) suggesting similar origin by fractional crystallization of mantle derived basaltic magma by low-pressure fractionation rather than by partial melting of crust rocks.

In addition, Ta/Nb ratio might be a useful index of crustal contamination (Thompson et al., 1984, as cited in Wilson, 1989). For instance OIB and kimberlitic rocks all have a Ta/Nb <1, while CFB with crustal contamination have Ta/Nb ratio of 0.5-7.0. The Ta/Nb ratio of the Aiba rhyolites (0.05-0.07) and Th/Nb (0.06-0.14) are very low suggesting very limited crustal contamination, if any. Furthermore, Nb, Th and U do not show any significant negative anomaly suggesting limited contamination. The Aiba volcanics has low Y/Nb (0.5-1.5) and Zr/Nb ratio (6.79-9.65). This low value shows all the basalt and rhyolites are derived from enriched source component of the mantle (Wilson 1989, fig

6.1d). In general, the basalts and rhyolites of the Aiba area could be considered to be derived from an enriched mantle source by low pressure fractional crystallization.

Comparison of the REE patterns of the Aiba rhyolites with those of other parts of the Ethiopian plateau such as at Lima limo, Jima, Wegel Tena and Debre Birhan (Fig. 6.2), shows that the plateau rhyolites in all localities are closely related to the basaltic counterparts, and are shown to be evolved by fractional crystallization (Dereje Ayalew et al., 1999; 2002; Dereje Ayalew and Gezahign, 2003) and that the Aiba rhyolites and basalts show very similar patterns to those of the Wegel Tena volcanic rocks in their the trace element ratio and concentration, where the rhyolites show moderately sloping LREE and nearly flat HREE, with no appreciable anomalies, unlike the Lima Limo, Jima and Debre Birhan rhyolites which show strong negative Eu anomaly.

Further, the positive anomaly of Pb and Rb Multi-element variation diagram Fig5.5, it may be due to mobility of the elements (Rollison, 1993). Little negative anomaly in Eu in the REE chondrite is the results of fractionation of Eu in the crystal structure of plagioclase and Calcic-alkali feldspar at high oxygen fugacity (Rollison, 1993). In addition, the negative anomaly of P, Ti, Ba, and Sr in the multi element variation diagram Fig5.5, suggested that the fractionation of Apatite, Fe-Ti oxide, k-feldspar and plagioclase feldspar mineral respectively. In addition, the negative correlation of the most compatible element such as Ni, Sc, Cr and Sr provide that the removal or fractionation of the mafic minerals such as oliven, clinopyroxene and Cr-spinel, plagioclase bearing mineral from the system.

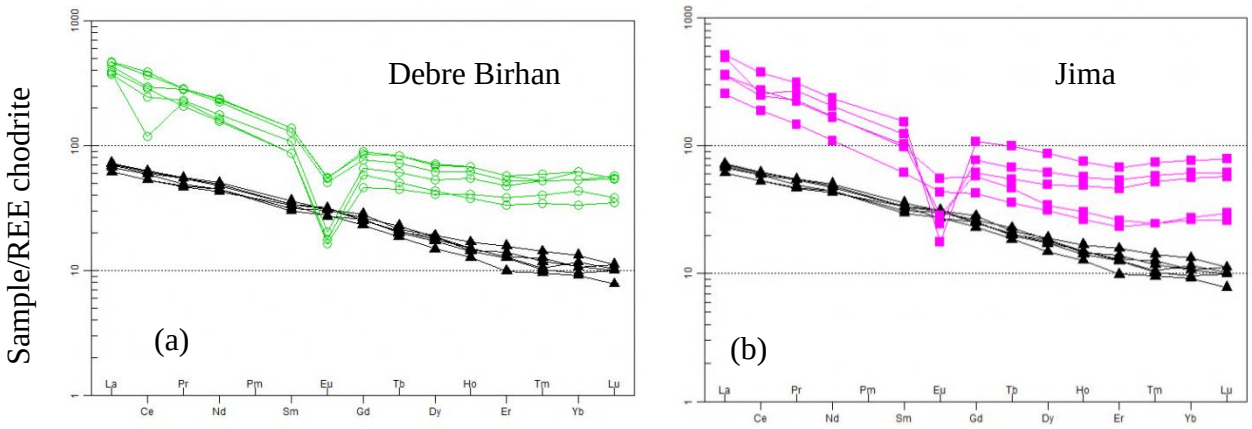

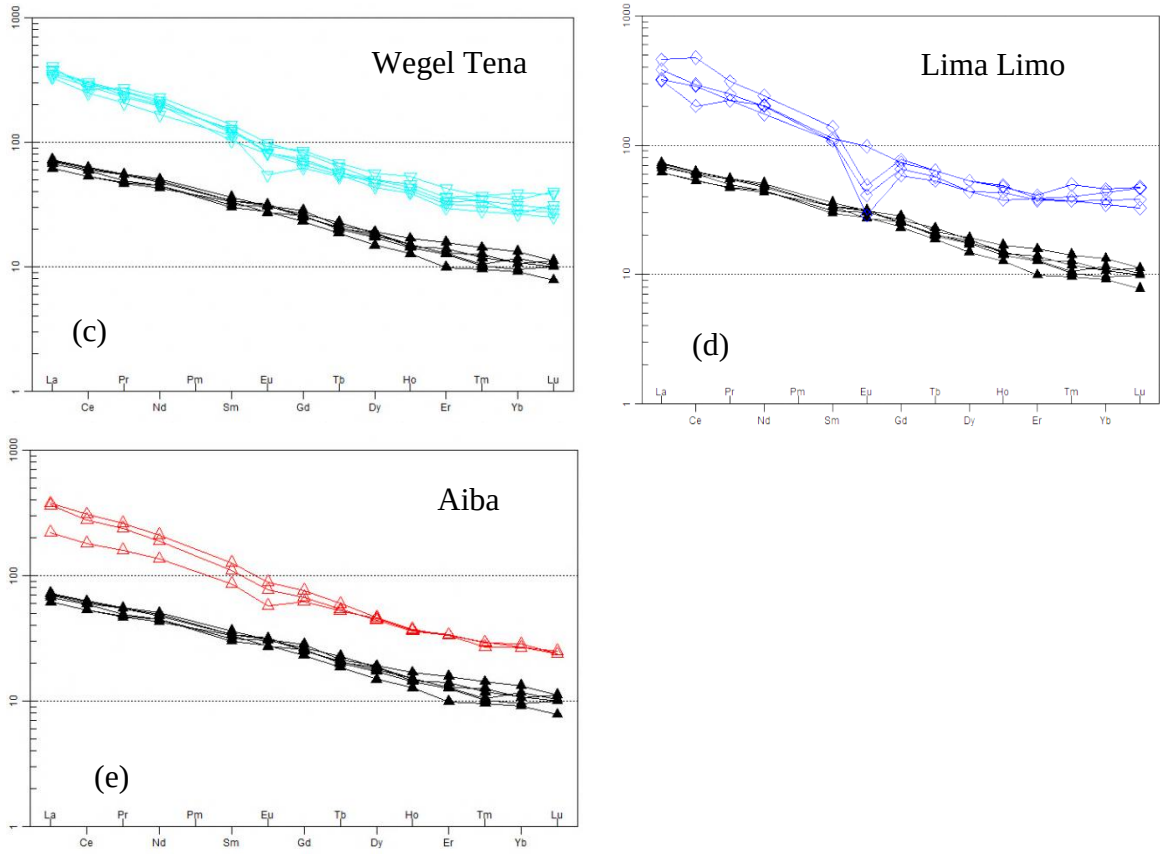

Fig. 6.2. Chondrite-normalized REE patterns for Ethiopian plateau rhyolites (a - d) and the Aiba area (e). Normalization values are from Boynton (1984). Ranges of REE patterns for the associated basalts (lower dark field is basalt from Aiba) are shown for comparison.

CHAPTER SEVEN

CONCLUSIONS AND RECOMMENDATION

7.1. Conclusions

1. The Alaje Formation volcanic rocks are comprised of three sequences of basaltic suites and three units of rhyolitic suites which can be traced in the whole mapped area, except in few localities where some of the units are missing due to removal by erosion or by faulting.
2. The volcanic rocks are affected by parallel series of joints and normal faults which are generally oriented NE-SW, parallel to the main trend of the Ethiopian rift system.
3. The basaltic rocks of the Alaje formation, which are tholeiitic to transitional, show some textural and compositional variation. Most of the units are porphyritic, plagioclase phenocryst dominated, followed by clinopyroxene, Fe-Ti oxide, and olivine mineral assemblage. The lower basaltic unit is olivine phenocrysts dominated, the middle basalt is more plagioclase and pyroxene dominated, while the upper basaltic is aphyric and comprises of more Fe- Ti oxides, indicating more fractionated basalts.
4. The basaltic suits (lower, intermediate and upper stratigraphy) show nearly flat LREE to HREE variation with slightly enriched values than chondrite. In general, the clustering of the basalts in the silica differentiation trend, and little variation in the highly incompatible trace element concentrations, indicate that the basaltic units are less fractionated, and the positive correlation of the highly incompatible element against Zr and trace element variation diagram shows possibly co-genetic, and evolved from homogeneous source parental magma.
5. The rhyolites are suites of rhyolitic lava flow, ignimbritic flow and rhyolitic fall, which are alkaline trachy-dacites to rhyolites, per alkaline in composition. The upper rhyolitic lava is significantly different from the rhyolitic tuff and rhyolitic ignimbrite, where the lava flow is less porphyritic, contains more quartz and rare rock fragments, and shows clear flow banding.
6. The rhyolitic rocks of the Aiba area show consistently similar geochemistry to the well-constrained rhyolitic rocks of Wegel Tena and Lima limo, which have been

indicated to be formed by low pressure crystal fractionation process, though They show very similar patterns to those of the Wegel Tena volcanic rocks, where the rhyolites show moderately sloping LREE and nearly flat HREE, with no appreciable anomalies in both.

7. The basaltic and rhyolitic suites of the different stratigraphic do not shows similar ratio of two highly incompatible, very low Ta/Nb and Nb, Th and U do not show any significant negative anomaly suggesting co genetic origin and with limited crustal contamination, if any.
8. All the major and trace element ratio and REE chondrite of the Aiba basaltic suits are classified with in HT1 geochemical signature.

7.2. Recommendation

Though the field, stratigraphic logging, geological mapping as well as the petrographic analysis and the limited number of major and trace element geochemical analysis provided enough background to the investigation of Petrogenesis of the Alaji Formation rocks in the Aiba area, the numbers of geochemical samples were very limited to draw definitive conclusions. It is therefore recommended to conduct more detailed geochemical analysis for major and trace elements in order to draw statistically significant analysis and geochemical modeling which will allow drawing definitive conclusions. In addition, Rb-Sr and Sm-Nd isotopic investigations are recommended for constraining magma sources and the Petrogenetic processes responsible for the formation of the rock suite.

Reference

Angesom Resom, Asfawossen Asrat,Tegenu Gossa, Erella Hovers.(2018). Petrogenesis and depositional history of felsic pyroclastic rocks from the Melka Wakena archaeological site-complex in south central Ethiopia .*Journal of African Earth Sciences, 1429:* 93-111.

Baker J., Snee, L. and Menzies, M. (1996). A brief Oligocene period of flood volcanism in Yemen. *Earth and Planetary Science Letters* 138: 39–55.

Beccaluva, L., Bianchini, G.,Natali,C. and Siena,F.(2009). Continental Flood Basalts and Mantle Plumes: a Case Study of the Northern Ethiopian Plateau. *Journal of Petrology.* (50):1377-1403.

Black, S., Macdonald, R., Kelly, M.R.(1997). Crustal origin for peralkaline rhyolites from Kenya: evidence from U-series disequilibria and Th-isotopes. *J. Petrol.* 38: 277–297.

Boccaletti M., Getaneh Asefa., Mazzuoli R., Tortorici L. and Trua T. (1995). Chemical variations in a bimodal magma system: The plio Quaternary volcanism in the Dera Nazret area (Main Ethiopian Rift, Ethiopia). *Afr. Geosci. Rev.* 2: 37–60.

Boynton W.V. (1984). Geochemistry of rare earth elements: meteorite studies, In: Henderson P. (ed.), *rare earth element geochemistry. 63-114.*

Chorowicz, J., (2005). The East African Rift System. *Journal of African Earth Sciences* 43:379-410.

Corti, G. (2009). Continental rift evolution: From rift initiation to incipient break-up in the Main Ethiopian Rift. *East Africa .Earth-Science Reviews*, 96: 1–53.

Dereje Ayalew, Gezahign Yirgu and Pik,R. (1999). Geochemical and isotopic (Sr, Nd and Pb) characteristics of volcanic rocks from southwestern Ethiopia. *Journal of African Earth Sciences,* 29: 381-391.

Dereje Ayalew (2000).Origin by fractional crystallization of transitional basalt for the Asela-Ziway pantellerite. Crustal control in the genesis of Plio-Quaternary bimodal magmatism of the Main Ethiopian Rift MER: geochemical and isotopic Sr, Nd, Pb evidence by Trua et al. 1999.*Chemical Geology*, 168: 2000 1–3.

Dereje Ayalew, Barbey P., Marty B,. LaReisberg L., Gezahign Yirgu, and Pik R,. (2002). Source, genesis, and timing of giant ignimbrite deposits associated with Ethiopian continental flood basalts.*Geochimica et Cosmochimica Acta*,66(8): 1429–1448.

Dereje Ayalew and Gezahegn Yirgu (2003). Crustal contribution to the genesis of Ethiopian plateau rhyolitic ignimbrites: Basalt and rhyolite geochemical provinciality. *Journal of the Geological Society*, 160: 47-56.

Dereje Ayalew, Ebinger, C., Bourdon, E., Wolfenden, E., Gezahign Yirgu and Grassineau, N. (2006). Temporal compositional variation of syn-rift rhyolites along the western margin of the southern Red Sea and northern Main Ethiopian Rift. In: Gezahign Yirgu, Ebinger, C.J., Maguire, P.K.H. (Eds.), the Afar Volcanic Province within the East African Rift System: *Geological Society Special Publication,* 259: 121–130.

Dereje Ayalew (2011).The relations between felsic and mafic volcanic rocks in continental flood basalts of Ethiopia: implication for the thermal weakening of the crust. *Geological Society, London, Special Publications,* 357: 253-264.

Dereje Ayalew., Jung, S., Romer, R.L, Kersten, F., fänder .J.A.P., Garbe-Schönberg .D.(2016). Petrogenesis and origin of modern Ethiopian rift basalts:Constraints from isotope and trace element geochemistry. *Lithos* 258–259: 1–14

Ebinger, C.J., Tilahun Yemane, Giday Weldegebriel, Aronson, J.L. and Walter, R.C. (1993). Late Eocene Recent volcanism and faulting in the southern main Ethiopian rift. *Journal of the Geological Society of London*, 150: 99–108.

Ebinger, C.J., Sleep, N.H.(1988). Cenozoic magmatism throughout east Africa resulting from impact of single plume. *Nature,* 395:788-791.

Furman, T., Bryce, J.G., Karson, J., Iotti, A.(2004). East African Rift System (EARS) plume structure: insights from Quaternary mafic lavas of Turkana, Kenya. *J. Petrology* 45: 1069-1088.

Furman T., Bryce J., Rooney T., Hanan B., Gezahign Yirgu and Dereje Ayalew. (2006). Heads and tails: 30 million years of the Afar plume. Gezahign Yirgu, G. and Ebinger, C. J. (eds.). The Afar Volcanic the East African Rift System. *Geol. Soc. Spec. Pubs.* 256: 95–119.

Furman, T. (2007). Geochemistry of East African Rift basalts: an overview. *J. Afr. Earth Sci*. 48: 147–160.

Furman T, Nelson W.R., Tanton, E.L.(2016). Evolution of the East African rift: Drip magmatism, lithospheric thinning and mafic volcanism. *Geochimica et Cosmochimica Acta* 185:18–434.

Gasparon, M., Innocenti, F., Manetti, P., Peccerillo, A. and Tsegaye Abebe (1993). Genesis of the Pliocene to Recent bimodal mafic–felsic volcanism in the Debre–Zeyt area, central Ethiopia: volcano logical and geochemical constraints. *Journal of African Earth Sciences,* 17: 145–165.

George, R., Rogers, N. and Kelly, S. (1998). Earliest magmatism in Ethiopia: evidence for two mantle plumes in one flood basalt province. *Geology*, 26: 923-926.

Giday Weldegebriel, G., Aronson, J.L. and Walter, R.C. (1990). Geology, geochronology, and rift basin development in the central sector of the Main Ethiopia Rift. *Geological Society of America Bulletin,* 102: 439–458.

Giday Weldegebriel and Heiken, G. White, T, D. Berhane Asfaw,Hart,W. K. and Renne, P. R. (2000).Volcanism, tectonism, sedimentation, and the paleoanthropological record in the Ethiopian Rift System. Geological Society of America. Special Paper, 345: 83-98.

Giordano, F., D'Antonio M. ,Civetta L., Tonarini S., Orsi G., Dereje Ayalew, Gezahign Yirgu, Dell'Erba F., Di Vito M.A. and Isaia R. (2014). Genesis and evolution of mafic and felsic magmas at Quaternary volcanoes within the Main Ethiopian Rift: Insights from Gedemsa and Fanta 'Ale complexes. *Lithos,* 188: 130–144.

Hart, W. K, Giday Woldegabriel, Walte,R.C. and Mertzman.S.A.(1989). Basaltic Volcanism in Ethiopia: Constraints on Continental Rifting and Mantle Interactions. Journal Of Geophysical *Research*, l(94): (7731-7748).

Hofmann, C., Courtillot, V., Féraud, G., Rochette, P., Gezahegn Yirgu, Ketefo, E., and Pik, R. (1997). Timing of the Ethiopian flood basalt event and implications for plume birth and global change: *Nature*, 389: 838–841.

http://En.climate-data.org.

http://en.m.wikipidia.org.>wiki>mayc.

Kieffer, B., Arndt, N., LaPierre, H., Bastien, F., Bosch, D., Pecher, A., Gezahegn Yirgu, Dereje Ayalew, Weis, D., Jerram, D., Keller and F., Meugniot, C. (2004). Flood and shield basalts from Ethiopia: magmas from the African Super swell. *Journal of Petrology*, 45: 793–834.

Kurkura Kabeto, Sawnda,Y and Roser B. (2009). Compositional differences between felsic volcanic rocks from the margin and center of the northern Main Ethiopian Rift. *MEJS*, 1(1): 4-35.

Kurkura Kabeto (2010). Geological and geochemical variations in Mid-Tertiary Ethiopian Flood Basalt Province, Maychew, Tigray Region, Ethiopia. *MEJS2 (1): 4-25.*

Macdonald, R. (1974). Nomenclature and petrochemistry of the peralkaline oversaturated extrusive rocks. *Bull, Volcanol*. 38 (2):498-516

Mahoney, J.J., Saunders, A.D., Storey, M., Randriamanantenasoa, A.(2008). Geochemistry of the volcan de l' androy basalt–rhyolite complex, Madagascar cretaceous igneous province. *J. Petrol*. 49:1069–1096.

Marty, B., Pik, R.E, Gezahign Yirgu.(1996).Helium isotopic variations in Ethiopian plume lavas: nature of magmatic sources and limit on lower mantle contribution. *Earth and Planetary Science Letters*, 144:223-237.

Mengesha Tefera, Tadious Chernet, and Workineh Haro (1996). Exploration of the geological map of Ethiopia (1:20,000,000). Ethiopian institutes of geological surveys Addis Ababa, Ethiopia, 83pp.

Merla, G., Erenesto Abbate, Azzaroli, A., Bruni, P., Caunti, P., Fazzuoli, M., Sagri, M. and Tacconi, P. (1979). Geological map of Ethiopia and Somalia (1973):1:2,000,000 and comment with major land forms. 2-98.

Middlemost, E. A.K. (1994). Naming materials in the magma/igneous rock system. *Elsevier, Earth science review, 37:215*-224.

Miruts Hagos, Koeberl C, Kurkura Kebeto, Koller,F.(2010).Geology, petrology and geochemistry of the basaltic rock of the Axum area, northern Ethiopia. In: Ray J et al (eds) Topics in igneous petrology. Springer, Berlin, pp 69–93.

Miruts Hagos, Koeberl,C., Vries,B.V.W.D. .(2016). The Quaternary volcanic rocks of the northern afar Depression (northern Ethiopia): Perspectives on petrology, geochemistry, and tectonics. Journal of African Earth Sciences 117: 29-47

Mohr, P.A. (1983). Ethiopian Flood basalt provinces. *Nature*, 303: 577-583

Mohr P. and Zanettin B. (1988).The Ethiopian flood basalt province. In Continental Flood Basalts (ed. J. D. Macdougall).*Kluwer Academic, Dordrecht, pp*. 63–110

Mulugeta Alene, Hart, W.K., Saylor, B.Z.,Deino,A., Mertzman,S., Yohannes Haile Selassie, Gibert,L.B.(2017).Geochemistry of Woranso–Mille Pliocene basalts from west-central Afar, Ethiopia: Implications for mantle source characteristics and rift evolution. *lithos* ,282-283:187-200.

Natali, C., Beccaluva L, Bianchini G, Siena F.(2011).Rhyolite associated to Ethiopian CFB: clues for initial rifting at the Afar plume axis. *Earth Planet Sci Lett*, 312:59–68.

Natali,C., Beccaluva L, Bianchini G, Siena F.(2013).The Axum–Adwa basalt–trachyte complex: a late magmatic activity at the periphery of the Afar plume. *Contrib Mineral Petrol*, 166: 351–370.

Peccerillo, E.M., Justin-Visentin.E, Zanettin,B. Joron,J.L. and M. Treuil.M.(1979). Geodynamic evolution from plateau to rift: major and trace element geochemistry of the central eastern Ethiopian Plateau volcanics. *Neues Jb. Geol. Palaont. Abh.* 158:139-179.

Peccerillo, A., Barberio, M.R., Gezahign Yirgu, Dereje Ayalew, Barberi, M. and Wu, T.W. (2003). Relationships between mafic and acid peralkaline magmatism in continental rift settings: a petrological, geochemical and isotopic study of the Gedemsa volcano, central Ethiopian Rift. *Journal of Petrology*, 44(11): 2003-2032.

Peccerillo, A., Donati C., Santo, A. P., Orlando, A., Gezahign Yirgu and Dereje Ayalew (2007). Petrogenesis of silicic peralkaline rocks in the Ethiopian rift: geochemical evidence and volcano logical implications. *Journal of African Earth Sciences*, 48: 161–173.

Pik, R., Deniel, C., Coulon, C., Gezahign Yirgu, Hofmann, C., Dereje Ayalew (1998). The Northwest Ethiopian plateau flood basalts: classification and spatial distribution of magma types. *Journal of Volcanology and Geothermal Research*, 81: 91–111.

Pik, R., Deniel, C., Coulon, C., Gezahign Yirgu and Marty B. (1999). Isotopic and trace element signatures of Ethiopian flood basalts: Evidence for plume–lithosphere interactions.*Geochimica Cosmochimica Acta*, 63(15): 2263–2279.

Pik, R., Marty, B., Hilton, D.R. (2006). How many mantle plumes in Africa? The Geochemical point of view. *Chemical Geology*, 226:100-114.

Rogers, N., Macdonald, R., fitton, J.G., george, R., smith, M. and Barreiro, B. (2000). Two mantle plumes beneath the East African Rift System: Sr, Nd and Pb isotope evidence from Kenya Rift basalts. *Earth and Planeta~ Science Letters*, 176: 387-400.

Rollinson, H., (1993). Using geochemical data: evaluation, presentation, interpretation. Pearson, *prentice hall*, 380pp.

Rooney, T., Furman T., Gezahign Yirgu, Dereje Ayalew. (2005). Structure of the Ethiopian lithosphere: Xenolith evidence in the Main Ethiopian Rift. *Geochim Cosmochim Acta*, 69(15):3889–3910.

Rooney, T. O., Furman T., Bastow, Dereje Ayalew and Gezahign Yirgu (2007). Lithospheric modification during crustal extension in the Main Ethiopian Rift. *J. Geophysics*. Res. 112.

Rooney, T.O., Hanan, B.B., Graham, D.W., Furman, T., Blichert-Toft, J., Schilling, J.G.(2012). Upper mantle pollution during afar plume–continental rift interaction. *Journal of Petrology*, 53: 365–389.

Seife Micahel Berhe, Berhe Desta, Nicoletti, M. and Mengesha Tefera (1987). Geology, geochronology and geodynamic implications of the Cenozoic magmatic province in W and SE Ethiopia. *Journal of the Geological Society, London,* **144**: 213- 226.

Sembroni, A., C. Faccenna, T. W. Becker, P. Molin, and Bekele Abebe (2016). Longterm, deep mantle support of the Ethiopia-Yemen Plateau, Tectonics, 35:469–488.

Stewart. and Rogers N. (1996). Mantle plume and lithosphere contributions to basalts from southern Ethiopia. *Earth and Planetary Science*, 139:195-211

Sun, S.S., McDonough, W.F. (1989). Chemical and isotopic systematics of oceanic basalts: implication for mantle composition and processes. In: Saunders, A.D., Norry, M.J. (Eds.), Magmatism in the ocean basins. *Geological Society Special Publication*, 42:313-345.

Tadiwos Chernet, Hart, W.K., Aronson, J.L. and Walter, R.C. (1998). New age constraints on the timing of volcanism and tectonism in the northern Main Ethiopian Rift-southern Afar transition zone (Ethiopia). *Journal of Volcanology and Geothermal Research,* **80**: 267–280.

Tadiows Chernet and Hart W.K. (1999). Petrology and Geochemistry of volcanism in the northern Main Ethiopian Rift- southern Afar transition region. *Actavolcanologica,* **11**(1): 21-41.

Thompson, R.N., Morrison, M.A., Hendry, G.L., Parry, S.J. (1984). An assessment of the relative roles of a crustal and mantle in magma genesis: an elemental approach. Phil Trans Royal Society London, 310:549-590.

Trua, T., Deniel, C. and Mazzuoli, R. (1999). Crustal control in the genesis of Plio-Quaternary bimodal magmatism of the Main Ethiopian Rift (MER): Geochemical and isotopic (Sr, Nd and Pb) evidence. *Chemical Geology*, 155: 201–231.

Ukstins, A., Paul R. ,Renne ., Ellen W ., Joel .,Dereje Ayalew., Martin .(2002). Matching conjugate volcanic rifted margins: 40Ar/39Ar chrono-stratigraphy of pre- and syn-rift bimodal food volcanism in Ethiopia and Yemen. *Earth and Planetary Science Letters*, 198: 289-306.

Wilson, M. (1989). Igneous Petrogenesis A global tectonic Approach. *Unwin Hyman*, London, and 480pp.

Wolfenden, E., Ebinger, C., Gezahegn Yirgu, Deino, A. and Dereje Ayalew (2004). Evolution of the northern Main Ethiopian rift: birth of a triple junction. *Earth and Planetary Science Letters*, 224: 213–228.

Zanettine, B., Justin-Visentin, E., Nicoletti, M. and Petrucciani, C. (1978). Evolution of the Chencha escarpment and the Ganjiuli graben (Lake Abaya) in the southern Ethiopian rift. Neues Jahrbuch fur Geologie und Palaontologie. Monatshefte ,8:473–490.

Zanettine, B., Justin-Visentin, E., Nicoletti, M. and Piccirillo, E.M. (1980). Correlations among Ethiopian Volcanic Formations with special reference to the chronological and stratigraphic problems of the Trap Series. *Accad. Naz. dei Lincei*, Rome, 47: 231–252.

List of appendix

Appendix I : Structural measurement

Joint measurement

Easting	Northing	Strike	Dip amount	Dip direction
559466	1418911	30NE	60	45SE
559469	1418913	30NE	65	45SE
559484	1418920	30NE	70	40SE
559565	1418959	30NE	70	70SE
559349	1418903	029NE	75	26SE
559351	1418903	15NE	75	50SE
559460	1411891	65NW	40	30NE
559570	1418960	30NE	60	60SW
559577	1418964	15NE	70	90NE
559577	1418964	20NE	80	70SE
559689	1419042	10NE	35	75SE
560505	1419598	25NE	75	60SE
560503	1411983	30NE	65	65SE
560500	1419459	35NE	70	S45E
560520	1419388	30NE	60	50SE
558137	1425467	N20W	70	45NE
558295	1425562	10NE	70	37SE
55833	1425615	24NE	66	28SE
557203	1417772	N30E	70	35SE
557279	1419318	24NE	50	60SE
559621	1418976	27NE	80	35SE
558033	1423259	25NE	55	60SE
557589	1422542	30NE	80	40SE
557279	1419343	30NE	50	48SE

Normal fault measurement

Easting	Northing	Strike	Dip amount	Dip direction
5506617	1419356	40NE	70	30SE
550741	1240240	30NE	60	25SE
561072	1420079	27NE	50	45SE
5594451	1419966	35NE	65	50SE
558835	1420427	27NE	48	40SE
557533	1420177	35NE	75	75SE

Appendix II: Sample location for petrography and Geochemistry

Easting	Northing	Sample code	Elevation
559012	1419500	LAB-01	2946
558741	1420240	ASR-03	3120
554944	1423347	LTSB-04	3500
554182	1421632	UTSB-06	3925
560741	1420252	UASB-08	3265
557533	1420177	ASR-15	3134
559622	1420605	UASB-17	3312
559451	1419966	ASR-20	3134
558520	1425653	LCST-20	2935
557589	1422542	ASI-16	3060
560643	1419335	lab-02	2961
554931	1422910	TSR-05	3510
560457	1425000	CSI-20	3200
559013	1425612	CSB-22	3100
554517	1422069	UTSB-07	3813
559621	1418978	LAST-20	2860

Appendix III: Sum and ratio of major oxide

Na2O	K2O	CaO	Al2O3	K2O/Na2O	CaO/Al2O3	K2O+Na2O
1.91	0.62	10.13	11.3	0.32460733	0.896460177	2.53
2.91	0.89	10.38	15.68	0.305841924	0.661989796	3.8
5.9	5	0.76	14.77	0.847457627	0.051455653	10.9
2.96	0.9	10.43	15.46	0.304054054	0.674644243	3.86
2.89	0.95	10.45	15.52	0.328719723	0.673324742	3.84
2.47	0.38	10.85	13.37	0.153846154	0.811518325	2.85
1.93	3.97	0.59	8.63	2.056994819	0.068366165	5.9
2.12	0.59	11.38	12.04	0.278301887	0.945182724	2.71
5.99	5.35	0.77	14.79	0.893155259	0.052062204	11.34

Appendix IV: Selected REE from Ethiopian plateau Rhyolite

Code	La	Ce	Pr	Nd	Sm	Eu	Gd	Tb	Dy	Ho	Er	Tm	Yb	Lu
Lima limo														
AD27	98	162	27	122	22	7.2	19	3	17	3.5	8.1	1.2	7.2	1.05
98-150	100	231	27	104	21	2.1	15	2.5	14	2.7	8.1	1.3	9	1.49
AD26	119	237	30	120	21	3	17	2.7	14	3.1	7.8	1.2	7.8	1.22
98-138	142	384	38	144	27	3.6	20	3	17	3.4	8.6	1.6	9.5	1.52
Jima														
98-13	79	152	18	66	12	3.2	11	1.7	10	1.9	4.9	0.8	5.7	0.96
98-7	110	221	27	100	20	2.1	16	2.6	16	3.5	9.7	1.7	11.7	1.85
98-5	111	199	28	102	19	4.1	15	2.2	11	2.2	5.5	0.8	5.5	0.84
98-8	152	205	33	122	24	1.8	20	3.2	20	4.1	11.3	1.9	12.9	1.98
98-10	160	304	38	142	30	1.3	28	4.7	28	5.4	14.	2.4	16.	2.5
Wegel Tena														
AD14	117	246	31	124	24	6	19	2.7	15	2.9	6.7	1	6	0.88
AD40	126	212	33	137	27	7.2	21	3	16	3.3	7.6	1.1	6.5	0.93
AD12	110	246	29	119	20	5.9	17	2.6	14	2.8	6.2	0.9	5.5	0.8
AD74	102	199	25	99	22	4	16	2.5	16	3.3	7.5	1.2	8.1	1.23
AD9	106	227	28	116	25	6.1	18	2.7	16	3.1	7	1.1	5.5	1.01
AD57	119	233	31	129	23	6.8	22	3.2	18	3.8	8.9	1.2	7.2	1.28

Debre Birhan														
AD30	134	236	34	133	25	3.7	20	3.4	20	4.4	11	1.7	11	1.84
AD28	143	296	35	141	27	4	23	3.9	22	4.9	12	1.7	13	1.77
AD29	145	312	35	143	27	4.1	22	3.9	23	4.9	12	1.9	13	1.77
AD79	118	95	27	97	17	1.2	12	2.1	13	2.9	8	1.3	9	1.24
AD32	115	196	28	106	21	1.5	17	2.9	17	3.9	10	1.7	11	1.72
98-62	122	229	25	94	17	1.3	15.1	2.4	14	2.7	7	1.11	7	1.12

N.B. Data source for the plateau rhyolite: Dereje Ayalew et al., 2002

REE data of the High Titanium and low Titanium Oligocene flood basalt from North Ethiopia

HT2														
	La	Ce	Pr	Nd	Sm	Eu	Gd	Tb	Dy	Ho	Er	Tm	Yb	Lu
E235	32.8	69.4	8.5	34.8	7.09	2.22	6.99	0.99	5.74	1.08	2.84	0.386	2.35	0.355
E31	29.9	71.8	9.5	41.9	9.47	2.77	8.43	1.17	6	1.06	2.53	0.32	1.84	0.26
E35	31	70	9.7	44	9.6	3	9.03	1.4	7.2	1.29	3.1	0.4	2.4	0.35
E37	37	87	11.6	52	11.1	3.5	10.7	1.5	8.2	1.46	3.5	0.45	2.7	0.39
E38	43.9	103.6	13.2	57.3	12.3	3.6	10.8	1.46	7.55	1.32	3.21	0.41	2.4	0.34
E40	27.1	65	8.8	38.3	8.54	2,56	7.94	1.1	5.93	1.07	2.62	0.33	1.98	0.27
E233	27.9	67.9	9.1	42.2	9.3	2.9	8.8	1.2	6.4	1.11	2.7	0.34	2	0.3
E226	17.9	40.7	8	25.7	6.15	1.99	6.55	0.94	5.34	0.97	2.5	0.35	1.97	0.31
LT														
E166	7.9	18.5	2.7	13.5	3.76	1.32	4.3	0.7	4.44	0.88	2.55	0.351	2.2	0.341
E168	11.9	27.1	3.8	18.7	5.15	1.67	5.93	0.96	6.11	1.24	3.64	0.497	3.2	0.492
E178	7.8	19.2	2.9	14.8	4.44	1.56	5.31	0.85	5.5	1.12	3.14	0.437	2.72	0.443
E181	13.4	24.4	3.6	17.6	4.69	1.64	5.35	0.84	5.23	1	2.87	0.378	2.3	0.364
PM6	9.4	18.2	2.5	11.6	3	1.14	3.82	0.63	4.03	0.85	2.44	0.36	2.36	0.355
E210	8.7	21.5	3.1	15	4.07	1.45	4.85	0.76	4.78	0.96	2.61	0.36	2.2	0.335
E90	8.8	24.9	3.8	19.7	5.22	1.92	5.92	0.89	5.45	1.08	2.82	0.29	2.41	0.389
E88	9.3	23	3.4	15.9	4.1	1.5	5	0.8	4.9	1.97	2.6	0.33	2.3	0.35
E84	2.9	8.2	1.3	7.2	2.4	1	3.3	0.56	3.6	0.75	2	0.368	1.9	0.229
E202	4.7	12.5	1.9	9.8	2.9	1.58	3.7	0.64	4	0.83	2.3	0.56	2.1	0.33

N.B. LT and HT REE data source Pik et al., 1999

Ti,Y,and Nb data from the north western Ethiopia plateau(from Pik et al., 1998)

HT2								LT									
Ti	E31	E33	E35	E37	E38	E40	E225	E226	E232	E166	E168	E171	E178	E181	PM6	E210	E90	E88
Y	4.02	4.28	4.62	4.99	3.79	3.92	2.62	3.77	4.39	1.58	2.1	1.88	1.98	1.32	1.8	2.26	1.59	1.08
Nb	32	29	32	37.5	33.9	28.9	29.4	29.4	32.3	28.7	39.9	36.1	32.1	26.1	34.7	31	26.8	20.7